UNIVERSITÀ DI PARMA

UNIVERSITA' DEGLI STUDI DI PARMA

DOTTORATO DI RICERCA IN

"*Scienze del Farmaco, delle Biomolecole e dei*

Prodotti per la Salute"

CICLO XXXIV°

INFLUENCE OF PROPROTEIN CONVERTASE SUBTILISIN/KEXIN TYPE 9 (PCSK9) ON BRAIN CHOLESTEROL METABOLISM AND POTENTIAL IMPACT ON ALZHEIMER'S DISEASE PATHOGENESIS

Coordinatore:

Chiar.mo Prof. Marco Mor

Tutore:

Chiar.mo Prof. Franco Bernini

Dottoranda: Bianca Papotti

Anni Accademici 2018/2019 – 2020/2021

ABSTRACT

Alzheimer's Disease (AD) represents the most common and burdening form of dementia against which, currently, no drug is effective in slowing or counteracting the disease. The most challenging aspect is represented by the fact that the etiopathological processes leading to AD development are not yet fully clarified. Among other hypotheses, the involvement of lipid metabolism has been postulated. Cholesterol, indeed, actively participates in several relevant processes for brain homeostasis and disturbances in its metabolism have been described in several neurodegenerative diseases, including AD. Brain relies on *in situ* cholesterol biosynthesis, due to the presence of BBB; moreover, adult neurons strongly depend on cholesterol provided by astrocytes, as their endogenous cholesterol biosynthetic rate is limited. Hence, brain cholesterol transport from astrocytes to neurons, specifically mediated by apoE-containing lipoparticles, represents a crucial step for neuronal homeostasis. Proprotein Convertase Subtilisin/Kexin type 9 (PCSK9), one of the major regulators of plasma LDL-C levels, whose involvement in different processes relevant for CNS homeostasis has been described, may possibly impact directly on brain cholesterol transport by degrading cerebral lipoprotein receptors. However, the currently available evidence of an involvement of PCSK9 in AD, possibly by disturbing brain cholesterol transport, is still limited and controversial.

This research work stems from the previous observation by our research group of increased PCSK9 concentrations in cerebrospinal fluid (CSF) of AD subjects as compared to controls. The main objective of this work is the investigation of the potential involvement of PCSK9 in brain cholesterol dysregulation, which represents a central aspect of AD, aiming at clarifying its role in the disease etiopathogenesis and potentially identifying PCSK9 as a possible disease-related biomarker and a pharmacological target.
To this aim, a translational study was set up, following three different experimental approaches including *in vitro* studies on cultured astrocytes and neuronal cell models, and *ex vivo* analyses upon samples isolated from both animal models of the disease and patients with different degrees of cognitive impairment.

In the first part of the present research work, the impact of PCSK9 on the most relevant steps of brain cholesterol transport has been explored. In cultured astrocytes, PCSK9 induced an increase in endogenous cholesterol biosynthesis, which, however, wasn't able to counterbalance the impairment of cholesterol endocytosis due to its degrading effect on lipoprotein receptor, leading to an overall reduction in astrocyte cholesterol content, furtherly lowered by the co-incubation with $A\beta_{1-42}$ fibrils. The observed impairment of astrocyte cholesterol homeostasis, namely reduced intracellular cholesterol, may eventually translate into reduced supply to neurons. Consistently, in cultured neurons PCSK9 furtherly promoted cellular cholesterol depletion by impairing both the endocytic process as well as by reducing intracellular cholesterol biosynthesis, possibly resulting in compromised neuronal viability.

In the second part of the present research work, the impact of PCSK9 on cholesterol homeostasis was investigated in a transgenic mouse model of AD lacking PCSK9. Specifically, the PCSK9 heterozygous and, even more, the homozygous mutation in mice led to a significant decrease in both serum and cerebral cholesterol content. Interestingly, transgenic AD mice were characterized by an overall reduction of total circulating as well as cerebral cholesterol levels, more exacerbated in mice bearing PCSK9 homozygous or heterozygous deletion. This evidence supports the involvement of PCSK9 in cerebral cholesterol homeostasis, thus reinforcing the previously described *in vitro* evidence.

In the third part of the present research work, a case-control study has been performed to explore PCSK9 as well as the main lipid levels in 83 subjects with different degrees of cognitive impairment, namely subjects with stable mild cognitive impairment (MCI), patients with MCI that furtherly degenerated to AD at follow-up, and patients with clinically diagnosed AD. CSF and serum PCSK9 levels were similar among the three considered groups, but CSF PCSK9 concentration was higher as compared to that of a control group previously analysed. This evidence suggests that CSF PCSK9 levels may start to increase during the prodromal phases of the disease. AD subjects carrying at least one apoE ε4 allele showed higher PCSK9 concentrations as compared to non-carriers. Furthermore, a positive correlation between serum and CSF PCSK9 levels was highlighted in AD patients, suggesting that an exchange between peripheral and central PCSK9 levels may occur, possibly as a consequence of an increased BBB permeability, that has been previously reported.

In conclusion, the results of this translational study, performed upon *in vitro* as well as *ex vivo* experimental approaches, indicate the involvement of PCSK9 in AD pathogenesis, possibly through the modulation of brain cholesterol homeostasis. Altogether, these data support the possibility to recognize PCSK9 as a pharmacological target in AD, for which effective therapies are still lacking. Hence, the development of small lipophilic molecules inhibiting PCSK9 and being able to cross BBB may represent an interesting future pharmacological perspective to restore brain cholesterol homeostasis, thus providing a potential future innovative therapy for AD.

TABLE OF CONTENTS

Main abbreviation list (alphabetic order)

Aβ: Amyloid β

ABC: ATP Binding cassette

AD: Alzheimer's Disease

apoA-1: apolipoprotein A-I

apoE: apolipoprotein E

apoER2: apolipoprotein E receptor 2

BBB: Blood Brain Barrier

CSF: Cerebrospinal Fluid

EOAD: Early Onset AD

GOF: gain of function

HDL: High-density lipoprotein

LC-MS/MS: Liquid Chromatography-Tandem Mass Spectrometry

LOAD: Late Onset AD

LOF: loss of function

LDL: Low-density lipoprotein

LDLR: Low-density lipoprotein receptor

LRP1: LDL receptor-related protein 1

LXR: Liver X Receptor

mAbs: monoclonal antibodies

MCI: Mild Cognitive Impairment

NFT: Neurofibrillary Tangles

PCSK9: proprotein convertase subtilisin/kexin type 9

RXR: Retinoid X Receptor

SNP: Single Nucleotide Polimorphism

SREBP: Sterol regulatory Element Binding Protein

VLDLR: Very low-density lipoprotein receptor

24-OHC: 24-hydroxycholesterol

25-OHC: 25-Hydroxysterol

27-OHC: 27-Hydroxysterol

INTRODUCTION

1. ALZHEIMER'S DISEASE

Alzheimer's disease (AD; OMIM #104300) refers to an age-related cognitive and functional decline eventually resulting in death [1]. AD dementia was first described in 1906 by Alois Alzheimer, referring to disorientation and cognitive alterations in a 51-year-old woman, associated with brain atrophy and anatomopathological abnormalities in her post-mortem neurohystological sections [2]. Currently, the diagnostic parameters for AD include memory and cognitive assessment tests, as well as the evaluation of specific parameters including structural brain imaging, amyloid brain positron emission tomography (PET) and cerebrospinal fluid (CSF) analysis [3].

1.1 EPIDEMIOLOGY

AD is the most common form of dementia, representing one of the most lethal and burdening pathological conditions, with an estimated prevalence of about 50 million people worldwide, two-thirds of which are living in low- and middle-income countries [4]. The incidence of AD in Europe is destined to double by 2050 [5]. Concerning patients' survival, AD is accompanied by a shorter life expectancy, varying between 3-12 years after diagnosis, based on different factors such as patients characteristics, comorbidities and their management [6]. A recent multicentre study investigated the duration of both dementia stage as well as of its prodromal phase, characterized by a mild cognitive impairment (MCI), showing that in subjects with a mean age of 70 years, the duration of preclinical AD stage was 10 years, followed by a mean 4 years of prodromal AD and overt dementia for 6 years [7]. Specific screening tests, including Mini-Mental Scale Examination (MMSE) and Montreal Cognitive Assessment (MoCa), are usually used to support clinical diagnosis and to monitor patients' cognitive decline [8]. The strongest risk factors for AD are related to age, gender, with more affected females than men (1.5 relative risk) and apolipoprotein (apo) E genotype, with carriers of at least one apoE isoform ε4 at high risk of developing AD [3]. Among modifiable risk factors, vascular diseases (diabetes, hypertension, dyslipidaemia, obesity), tobacco habit, low physical activity, cerebrovascular or traumatic brain injury and low cognitive reserve due to low educational or professional achievement are noteworthy [9]. AD is typically referred as early-onset AD (EOAD), representing 5-10% of all AD cases, or late-onset AD (LOAD) based on the age of onset, whose cut-off is typically among 60-65 years [10]. Two different patterns have been observed in EOAD: mendelian (mEOAD), with an autosomal

dominant inheritance, that will be furtherly discussed in paragraph 1.2.3, and non-mendelian or sporadic (nmEOAD), with variable inheritance pattern [11].

1.2 ETIOLOGY

AD is a multifactorial disease, in which many risk factors may concur, as mentioned in paragraph 1.1. Currently, the underlying causes of AD are not fully defined. In this complex framework, different hypotheses have been postulated and coexist, in order to explain and describe the pathological alterations that characterize AD.

1.2.1 Amyloid hypothesis

One of the most validated hypotheses concerning AD aetiology is related to amyloid plaque deposition, which would be responsible for neuronal death in specific brain districts. This hypothesis was first formulated in 1984, after the isolation of Amyloid β (Aβ) plaques in the brain cortex of AD patients [12] and then reinterpreted several times, leading to a more recent insight, in which pathological Aβ deposition is a result of an imbalance between Aβ production and its clearance [13]. This evidence was also confirmed by genetic studies showing that mutations in amyloid precursor protein (APP), Presenilin (Psen)1 and Psen2 were related to an autosomal dominant AD form [14]. Specifically, in the non-amyloidogenic pathway, APP is constitutively cleaved by α- secretases such as ADAM10 and ADAM17 between Lysine16 and Lysine17 residues inside the Aβ domain, thus originating soluble protein called sAPPα and the membrane-bound fragment of 83 amino acid, C83, then processed by γ-secretase into p3 protein. sAPPα is involved in synaptic plasticity, neuronal signalling, survival and protection, as well as in the maintenance of memory, emotional and learning ability [15]. In the amyloidogenic process, β-secretases (BACE1) and γ-secretases, aspartyl proteases complex composed of Psen1, anterior pharynx-defective 1 (Aph1), nicastrin and Psen2, cleave APP between Aspartate 1 and Glutamic acid 11, leading to insoluble Aβ fragments. These latter are furtherly self-polymerized into oligomers and then fibrils, that finally aggregate in plaques and contribute to neurotoxicity [16]. Specifically, APP is a 770 amino acid plasma membrane integral protein encoded by a gene located on chromosome 21, which is cleaved either through the amyloidogenic or non-amyloidogenic pathway by different proteases, exerting different physiological functions involved in neuronal survival and growth. The relevance of this protein in physiological conditions is highlighted by recent experimental evidence, in which *in utero* electroporation of short hairpin RNA (shRNA) to knock-down

APP in rats results in reduced migration of neuronal precursors in the cortical plate [17]. Different *in vitro* studies showed that following γ-secretase processing, the C99 fragment originates different peptides, with a length comprised between 37 and 42 amino acids; among them $A\beta_{40}$ and, especially, $A\beta_{42}$ are more prone to self-aggregation. Different *in vitro* studies investigated the fibril formation process, during which Aβ monomers interact spontaneously with one another leading to oligomers formation in the first and slow nucleation phase [18]. These polymorphic Aβ species are arranged into 3-dimensional structures and furtherly aggregated into larger β-strand fibrils [19] in a second elongation phase, leading to the aggregation of different structures with different molecular weights finally resulting in fibrils [20]. The pathological alteration of this process is currently not fully clarified, and probably arise from increased production or reduced clearance of Aβ, with subsequent aggregation into oligomers and then fibrils and plaques. The resulting deposition of Aβ in the brain is related to the correct equilibrium between its production and its catabolism or clearance [13]. A physiological overproduction of Aβ is related to increased age, during which its catabolism is also reduced as a result of decreased activity of degrading enzymes such as neprilysin [21], and due to different age-related processes such as immune system dysregulation [22], diabetes and mitochondrial and oxidative stress [23], and also cholesterol metabolism alteration [24]. All those listed processes are considered risk factors for AD. In parallel, Aβ formation may be promoted by some mutations, such as on APP, Psen1 and Psen2 encoding genes, leading to a strong increase in Aβ deposition, leading to a fast neurodegeneration [25]. Aβ plaques induce a series of downstream processes that lead, in turn, to neurotoxicity, such as ion channel blockage, alteration in neuronal calcium homeostasis, mitochondrial oxidative stress, excitotoxicity, protein tau hyperphosphorylation and lower neuronal energy metabolism and glucose homeostasis alteration, leading to cell death and alteration in neurotransmitters, especially acetylcholine. In addition, Aβ seems to exert a direct effect on synapses and dendritic spines, as demonstrated in mice characterized by a virus-mediated overproduction of Aβ, and in 5xFAD mice, an experimental model of AD. In these models, the N-methyl-D-aspartate receptors (NMDARs), extremely important for synaptic plasticity, learning and memory, subunits GluN1, GluN2 and GluN3 equally contributed to Aβ-mediated decrease in the number of postsynaptic receptors in hippocampal neurons, essential for neuronal plasticity and short-term memory [26,27]. Hence, this specific loss of postsynaptic receptor due to Aβ may explain the specific AD-related memory impairment. Other than the well-known neurotoxic effect of Aβ fibrils, also different

evidence pointing to an Aβ oligomer-induced toxicity are currently available, despite the difficulties due to their heterogeneous structure and unstable characteristics. Indeed, oligomers interact with at least 20 different cell membranes receptors, including glutamate receptors, adrenergic receptors (β2-AR), p75 neurotrophin receptors and cellular prion protein receptor (PrPc) [19]. As demonstrated by an *in vivo* study, the coincubation of cultured astrocytes with Aβ oligomers leads to a strong increase in glutamate release, probably, as a consequence of their interaction with calcium-permeable ion channel astrocytic a7 nicotinic acetylcholine receptors (a7 nAChR) [28]. Again, the interaction of Aβ oligomers and PrPc is known to activate the kinase Fyn, with consequent reduction of NMDAR in neuronal synapses, thus leading to dendritic spine loss [29]. Together with oligomers-induced aberrant signalling, it has been demonstrated that they can also directly affect intracellular homeostasis. In this regard, Aβ oligomers promoted endothelial reticulum (ER) distress through the activation of phospholipase C, with subsequent pro-apoptotic caspase 3 activation [30]. Finally, Aβ oligomers seem to be involved in mitochondrial dysfunction, by promoting cytochrome c release, lysosomal and endosomal membrane disruption and brain-derived neurotrophic factor (BDNF) signal perturbation, essential to synaptic plasticity and memory [18]. Since BACE1 represents the rate-limiting step in Aβ formations, is currently considered an attractive druggable target for AD, also supported by *in vivo* evidence in which BACE1 Knock out (KO) mice lacked brain Aβ deposition and showed normal behaviour [31], and different BACE1 inhibitors have been developed and tested in clinical trials. Among them, MK8931 (Verubecestat), AZD-3293 (Lanabecestat), JNJ-54861911 (Atabecestat), E2609 (Elenbecestat) and CNP520 (Umibecestat), all tested in Phase II/III clinical trials but prematurely interrupted due to lacking amelioration in patients' cognition and Aβ deposition compared to placebo group [32], suggesting that their therapeutic potential in AD may be reviewed. Another field of investigation in AD drug discovery is related to the investigation of the therapeutic potential of active anti-amyloid immunotherapies, showing, however, important side effects such as severe meningoencephalitis or fatal immune response [33,34], thus clearing the path to safer and more controllable passive immunisation with monoclonal antibodies (mAbs) against Aβ. Among them, aducanumab, a human immunoglobulin gamma 1 (IgG1) is able to specifically target the aggregated soluble and insoluble Aβ. A preclinical study conducted upon Tg2576 transgenic mice showed that aducanumab is able to cross BBB and reach the brain, where it binds and reduces Aβ soluble and insoluble aggregates in a dose-dependent fashion [35].

Concerning clinical studies, the two Phase III clinical trials, EMERGE (NCT02484547) and ENGAGE (NCT02477800), tested aducanumab efficacy and safety in patients in the early stage of AD showing MCI and confirmed Aβ deposition. However, the clinical impact on the primary outcome, namely cognitive function, was modest, partially explained by the low rate of brain penetration of aducanumab and its selectivity for insoluble Aβ fibrils and plaques (-59% in ENGAGE trial and -71% in EMERGE trial) but not for oligomers [36]. However, considering the therapeutic potential of aducanumab and the lack of effective alternatives, it received FDA approval in June 2021 under the trade name of Aduhelm.

1.2.2 Tauopathy hypothesis

Despite the Aβ hypothesis holding a pivotal role in AD pathogenesis, different observations opened the path for additional hypotheses concerning AD-related physio-pathological processes. As an example, the brain areas with the most important Aβ deposition are different from those affected by neurofibrillary tangles (NFT) formation and neuronal death; moreover, evidence taken from a cohort of 107 patients with MCI and confirmed AD, suggested that the symptoms only arise in concomitance of elevated tau protein phosphorylation [37,38]. Tau protein is encoded by a gene located on chromosome 17 and, after alternative splicing of exon 2,3 ad 10, six possible isoforms, each composed of 352-441 amino acidic residues, can be obtained. Tau protein is a major member of Microtubules Associated Proteins (MAPs), able to bind with tubulin dimers and promote their subsequential association and dissociation, thus allowing neurons to maintain their axonal structure and polarity, and to guarantee organelles and signalling molecules transport [39]. Tau proteins are composed of an N-terminus and a C-terminus part, the latter of which contains repeated sequences that constitute the microtubules binding region (MTBR) [40]. Normally, tau protein's biological activity strictly depends on its degree of phosphorylation: in its non-phosphorylated form is extremely soluble, flexible and seems to promote synaptic activity and neuronal growth [41]. However, different neurodegenerative diseases, defined as "tauopathies" among which also AD is listed, are characterized by an alteration of the phosphorylated residues as a consequence of the deregulation of kinases and phosphatases, the enzymes responsible for phosphorylation and dephosphorylation, respectively [40]. The most important kinases in CNS are Glycogen Synthase Kinase-3β (GSK3β), Mitogen-Activated Protein Kinases (MAPK), Extracellular signal-regulated kinases 1 and 2 (Erk1/2) and c-Jun N-terminal kinases (JNK) [42]. Among them, GSK3β plays a key role in tau phosphorylation, being

responsible for the phosphorylation of Serine (Ser)199, Threonine (Thr)231, Ser396, Ser400, Ser404 and Ser413 residues in paired helical filaments (PHF) that constitute pathological NFTs, as demonstrated in isolated tau protein from human AD brain [43]. On the other side, tau dephosphorylating phosphatase (PP)2A activity was significantly lower in specific areas of brains isolated from AD patients [44]. Increased tau phosphorylation and decreased dephosphorylation lead to an overall 3- or 4-fold level of hyperphosphorylation in AD patients compared to aged subjects with preserved cognitive function [45]. Besides, tau protein isolated from AD patients is highly acetylated compared to healthy brains, possibly as a consequence of the altered acetylating activity of histone acetyltransferase p300 (p300 HAT) and cAMP-responsive element-binding protein (CREB)-binding protein enzymes [46]. Abnormal acetylation is thought to promote tau cleavage and inhibits its ubiquitin-mediated turnover, thus leading to abnormal tau deposition and aggregation [46]. However, the above-described tau alterations aren't the only cause of filament aggregation, as evidence of physiological phosphorylation has been also found in healthy brains in absence of tauopathy, thus suggesting that additional mechanisms may interfere in the fibrillogenic process, which is slow and organized in sequential phases in which several mechanisms take part. As an example, an *in vitro* study using tau cDNA clones expressed in *Escherichia coli* demonstrated that the repeat sequences in short tau fragment may be mostly responsible for the whole protein aggregation [47]; moreover, disulphide bridges among PHF monomers are preferentially formed under an oxidising environment, while polyanions seem to significantly accelerate the polymerization phase [48]. Besides, a recent cryo-electron microscopy (cryo-EM) study using 3.4-3.5 Ångstrom resolution demonstrated that in brains isolated from an AD-deceased patient, two filaments containing 306-378 residues of tau protein assemble in a cross-β/β-helix, thus clearing the path for subsequential further tau aggregation [49]. Based on this evidence, several attempts to develop an effective AD therapy by targeting tau protein are currently ongoing. Specifically, tau-targeting drugs can be divided into PP2A activators, such as memantine, GSK3β inhibitors, such as tideglusib, aggregation inhibitors and microtubule stabilisers that have been or currently are under investigation in clinical trials, with modest and unclear results [50]. Thus, other pharmacological approaches are currently under investigation. Among them, active immunization showed promising evidence by reducing tau deposition in preclinical models, but several adverse immune reactions have been recorded [51]. However, a randomized Phase II clinical trial was recently concluded, showing that the active peptide vaccine AADvac1 administered in patients with mild AD-

related dementia was well tolerated and able to induce antibodies production, despite no significant effects on cognitive function were recorded [52]. Passive immunization, on the other side, represents a possible solution, as the mAbs guarantee a lower risk of immunological adverse effects and greater target specificity. Among them, BMS-986168, able to recognize the 9-18 residues on the amino-terminal tau fragment, and RO7105705, able to recognize phosphorylated Ser409 on tau protein were tested in phase I and II clinical trials, furtherly interrupted as they didn't meet the primary outcomes related to efficacy. Other mAbs, such as LY3303560 (NCT03518073) and JNJ-63733657 (NCT04619420) are currently under investigation in early-phases clinical trials in patients with prodromic AD.

1.2.3 Genetic hypothesis

AD is generally considered a polygenic disorder; the evidence that mutations in three genetic sequences encoding for APP, Psen1 and Psen2 are directly related to autosomal dominant AD [14] lead to an increased effort to investigate further genic alteration that may concur to its pathogenesis. APP, Psen1 and Psen2 combined mutations are responsible for about 11% of all EOAD cases, and only 0.6% of all LOAD cases [53]; moreover since the APP encoding gene is located on chromosome 21, patients with Down's syndrome are more prone to develop AD-related Aβ deposition [54]. Consistently, duplication of APP encoding gene is associated with autosomal dominant AD [55], while a rare mutation in its sequence, known as "Icelandic mutation" is protective [56]. In this context, a French study on a large cohort of patients with EOAD demonstrated that mutations in APP encoding gene were present in about 26% of patients and Psen1 and Psen2 in 67% and 7%, respectively [57]. Concerning LOAD, studies conducted in twins showed a heritability of the disease ranging from 60% to 80% [58], and about 27% of which can be attributed to apoE isoform Ɛ4 [59], currently considered the major genetic risk factor for LOAD. Specifically, apoE is an apolipoprotein whose involvement in lipid metabolism and transport will be extensively treated in the forthcoming paragraphs. ApoE can be found in three different isoforms, as a result of polymorphisms in its encoding gene thus resulting in amino acid substitution: in the most common isoform, apoE Ɛ3, a cysteine and arginine residues are located in position 112 and 158, respectively, while apoE Ɛ4 is characterized by arginine in both residues and apoE Ɛ2, the least common isoform, by cysteine in both residues. Concerning apoE Ɛ4, the amino acid substitution leads to a salt-bridge formation between Arginine61 residue and Glutamine255 residue, with

consequent higher interaction between N-terminal and C-terminal protein region, otherwise separated in apoE Ɛ2 and Ɛ3 [60], thus affecting apoE structure and function. Corder and co-workers demonstrated that the Ɛ4 isoform in heterozygosis is associated with a 2-4-fold risk to develop AD, while its presence in homozygosis furtherly increases this risk up to 8-12-fold. On the other side, Ɛ2 isoform is associated with a lower AD risk [60]. In this complex picture, genome-wide association studies (GWAS) helped to identify genetic variants such as single nucleotide polymorphisms (SNPs) associated with AD. The most recent one, analysed 94437 patients with LOAD, confirmed 20 previously known risk loci, such as PICALM, BIN1, CD2AP, CLU, ABCA7, SORL1, CD33, TREM2, HLA and, above all, APOE, and also identified 5 new risk loci (IQCK, ADAM10, ACE, ADAMTS1, WMOX), all involved in synaptic functionality, Aβ and tau processing, inflammation and lipid metabolism [61]. The identification of risk loci for AD is extremely important, given the complexity of its pathogenesis, which is still partially unknown, as it may help in identifying new disease-related mechanisms and new targets for therapies and to establish individual polygenic hazard scores [62].

1.2.4 Cholinergic hypothesis

The cholinergic hypothesis is based on three main pillars. First, in severe AD-related neurodegeneration the nucleus basalis of Meynert (NBM), one of the main cortical cholinergic sources with different cortex projections, undergoes atrophy [63]; second, presynaptic cholinergic lesions have been found in the cerebral cortex of AD patients [64]; third, cholinergic agonists may positively affect memory [65]. Acetylcholine (Ach) represents the most relevant cortex, basal ganglia and basal forebrain neurotransmitter, acting on postsynaptic nicotinic and muscarinic receptors. In this regard, studies upon human post-mortem brain autopsies revealed a diminished number of nicotinic receptors [66]. Ach is involved in different fundamental cerebral functions, such as the synchronization of brain activity, neuroplasticity induced by experience, and connectivity: indeed, the stimulation of rat NBM lead to cortical remodelling and modulation of sensory map [66] and stimulated cerebral perfusion [67], thus affecting both cerebral neuroplasticity and haemodynamic. Interestingly, cholinergic alterations play a complex but established interaction with many typical AD-related hallmarks, such as Aβ deposition, NFT formation and neuroinflammation. Indeed, NFT deposition is probably the causing phenomenon leading to loss of cholinergic neurons in the NBM, the most sensitive area to neurofibrillary degeneration, as demonstrated by immunohistochemical

analyses on post-mortem AD brains compared to those of healthy controls [68]. Concerning Aβ deposition, Beach and co-workers found that choline acetyltransferase activity, the enzyme involved in Ach synthesis, was lower in presence of high Aβ deposition in post mortem brain of cognitively impaired subjects [69]. These observations were also supported by evidence in preclinical studies: as an example, the experimental induction of cholinergic lesions with murine p75 saporin in amyloid-prone APPswe/PS1dE9 mice lead to an increase in Aβ deposition and tau phosphorylation, also reflected by alteration in memory function [70]. In addition, several experimental evidence points to an anti-inflammatory effect derived by the stimulation of the α7 nicotinic receptor, probably as a consequence of the downregulation of nuclear factor kappa-light-chain-enhancer of activated B cells (NFκB) pathway [71]. Finally, concerning apoE isoforms, the main genetic risk factor for AD predisposition, it has been recently demonstrated that transgenic mice expressing human apoE ε4 isoform were characterized by cholinergic alterations in the hippocampal compensatory sprouting process [72], thus opening a new investigation field to clarify the exact molecular mechanisms. Starting from these observations, different therapies aiming at increasing Ach in the deficient brain areas and also inhibiting its degradation have been developed and currently represent one of the few FDA-approved drugs for AD. Among them, acetylcholinesterase inhibitors such as donepezil, rivastigmine and galantamine are able to promote a modest but consistent improvement in cognitive functions and slow decline compared to placebo-treated AD patients, as reported by a meta-analysis of 26 double-blind randomized controlled trials (RCT) [73].

1.2.5 Inflammatory hypothesis

In the complex interplay between the pathological events of AD, involving Aβ and NFT formation, neuroinflammation seems to play a significant role, thus concurring to neurodegeneration. Microglial cells and astrocytes represent the main brain immune effector cells and, as demonstrated by a seminal work upon transgenic mice expressing green fluorescent protein (GFP) in resident microglia, they preside CNS immune surveillance [74]. Specifically, neuroinflammation refers to CNS inflammation, caused either by pathogens or by pathological conditions such as trauma, ischaemia, with rapid release mainly by microglia and astrocytes of pro-inflammatory such as interleukin (IL)-1β, IL-6, tumour necrosis factor (TNF), different chemokines and reactive oxygen species (ROS) [75], that may lead to synaptic loss and neuronal death [76]. All these pro-inflammatory molecules furtherly stimulates microglial inflammasome accumulation, leading to a

vicious circle [77]. As an example, IL-1β infusion in rats is associated with a reduction in synaptic connections as a consequence of the prostaglandin E2 release, with consequent presynaptic glutamate release and NMDA activation [78]. Neuroinflammation also implies the activation of the complement system, mainly of C3 protein, that exacerbates the phagocytic activity of microglia and, if not controlled, may engulf synaptic material, as demonstrated in AD-mutant hAPP Tg mice [79]. Finally, together with pro-inflammatory cytokines secretion, activated microglia also produces anti-inflammatory mediators, such as IL-1 receptor antagonist, IL-4 and IL-10 and upregulates its phagocytic activity, in order to dampen excessive inflammation. However, in neurodegenerative disease this process is defective and neuroinflammation becomes a chronic condition [75]. Concerning AD, it has been widely described a strong connection between neuroinflammation and pathology [80]. Data obtained through *in vivo* brain imaging in transgenic AD-prone mice (APP_{KM670}/671NL and $PS1_{L166P}$) with microglial cells overexpressing GFP, revealed a rapid and dramatic microglia activation and proliferation in presence of Aβ deposition, that, however, isn't able to completely remove the deposits [81]. In this context, Toll-like receptors (TLRs), belonging to the Pattern Recognition Receptors (PRRs) play a great role in innate immune activation. In mammals, at least 10 TRLs have been identified, each with a distinct function and ligand selectivity, despite their structural similarity. The binding of TLRs to their specific ligand promotes the transduction of an intracellular signalling cascade, that can be classified as myeloid differentiation primary response gene 88 (MyD88)-dependent or TIR domain-containing adaptor-inducing interferon (IFN)-β (TRIF)-dependent pathway. The MyD88-dependent pathway involves the NF-κB activation through IκB kinase (IKK) complex and mitogen-activated protein kinase (MAPK) phosphorylation, leading to pro-inflammatory cytokines and chemokines secretion [80]. Similarly, TRIF-dependent signalling leads to NF-κB activation and IFN-β induction through the engagement of a different signalling pathway which involves tumour necrosis factor receptor-associated factor (TRAF)6 and transforming growth factor-β-activated kinase (TAK)1 [82]. Interestingly, in this regard, immunostaining of brain slices of APP TgCRND8 AD-prone mice revealed an increased expression of innate immune receptors, such as CD14, mainly localized near Aβ cerebral deposits [83] and, similarly, Walter and co-workers recorded an increased TRL4 mRNA in the same experimental model, furtherly confirmed by a parallel Aβ-associated increase in TRL4 expression in the entorhinal cortex of AD patients [84]. Consistently, a polymorphism in the TRL4 encoding gene caused by an adenine to guanine substitution, leading to aspartic

acid replacement instead of glycine in position 299 (Asp299Gly) is associated with a reduction in LOAD risk (-2.7 fold), probably as a consequence of a reduction in TLR ability to promote neuroinflammation [85]. The molecular mechanism explaining the innate immune activation in AD has been proposed by Stewart and co-workers using both *in vitro* and *in vivo* mouse models and demonstrating for the first time that Aβ is recognized by scavenger receptor CD36 in microglial cells, thus promoting the heterodimerization of TLR4 and TRL6 with the consequent engagement of both MyD88- and TRIF-dependent pathways and release of many pro-inflammatory mediators such as chemokines, cytokines, nitric oxide (NO) and ROS [86]. Notably, it has been previously demonstrated in transgenic PS1/APPsw mice that the amount of pro-inflammatory cytokines, including IL-1β, IL-6 and TNF-α, is strictly dependent on the burden of Aβ deposition [87]. TRL-dependent signal transduction seems to be also involved in neuronal apoptosis, as suggested by the evidence that conditioned media derived from Aβ-treated microglia lead to hippocampal neuron death [84]. In addition, activated microglia may recognize Aβ-damaged neurons, thus promoting their apoptosis through a CD14-dependent mechanism [88], probably as a consequence of the recognition of neuronal Aβ-induced phenotypic alterations. Another interesting aspect concerning neuroinflammation is related to the regulation of the Wnt pathway that has recently become a research hotspot, as Wnt in CNS is involved in the development of BBB, vascular protection and immune surveillance [89,90]. Specifically, upon Wnt canonical pathway activation, microglial cells switch from a "resting" to acquire an activated pro-inflammatory phenotype with high phagocytic ability, which is thought to play a great role in AD development, as the *in vivo* stimulation of Wnt pathway in AD-prone mice is associated to improvement in both behavioural assays and low Aβ deposition [91]. However, Aβ seems to induce β-catenin phosphorylation and degradation, thus blocking the Wnt pathway, despite to date no direct evidence about the molecular mechanisms are available [92]. In addition, tau protein, which in physiological conditions is involved in β-catenin binding and stabilization, upon hyper-phosphorylation loses this ability, with consequent damage to Wnt protective pathway [93]. Hence, the dysfunction of Wnt pathway, together with the increasing Aβ deposition, may lead microglial cells to secrete increasing concentrations of pro-inflammatory mediators while failing in phagocytosing Aβ [90].

1.2.6 Other hypotheses

The multifactorial nature of AD also implies other coexisting hypotheses, based on clinical and anatomopathological evidence, the most relevant of which will be discussed in the present paragraph.

The vascular hypothesis is based on the evidence that cerebral amyloid angiopathy (CCA), characterized by Aβ deposition within cerebral vessels and meninges with a further reduction of the internal diameter, is one of the most typical events associated with AD, with an estimated incidence of 70-97% [94,95]. The proposed two-step mechanism is that the initial vascular dysfunction, to which several risk factors such as hypertension, diabetes and dyslipidaemia may contribute, leads to a series of pathological processes including BBB and neurovascular unit (NVU) dysfunction, lower blood flow and neuronal death [96]. All these events may affect the correct Aβ clearance, thus leading to an accelerated deposition, as demonstrated in a cohort of cognitively impaired AD patients compared to healthy age-matched controls [97]. Interestingly, $A\beta_{1-40}$ peptide seems to be highly associated with CAA, while $A\beta_{1-42}$ with AD development [98]. In particular, NVU is an anatomic district composed of brain cells such as microglia, astrocytes, oligodendrocytes, neurons, and pericytes, smooth muscle cells and brain endothelial cells, and is involved in maintaining BBB functionality, cerebral blood flow and neuronal sustainment [99]. Interestingly, a strong derangement of hippocampus and cortex pericytes' number and coverage has been reported by immunohistochemical analyses upon post-mortem brain tissues of AD individuals [100]. Notably, AD apoE Ɛ4 carriers showed accelerated pericytes dysfunction and BBB breakdown compared to AD apoE Ɛ3 subjects, thus suggesting a direct role of apoE Ɛ4 in vascular protection [101].

Mitochondrial dysfunction represents another compelling hypothesis in AD pathogenesis and arises from the evidence that mitochondrial DNA (mtDNA) inheritance is strictly maternal and subjects with cases of AD in their maternal lineage are characterized by lower brain glucose and oxygen metabolism, higher PET PiB signs compared to individuals with a paternal history of AD [102]. Consistently, different studies conducted in cohorts of AD patients demonstrated an altered glucose metabolism in specific brain regions, such as in the temporoparietal cortex, resulting in lower 18-FDG uptake which is currently considered a specific diagnostic tool for AD [103,104]. Together with glucose metabolism, also oxygen consumption has been reported as altered in AD: a study

conducted upon 19 post-mortem AD brains highlighted a higher reduction of cytochrome oxidase activity in the frontal and temporal cortex compared to those of 30 controls, which may be associated with low ATP levels and increased ROS production [105]. Different studies performed in animal models suggested a direct involvement of mitochondrial dysfunction in Aβ and tau deposition. As an example, the administration of sodium azide, a complex IV inhibitor, in rats is associated with tau hyperphosphorylation and NFT deposition, neuronal loss and cognitive impairment [106], while rotenone treatment, a complex I inhibitor, is associated with high tau protein deposition in neurons, astrocytes and oligodendrocytes in rats [107]. Similarly, it has been demonstrated that the *in vitro* treatment of PC12 cells with Aβ is associated with inhibition of respiratory chain complexes I, III and IV, mitochondrial membrane depolarization and lower oxygen metabolism [108]. In addition, Aβ seems to negatively affect mitochondrial functionality by dysregulating also fission and fusion processes; as proof of that, post-mortem brain immunohistochemical analyses of M17 cells isolated from AD-prone APPswe mice revealed an increase in Dynamin-1-like protein (Drp1) and Opa1 and decrease in Mitochondrial fission 1 protein (Fis1) compared to control mice, with consequent lower mitochondrial fragmentation and abnormal mitochondrial distribution along neuronal axons, thus possibly leading to neuronal dysfunction [109]. In addition, a study performed in a triple transgenic mouse model characterized by contemporary Aβ deposition and tau protein hyperphosphorylation, suggest a putative synergistic action of these two pathological events in mitochondrial dysfunction, as highlighted by strong ROS production and altered functionality of the respiratory chain [110].

1.3 CLINICAL MANIFESTATION

AD is characterized by worsening cognitive decline, with loss of episodic memory, difficulty in remembering objects' and peoples' names, disorientation and visuospatial deficits, leading to a reduced ability to orientate in familial spaces. In addition, patients show progressive language decline, with paraphrastic errors and difficulties to find words and formulate long sentences [111]. AD is also accompanied by neuropsychiatric, sleep and behavioural changes, with signs of depression, withdrawal from social activities, maniac and executive changes, usually accompanied by psychomotor agitation, hallucinations, with the progressive inability of self-care [112]. As stated before, the prodromal phase of the disease is characterized by MCI. Altogether, about 15-20% of people older than 64 years present MCI and, among them, about 15% will furtherly degenerate into AD dementia.

The transition from MCI to overt AD occurs in case of new difficulties in accomplishing instrumental activities of daily living (iADLs), also associated with additional cognitive alteration which cannot be explained by a parallel alteration in patients' health [113].

1.4 ANATOMOPATHOLOGICAL ALTERATIONS

The most characteristic feature of AD is the deposition and accumulation of Aβ plaques outside neurons, together with NFT of protein tau inside neurons, ultimately leading to neuritic plaque and neuronal death with subsequent brain atrophy, gliosis and inflammation due to microglia activation [114,115]. In addition, AD patients usually show signs of α-synuclein deposition, transactive response DNA binding protein 42 kDa (TDP-42) hyperphosphorylation and microinfarcts [116]. Functional loss is mainly localized in the cerebral cortex and specific subcortical areas, such as the hippocampus, involved in memory function [117]. All these brain alterations may start years before the cognitive impairment is noticed and are currently considered AD biomarkers, important to support AD diagnosis, especially when patients show atypical signs, or for differential diagnosis with other dementia-related diseases [118]. The pathologic alterations are reflected by a decrease in CSF $A\beta_{1-42}$ and an increase in p-tau concentration, as a consequence of higher Aβ plaque deposition and NFT density, with subsequent neuronal degeneration [119]. Additionally, amyloid PET scans help in the confirmation of Aβ plaques density, using different tracers such as Pittsburgh Compound B (PiB), Amyvid (18F-Florbetapir), Vizamyl (18F-Flutemetamol) and Neuraceq (18-Florbetaben), currently approved by both FDA and EMA [120]. Additionally, tau and synapse PET scan may be helpful to confirm AD diagnosis, while hippocampal and parietal atrophy can be assessed through magnetic resonance imaging (MRI) and temporoparietal hypometabolism, all typical features of AD, though 18-fluorodeoxyglucose (18-FDG) PET [121]. Other biomarkers, currently used for research purposes include early biomarkers of blood-brain barrier (BBB) damage [122] and vascular dysfunction [123]. Additional blood and CSF markers of synaptic loss and neuronal injury, useful to monitor patient's cognition, have been recently approved by FDA [117].

2. CHOLESTEROL IN CENTRAL NERVOUS SYSTEM

Since its first identification in 1769 in human gallstones, cholesterol involvement in many physiological and pathological processes still represents a matter of extensive investigation. Chemically, unesterified cholesterol ($C_{27}H_{46}O$) is a hydrophobic sterol that is ubiquitously present in all eukaryote organisms, where it acts as a signalling molecule, being involved in the regulation of a plethora of cellular processes, including membrane permeability, fluidity and functionality, gene transcription and protein localization [124,125]. Cholesterol is also involved in the biosynthetic pathway of different steroid hormones and vitamins, such as Vitamin D, and, finally, takes part in the regulation of body development and growth [124]. Focusing on central nervous system, despite the brain's relatively low weight compared to the whole bodily mass (about 2.1%), free cholesterol accounts for about 23% of the whole human pool (approximately equal to 490mg/kg) [126]. The reasons for this disproportion are probably a consequence of the fundamental role that cholesterol plays in CNS. The vast majority of brain cholesterol is indeed localized into oligodendrocytes' myelin sheets, where it acts as a hydrophobic membrane surrounding neurons' axons, thus helping to increase the speed of electrical conduction. Hence, the disruption of this structure occurring in demyelinating diseases such as multiple sclerosis (MS), is associated with an alteration in neurotransmitter transduction [127]. Other than the structural maintenance of myelin sheets, cholesterol plays a great role in the regulation of brain physiology, representing a limiting factor for synaptogenesis, neuronal differentiation and plasticity. *In vitro* studies, indeed, demonstrated that apoE-bound cholesterol is essential for synaptogenesis in purified retinal ganglion cells [128]. Consistently, primary cultures of cortical and hippocampal neurons treated with BDNF, a well-known neurotrophin involved in synapses development and regulation, long-term potentiation and neuronal plasticity, are characterized by a strong increase in cholesterol biosynthesis [129]. As a matter of fact, neuronal pre- and post-synaptic areas are rich in lipid rafts, hence highlighting its fundamental role in neuronal functionality [130]. Notably, lipid rafts are small membrane microdomains extremely rich in cholesterol and other lipid subclasses involved in different fundamental cells' functions such as signal transduction. Lipid rafts alterations have been indeed described in different neurodegenerative diseases, including AD, MS, Parkinson's disease and Huntington's disease [131]. Concerning synaptic function, an *in vitro* study showed that cholesterol is also involved in synaptic vesicles biogenesis and maturation, through the interaction with synaptophysin protein in

neurosecretory PC12 cell line [132]. Moreover, cholesterol is essential for dendrite differentiation, as demonstrated in primary cortical neurons isolated from embryonic rats, in which cholesterol depletion was associated with a reduction in the number of dendrites [133]. Other relevant cholesterol functions in CNS are related to its ability to promote glial cell proliferation, microtubules stability and neurite outgrowth [133]. Neuronal cholesterol depletion is associated with an impairment of essential neuronal functions: as an example, the reduction of cholesterol levels in cultured hippocampal neurons is associated with a reduction in vesicle exocytosis [134]. Again, brain cholesterol depletion occurring in low-density lipoprotein receptor-related protein 1 (LRP1) Knock-out mice leads to an impairment of glutamate receptor subunits NMDAR1 and glutamate receptor 1 (GluR1), with consequent synapses impairment [135].

FIGURE 1

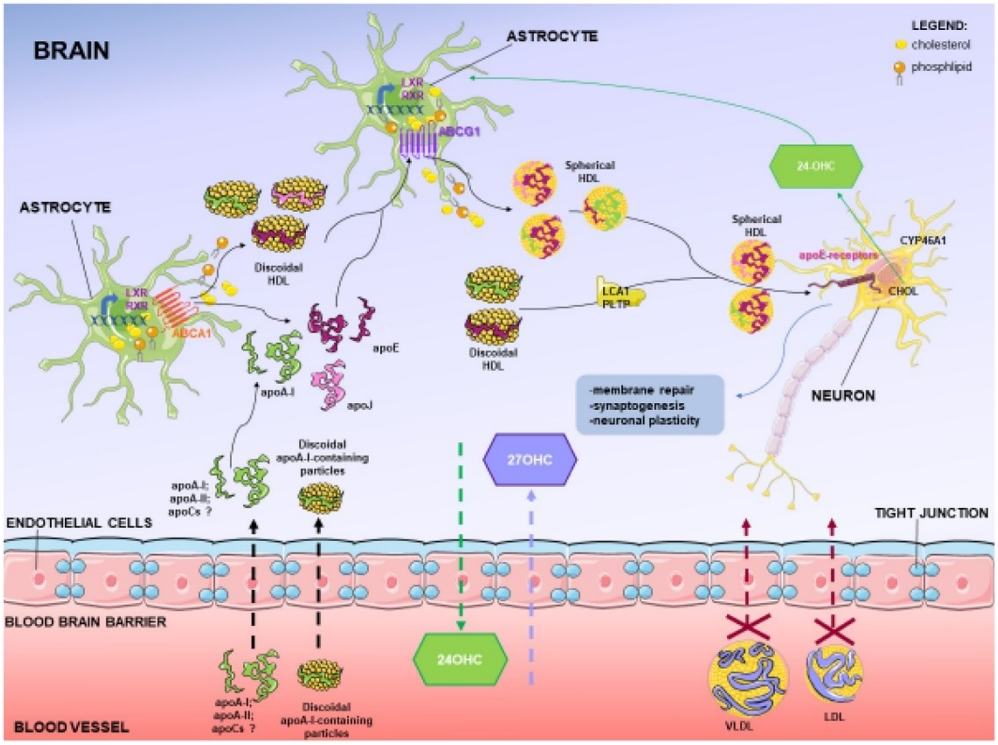

Figure 1. *Schematic representation of brain cholesterol homeostasis in CNS.* Peripheral and cerebral cholesterol pools are separated due to the presence of BBB, that allows only the passage of spherical HDL. In brain, cholesterol is mainly synthesized in astrocytes in a multi-step mevalonate pathway, then secreted in CSF, though an active process, forming discoidal lipoprotein particles containing mainly apoE and finally delivered to neurons. Excess cholesterol is converted into 24-hydroxycholesterol (OHC), that plays a significant regulatory role. 24-OHC is able to cross the BBB to be finally eliminated into the circulation. On the other side, 27-OHC is produced by peripheral tissues but there is a net flux from circulation to the brain, through the BBB. [136]

2.1 CHOLESTEROL HOMEOSTASIS

Cholesterol levels in SNC require a fine regulation; indeed, cholesterol deficiency can compromise correct brain development and function [133], but also cholesterol excess is associated with neurotoxicity. As an example, neuronal cholesterol accumulation is associated with NMDA-mediated excitotoxicity [137] and with an increased Aβ deposition due to the increased activity of γ-secretase [138]. Again, excess cholesterol leads to mitochondria dysfunction, with consequent ROS overproduction and, finally, several experimental evidence point to possible cholesterol- and 25-hydroxycholesterol (25-OHC)-dependent microglia activation, leading to neuroinflammation [139]. For these reasons, cellular cholesterol homeostasis is finely regulated through the concerted activity of different sterol-sensing mechanisms.

Liver X Receptors (LXRs) are transcription factors ubiquitously expressed, belonging to the superfamily of nuclear receptors and, since their discovery in the 1990s, their central role in cholesterol homeostasis, inflammation, immunity and several endocrine-related processes has been proposed [140]. Specifically, two LXRs isoforms have been identified: LXRα and LXRβ, respectively encoded by two distinct genes localized on chromosome 19. The first evidence connecting LXRs to cholesterol metabolism came from LXR-deficient mice, characterized, after cholesterol dietary intake, by the complete inability to induce the expression of CYP7A1 encoding gene, involved in cholesterol conversion into bile acids and subsequent excretion [141]. A series of experimental evidence supported the pivotal cholesterol-sensor activity of LXRs, demonstrating that LXRs are not only CYP7A1 promoters but are also involved in the up-regulation of ATP Binding Cassette (ABC) G5 and ABCG8, involved in cholesterol efflux in bile [142], and in the up-regulation of genes involved in cholesterol efflux, such as ABCA1, ABCG1 and ABCG4 [143,144] and in the reverse cholesterol transport (RCT) from peripheral tissues to liver [145]. In general, nuclear receptors are characterized by a DNA-binding domain (DBD) and, concerning LXRs, their two zinc-finger internal structure is able to recognize and bind to a specific sequence called LXR Responsive Element (LXRE; composed by two AGGTCA cores with four nucleotides) in genes' promotor region [146]. Another important feature is related to the C-terminal domain, able to dimerize with Retinoid X Receptor (RXR) [147]. Different experimental procedures were adopted to identify LXRs endogenous ligands, originally defined as "orphan receptors". Oxysterols, mainly 22(R)-hydroxycholesterol, 24(S),25-epoxycholesterol, 27-hydroxycholesterol (27-OHC) and desmosterol, currently known as

one of the major LXRs ligand [148], were first identified as LXRα ligands following the screening of about 70 molecules, using a high throughput co-transfection assay in CV-1 monkey kidney cells [149]. LXRs are physiologically bound to LXRE, thus recruiting co-repressors molecule that maintains chromatin in a compacted state through the activity of histone deacetylase enzyme. Following the interaction between the ligand and LXRs, a conformational change in its tertiary structure leads to its trans-activation, with the release of co-repressors, with parallel binding of co-activator and consequent epigenetic modifications to chromatin, thus inducing the transcription of target genes [140]. LXRs also possess a well-documented anti-inflammatory activity, as suggested by a strong decrease in pro-inflammatory mediators such as IL-1β, IL-6 NO in human peripheral blood monocytes after exposure to LXR/RXR agonists [150]. Interestingly, it has been proposed a different LXRs' activation mechanism, which involves small ubiquitin-like modifier (SUMO) proteins: in astrocytes, as an example, LXRs SUMOylation seems to inhibit the binding of signal transducer and activator of transcription 1 (STAT1) to specific promoters [151]. This proposed mechanism represents a matter of debate, as an *in vivo* study upon a mouse model of peritonitis suggests a canonical LXRs activation [152]. However, despite the debated mechanism, all this experimental evidence suggest the important connection between lipid homeostasis and neuroinflammation, which deserves further investigation. Indeed, LXRs can regulate brain cholesterol homeostasis through different mechanisms. First, LXR activation is associated with an increased expression of Inducible Degrader of the LDL receptor (IDOL), which promotes the degradation of Low-density lipoprotein receptor (LDLR), very low-density lipoprotein receptor (VLDLR) and apolipoprotein E receptor 2 (ApoER2) through its E3 ubiquitin ligase activity, as demonstrated by both *in vitro* and *in vivo* evidence [153]. Thus, LXRs seem to be involved in the down-regulation of exogenous cholesterol uptake, thus exerting a relevant neuroprotective role against excess cholesterol. Second, the *in vivo* mice treatment with a synthetic LXR agonist, T0-901317, is associated with an increased expression of ABCA1, ABCG1 and apoE, all involved in cholesterol efflux. This observation was also confirmed in Chinese hamster ovary (CHO) cells [154]. As a consequence, the increased cholesterol efflux and apoE secretion from astrocytes induced by LXR activation may enhance cholesterol supply to neurons [155]. Additionally, LXRs may exert a protective role against neuroinflammation: in a mouse model of intracerebral haemorrhage, indeed, the administration of T0-901317 leads to a significant reduction of cognitive deficits, brain oedema, accompanied by a reduction in neuronal death, BBB damage and markers of microglial-mediated inflammation, such as

JNK, MAPK and NF-κB [156]. In addition, in cultured SH-SY5Y neuroblastoma cells, the treatment with exogenous neuroprotective BDNF leads to a reduction in cholesterol uptake, as a consequence of increased LXRs expression, thus highlighting once again the protective role of LXRs in avoiding excess neuronal cholesterol accumulation [157].

Transcription factors Sterol Regulatory Element Binding Proteins (SREBPs) are helix-loop-helix leucine zipper proteins that can be found as $SREBP_{1a}$, $SREBP_{1c}$ and $SREBP_2$, all synthesized in ER membrane, where the C-terminus interacts with the sterol-sensing protein SREBP cleavage-activating protein (SCAP) [158]. Specifically, SREBP2 is synthesized by the *Srebf*2 gene, while $SREBP_{1a}$ and $SREBP_{1c}$ are two different isoforms encoded by the *Srebf1* gene [159] and have been extensively studied in hepatic and adipose tissue metabolism. When the intracellular cholesterol levels are low, SCAP promotes the translocation of SREBPs from the ER to the Golgi apparatus, for their processing through site 1 (S1P) and site 2 (S2P) proteases, releasing the mature SREBPs form, thus able to furtherly translocate to the nucleus and bind to the sterol regulatory elements (SREs) on the promoter sequence of target genes involved in the synthesis of cholesterol, triacylglycerol, phospholipids and fatty acids (FA) [158]. On the other side, in presence of a sustained intracellular cholesterol pool, SCAP/SREBPs are tightly bound to ER membrane, thus preventing SREBPs proteolytic activation [158]. Indeed, cholesterol directly binds to the SCAP sterol-sensing domain, thus changing its conformation and preventing its binding with the COPII proteins; as a consequence, SREBPs are no longer transported into Golgi for their further activation [158]. Insulin-induced gene (Insigs; Insig-1 and Insig-2) are ER proteins able to bind to SCAP and Hydroxy-3-methylglutaryl-CoA (HMGCoA) reductase enzyme in presence of high intracellular cholesterol pools, thus emphasising the SCAP/SREBP and HMCGoA reductase retainment into the ER and inhibiting intracellular cholesterol synthesis [158]. Noteworthy, once activated, SREBP promotes *Insig-1* mRNA transcription, thus acting in its own negative regulation [158]. Several experimental evidence suggests that SREBPs are involved in brain cholesterol homeostasis, also reinforced by the relevant role that cholesterol plays to maintain correct cerebral function, as discussed in paragraph 2. Nevertheless, a pathological alteration in brain cholesterol biosynthesis has been described in different neurodegenerative diseases and, in this regard, recent work demonstrated that the gene therapy providing an intra-striatal injection targeting astrocytes with a recombinant adeno-associated virus 2/5 (AAV2/5) carrying the activated human SREBP2 is associated with an amelioration of synaptic

function and behavioural abilities in mice [160]. The relevance of SREBP-mediated signalling in astrocytes for proper neuronal sustenance is also highlighted by the observation that SCAP deletion in astrocytes resulted in a reduction in cholesterol and phospholipids efflux *in vitro*, accompanied by a reduction of synapses and hippocampal plasticity in SCAP KO mice [161]. Interestingly, the genetic deficiency of $SREBP_{1c}$ in mice is associated with an altered, schizophrenic-like behaviour compared to WT controls [162], probably justified by a differential hippocampal expression of 7 genes [163]. Among those, they identified a decrease in glucagon-like peptide 2 receptors (GLP2R) expression, involved in neurogenesis and neuronal plasticity, and in necdin expression, involved in neuronal survival and differentiation [163]. In addition, the same experimental group also observed poor learning and memory ability in $SREBP_{1c}$-KO mice, together with an impairment in hippocampal dendritic length and complexity, and in dendritic spine density, thus possibly explaining the behavioural abnormalities [164]. Concerning $SREBP_{1a}$, Spell and co-workers identified a SNP, namely G→ΔG, in the 5' untranslated region (UTR) of $SREBP_{1a}$ encoding sequence associated with a lower incidence of AD in apoE ε4 carriers compared to apoE ε4 carriers with the wild-type $SREBP_{1a}$ form, thus acting as a protective factor [165], probably as a consequence of its involvement in cholesterol metabolism, despite the exact mechanisms still need to be clarified. Finally, concerning $SREBP_2$ expression and involvement in CNS homeostasis regulation, it has been confirmed its expression in both primary astrocytes, microglia and hippocampal neurons; moreover, its processing and activation are stimulated after ABCG1 or ABCG1 overexpression, paralleled by a decrease in intracellular cholesterol pool [166].

2.2 CHOLESTEROL BIOSYNTHESIS

Given the relevance of cholesterol in CNS, its pool needs to remain constant, with a tight regulation between cholesterol degradation, excretion and its *de novo* biosynthesis, aiming in supplying new bioactive sterols to astrocytes and neurons plasma membrane. Brain is a conserved district separated from the rest of the body due to the presence of intact BBB, whose endothelial cells, unlike those localized in other bodily capillary beds, don't present fenestrations, trans-endothelial vesicular transport and, on the other side, are characterized by extremely tight cell junctions and electrical resistance [135]. Several studies upon different experimental settings, including sheep, rodents and also humans, investigated whether plasma lipoprotein may cross BBB, thus contributing to brain cholesterol pool, all demonstrating that BBB represents a very selective barrier that

doesn't allow any net exchange of plasma lipoproteins, except for discoidal High-Density Lipoproteins (HDL), and neuronal cholesterol mostly derives from local synthesis [126,167]. At a cellular level, endogenous cholesterol biosynthesis is a complex and energy-intensive process, that takes place in the ER, starting from two Acetyl-Coenzyme A (Acetyl-CoA) molecules condensed into HMG-CoA by HMG-CoA synthase. HMG-CoA reductase then furtherly promotes the conversion of HMG-CoA into mevalonate: this reaction represents the rate-limiting step in cholesterol biosynthesis and the pharmacological target of statins, the main cholesterol-lowering agents currently available [135]. Mevalonate is then converted into 3-isoprenyl pyrophosphate, farnesyl pyrophosphate, squalene, lanosterol in 19-step condensation and oxidation reactions, finally leading to cholesterol formation [135]. Brain cholesterol biosynthesis is an essential process taking place since the early phases of development and, as a demonstration of its relevance, the brain homozygous deletion of SCAP in mice, leading to a reduction in cholesterol biosynthesis, is associated with microcephaly, gliosis and postnatal mortality, while its heterozygous deletion is associated with a significant reduction in synaptic activity and cognitive alteration [168]. However, the vast majority of newly-synthesized cholesterol is produced by oligodendrocytes during the myelination process, which takes place between the perinatal period and adolescence. The exact molecular mechanisms triggering the strong increase in brain cholesterol biosynthesis during this developmental phase are still poorly understood. Studies aiming at evaluating cholesterol biosynthesis *in vivo* demonstrated that in the first three weeks after birth, brain cholesterol concentration in mice greatly increases, ranging from 4 mg/g at birth to 12-13 mg/g, with about 250 μg of newly synthesised cholesterol per day [169]. After this period, cholesterol biosynthesis strongly decreases, with only 25-35 μg per day [169]. Moreover, different evidence suggests that endogenous cholesterol biosynthesis rate strongly depends on the specific brain area and correlates with the specific ultimate cholesterol concentration; as an example, the cerebrum is composed of 12 mg of cholesterol /g of tissue, the cerebellum of 14 mg/g, brainstem of 30 mg/g, mid-brain of 23 mg/g and the spinal cord of 38 mg/g. This experimental evidence suggests that cholesterol biosynthesis in the brain occurs locally to meet the requirements of the specific brain area [169]. Interestingly, it has been proposed that the daily renewal rate of cholesterol in adult neurons accounts for about 20% [167], suggesting that active cholesterol biosynthesis in CNS is still required also during adulthood. Despite this need, it has been demonstrated that in primary adult rat neurons the endogenous cholesterol synthesis is not sufficient and only restricted to neuronal

somata, as well as their ability to up-regulate the synthetic pathway is extremely lower compared to primary rat astrocytes, suggesting that adult neurons may strongly rely on these latter cellular types for their cholesterol need [170]. While the enzymatic reactions leading to endogenous cholesterol biosynthesis are common in all tissues, two different, interlinked and parallel processes have been proposed, namely the Kandutsch-Russell (K-R) and the Bloch pathways. In this regard, Nieweg and co-workers described a specific pattern of post-squalene precursors in primary astrocytes and neurons, highlighting higher precursors of Bloch pathway, such as desmosterol, in astrocytes, and an increase of lanosterol, 7-dehydrocholesterol and lathosterol in neurons, suggesting that K-R pathway may be prevalent in these cells [170]. Currently, the relevance of the specific precursors in the cholesterol biosynthetic pathway isn't fully clarified; however, some experimental indications suggest that the higher presence of desmosterol in astrocytes may promote cholesterol efflux to extracellular acceptors such as apoE, due to its ability to activate LXRs [171]. On the other side, specific neuronal cholesterol precursors such as lathosterol and 7-dehydrocholesterol may be involved in the stability of lipid rafts, thus contributing to synaptic activity [172]. Moreover, adult neurons are characterized by an extremely low activity of lathosterol-metabolising enzymes such as 24-dehydrocholesterol reductase (Dhcr24), and cytochrome P450 family 51 (Cyp51), involved in cholesterol synthesis down-regulation. These two enzymes probably undergo a transcriptional regulation process during neuronal differentiation: at this regard, an *in vitro* study demonstrated a strong reduction in Dhcr24 expression in human mesenchymal cells furtherly differentiated into adult neurons [173]. In this context, a recent study performed on primary cortical neurons and astrocytes isolated from dissected brain tissue of day 18 embryonic mice helped in clarify some element not yet fully known. By measuring several cholesterol biosynthesis intermediates during neuronal development trough Liquid chromatography–tandem mass spectrometry (LC-MS/MS), it was demonstrated that while neurons tend to accumulate newly synthesized cholesterol, astrocytes are more prone to secrete it. Moreover, they demonstrated that developing neurons preferentially synthesize cholesterol trough Bloch pathway and only during adulthood they switch to K-R pathway, as demonstrated by the high intracellular concentration of desmosterol compared to adult neurons [174].

2.3 CHOLESTEROL TRANSPORT

Central nervous system is divided by peripheral organs due to the presence of a competent barrier system, composed of BBB and blood-CSF barrier (BCSFB). Supporting the relevant separation between central and peripheric districts, an old, seminal study demonstrated that subjects that underwent liver transplantation expressed the donor's peripheric apoE isoform while maintaining their isoform in CNS [175]. Specifically, BBB is composed of endothelial cells within brain microvessels, organized in a sealed and organized cell-cell interaction with tight-junctions with occludins and claudins proteins, resulting in low transcellular and paracellular permeability and high electrical resistance [176]. Together with endothelial cells, also pericytes and astrocytes participate in BBB selective permeability, thus tightly regulating the passage of almost all the circulating molecules, except for those with high lipophilic properties or those having endothelial receptors or carriers that facilitate their CNS entrance [176]. In addition to BBB, BCSFB, localized in brain ventricles and specifically in choroid plexus (CP) where CSF is produced, is an anatomical district characterized by a high vascularized stroma and connective tissue within epithelial and endothelial convolutes [177]. Specifically, the stroma is composed of capillaries with fenestration of 60-80 nm diameter, and its ventricular side presents a monolayer of cuboidal epithelial cells and specific cells with high phagocytic activity [177]. BCSFB is generally more permeable compared to BBB, due to the presence of less tight junctions between epithelial cells and due to the presence of a differential expression of transporters [178]. In this regard, some experimental evidence suggests a low rate exchange of small HDL and some of their components [179], which will be furtherly discussed in the next sections. As an example, apolipoproteinA-I (apoA-I) bound to small and lipid poor HDL has been shown to be able to cross BBB in an *in vitro* experimental model [180]. Concerning lipid transport through BCSFB, the available studies are currently limited. ApoA-I and apoA-II are present in CSF [181], despite not being produced by brain cells; consequently, BCSFB may be permeable to their passage. In this regard, it has been demonstrated that the *in vivo* injection of recombinant fluorescent human apoA-I in mice localizes in the CP [182]. CSF is a colourless fluid mainly produced by CP (about 50% of the total production), while the remaining part originates from the ventricular ependymal-derived interstitial fluid, with an average daily production of 600 ml [177]. CSF production follows the stimulation of the autonomic nervous system and mainly depends on Na^+, K^+, Cl^-, $HCO3^-$ and H_2O aquaporin transporters creating an osmotic gradient that drives

water secretion [183]. CSF exerts several protective structural, hydrodynamic, immunologic and metabolic functions [184]. CSF, indeed, prevents collisions between brain and skull, maintains the correct electrolytic environment in CNS, supplies nutrients to glial cells and neurons, transports hormones, neurotrophic factors and neurotransmitters and, finally, removes catabolites and neurotoxic waste products through its convective exchange with interstitial fluid [184]. Specifically, as peripheral and brain cholesterol pools are almost completely separated districts [185], and due to the poor ability of neurons to provide to their own cellular cholesterol need [170], brain cholesterol transport represents a fundamental aspect in brain homeostasis and relies on the cooperation of specific molecules, transporters and receptors (**Figure 2**). Briefly, cholesterol synthesized from astrocytes is complexed with astrocyte-secreted apoE, thus originating apoE-containing lipoparticles, through the interaction with ABCA1, ABCG1 and ABCG4 transporters and remodelling enzymes [186]. Those particles interact with LDLR, LRP1, VLDLR and apoER2 on neuronal surface [187], thus supplying their cholesterol need.

FIGURE 2

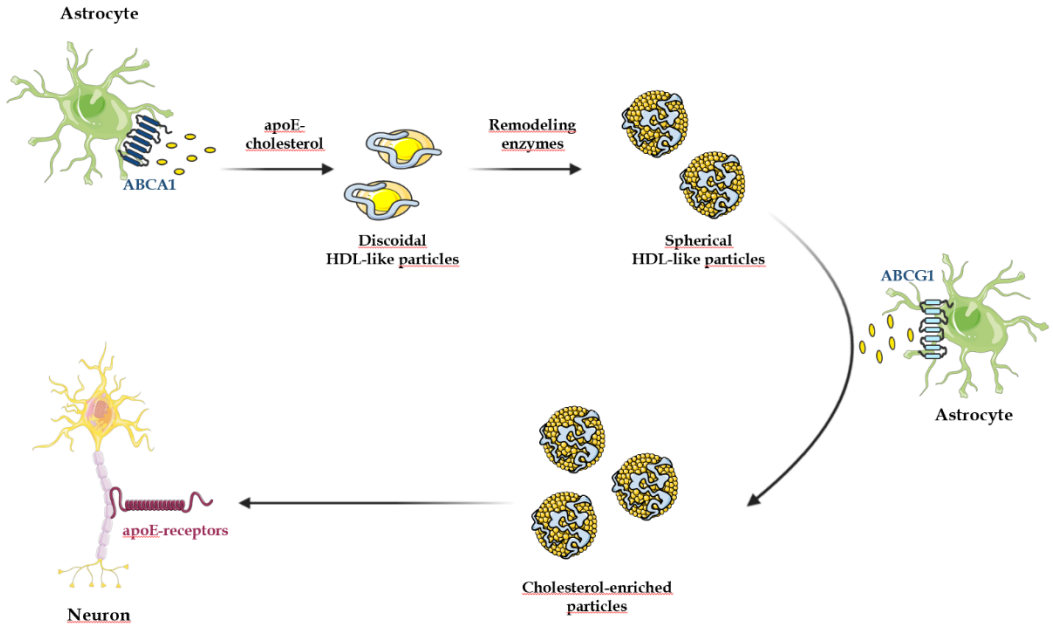

Figure 2. *Schematic representation of brain cholesterol transport.* *Pictures have been created by combining images from Smart Servier Medical Art (https://smart.servier.com/). Servier Medical Art by Servier is licensed under a Creative Commons Attribution 3.0 Unported License (https://creativecommons.org/licenses/by/3.0/).*

2.3.1. Lipoproteins

The vast majority of the experimental investigations aimed at characterizing brain lipoproteins have been conducted so far on CSF, due to its relatively easy accessibility. CSF lipoproteins have been defined as "HDL-like particles", due to their resemblance to plasma HDL for composition and size and, generally, their concentration in CSF is about 1-10% compared to plasma lipoproteins [185]. In this regard, Koch and co-workers isolated human CSF lipoproteins through affinity chromatography and observed that the main CSF lipoprotein fraction was composed of 12-20nm spherical particles bearing mainly apoE, but also apoA-I, apoA-IV, apoD, apoH and apoJ [185]. The other classes of CSF lipoprotein are far less numerous and consists of 13-18nm lipoparticles that present apoA-I and apoA-II, larger particles (18-22nm) characterized by apoA-I, apoA-IV, apoD, apoJ and finally small particles (10-12nm) with a low lipidic content, bearing apoA-IV, apoD, apoH and apoJ [185]. In addition, small peripheric HDLs may enter CNS through scavenger receptor class B type I (SR-BI). SR-BI is involved in hepatic HDL-cholesterol uptake, but it has also been found expressed in brain capillary endothelial cells, where it mediates the selective uptake of HDL [188]. Indeed, Fung and co-workers labelled HDL with a fluorescent dye, and, using high-resolution fluorescence microscopy on human cerebral cortex microvascular endothelial cells, observed that HDLs were internalized independently of caveolin, clathrin and scaffold protein Na/Pi Cotransporter C-Terminal-Associated Protein 1 (PDZK1), thus proposing transcytosis as a possible mechanism of HDL internalization through BBB [188]. The mechanism that regulates the formation of brain nascent lipoprotein is not fully understood. Astrocytes are the main cell type involved in CSF and brain tissue lipoproteins synthesis and, in this regard, an *in vitro* study on cultured astrocytes lacking in turn apoE or apoJ, demonstrated their ability to secrete nascent discoidal lipoproteins with phospholipids, cholesterol, apoE and apoJ, with apoE representing the main actor in the normal secretion of these lipoproteins [189]. However, in analogy with plasma HDL, nascent discoidal HDL undergo different remodeling processes, leading to the mature sperical lipoproteins isolated in CSF, despite the regulatory mechanisms are not fully clarified. Lecithin:cholesterol acyltransferase (LCAT) is a enzyme responsible for free cholesterol esterification, which is mainly sinthesized in liver. Interestingly, LCAT expression has also been found in astrocytes, where is responsible for the esterification of free cholesterol in nascent discoidal apoE-containing lipoproteins and consequently of lipoprotein maturation to larger and spherical particles [185,190]. As proof of that, *in vivo* LCAT deficiency in mice is associated with an increase in

apoE-HDL and a decrease in apoA-I-HDL in CSF [190]. CSF LCAT concentrations have been estimated to be about 5% compared to those of plasma and, since the major LCAT plasma activator is apoA-I, it has been proposed that in CNS apoE-containing lipoproteins may be the main LCAT substrates [190]. In plasma, also the Cholesteryl ester transfer protein (CETP) and phospholipid transfer protein (PLTP) play an important role in HDL remodelling and maturation. Albers and co-workers identified for the first time CETP expression also in human CSF (12% compared to plasma concentration) and in the conditioned media from human neuroblastoma and neuroglioma cells, thus suggesting that the synthesis of CETP occurs directly in the brain, where it seems to be involved in lipid-lipoprotein transfer, despite many aspects of its physiological role still need to be fully clarified [191].

2.3.2. Apolipoproteins

Apolipoproteins represent the lipoproteins' proteic constituent, able to regulate their metabolism and, concerning CNS, about 10 apolipoproteins have been identified, either directly synthesised *in situ*, like apoE, or diffused from periphery to brain across BBB, like apoA-I [192]. The most relevant apolipoproteins in CNS will be discussed in the following section.

ApoA-I is a 28.1 KDa protein composed of 243 amino acids and it represents the main lipoprotein in plasmatic HDL, determinant for HDL structure and function. ApoA-I is involved in reverse cholesterol transport through its interaction with ABCA1 transporter and thus promoting cholesterol efflux from macrophages [193]. Despite this well-known role in peripheric HDL metabolism, several experimental evidence suggests that plasmatic apoA-I crosses BBB through cholesterol-mediated endocytosis [194], where it may be involved in several cerebral protective effects.

ApoE is a 34 KDa glycoprotein mainly synthesized in the periphery by the liver, while, due to its inability to cross BBB, in CNS is directly produced *in situ*. ApoE is the major proteic component of HDL-like particles, despite its CSF concentration is much lower compared to plasma concentration. As also described in paragraph 1.4.3, apoE encoding gene may be present as a combination of three possible isoforms, apoE ε2, apoE ε3 and apoE ε4, characterized by different amino acid substitutions altering protein structure and functionality [195]. ApoE ε3 is the most common isoform, apoE ε2 seems to exert a protective effect on AD risk, while apoE ε4 is currently the strongest known risk factor for LOAD [195].

ApoJ, or clusterin, is a glycoprotein expressed in different tissues, including brain, where is mainly produced by astrocytes [195]. ApoJ is involved in the modulation of different physiological functions, such as apoptosis, complement inhibition and also lipid transport [195]. Concerning CNS, apoJ-bound lipoproteins are able to bind to Aβ clearance and promote its removal through the interaction with LRP2 in BBB [195].

2.3.3. Transporters

ABC transporters are ubiquitously expressed in cells and use ATP to generate energy to facilitate the transport of a series of substrates, including lipids, such as sterols and phospholipids, across biological membranes against their gradient of concentration [196]. Mammalian ABC transporters are generally composed of two trans-membrane domains with two nucleotide-binding domains and are divided into seven subfamilies, classified as A – G [196]. Given the relevance of lipids in brain, ABC transporters are likely to play an important role in lipid homeostasis maintenance; the most relevant will be discussed in the next section.

ABCA1 transporter expression is regulated by LXRs and RXRs and in periphery involved in the regulation of cholesterol efflux to lipid-free apoA-I and apoE, thus greatly contributing to the formation of nascent HDL and RCT, the most relevant anti-atherogenic process [197]. ABCA1 was first identified in 1998 in subjects with Tangier Disease, characterized by very low HDL levels due to alterations in ABCA1 encoding sequence and thus to impaired functionality [197]. In brain, ABCA1 is expressed by several cell types, including glial cells astrocytes, pericytes and brain capillary endothelial cells, where it transfers cholesterol to apoE, and in a lesser extent to apoA-I, that act as extracellular acceptors, thus contributing to the formation of discoidal apoE-containing HDLs and maintaining cholesterol supplying from astrocytes to neurons [197]. The relevance of ABCA1 in brain homeostasis is also highlighted by the evidence that mice lacking ABCA1 are characterized by a strong decrease in brain apoE, together with a reduction in dendritic density and cognitive function [198].

ABCG1 is expressed in a variety of cells, among which macrophages, and its synthesis is regulated by LXRs/RXRs agonists and is one of the key transporter involved in the regulation of cholesterol efflux to mature HDLs [196]. Different studies confirmed a strong ABCG1 expression in brain tissue, mainly localized in hippocampal neurons, in cortical areas as well as in the thalamus and nucleus striatum [196]. In addition, ABCG1 is also

expressed in microglial cells, including oligodendrocytes and astrocytes, and in the choroid plexus, where its synthesis is strongly induced by the presence of 24(S)-hydroxycholesterol (24-OHC) [196,199]. In CNS, ABCG1 preferentially promotes cholesterol efflux to lipid-enriched apoE-containing lipoproteins [200] and, interestingly, ABCG1 levels correlate with cholesterol efflux from cerebellar primary murine glial cells [201]. ABCG1 $^{-/-}$ mice were characterized by normal cerebral sterol levels, accompanied, however, by an increase of cholesterol biosynthetic intermediates such as desmosterol, lanosterol and lathosterol, together with a reduction in cholesterol efflux with consequent accumulation in astrocytes [171]. These observations suggest a direct involvement of ABCG1 in cholesterol biosynthesis, possibly involving $SREBP_2$ activation [166].

ABCG4, despite its similarity with ABCG1 (74% of identity in the amino acid composition), is exclusively found in brain tissue and in the neural retina, where it promotes cholesterol efflux to mature HDL, alone or directly bound to ABCG1, forming heterodimers [196]. Interestingly, ABCG4 expression is directly under the transcriptional control of LXRs only in astrocytes cells, but not in neurons and endothelial cells localized in BBB [202]. However, similarly to ABCG1, ABCG4 in murine neurons and astrocytes promotes $SREBP_2$ expression, thus inducing endogenous cholesterol biosynthesis [166]. Interestingly, intermediates products in cholesterol biosynthetic pathway such as desmosterol and lathosterol furtherly stabilize ABCG4 protein [202]. Bojanic and co-workers investigated the role of ABCG4 during CNS development, highlighting that its expression strongly increases in mice starting from the gestational age of 12.5 days and its deletion is associated with cholesterol and oxysterols accumulation in cerebral cells and retina, together with an alteration in LXRs and $SREBP_2$ target genes, resulting in memory impairment in adult mice [203].

2.3.4. Receptors

LDLR family comprises 7 extremely conserved membrane proteins: LDLR, VLDLR, apoER2, LRP1, LRP1B, megalin/LRP2, sortilin-related receptor (SorLA), LRP5 and LRP6, all expressed both during neurogenesis and in adult brain [204]. Structurally, LDLRs are all characterized by a ligand-binding domain, a transmembrane domain, one or more epidermal growth factor (EGF) domains and a cytoplasmic portion with one or more NPxY motifs, responsible for their endocytotic activity and signal transduction [204]. However, they differ in their physiological role, probably as a consequence of their

different ligand affinity, endocytosis rate and signalling pathway, as well as for their cellular and tissue expression. In brain, one of the main LDLR family ligands is apoE, which, as stated in the previous paragraphs, is the major protein constituent of cerebral lipoproteins, thus mediating the internalization of astrocyte-derived cholesterol into neurons. Hence, the interaction of apoE and LDLRs is fundamental. At this regard, as demonstrated in rat neuronal cultures, apoE-containing lipoproteins are necessary for the formation of neuronal synapses [128]. Consistently, mice lacking apoER2 and VLDLR showed alterations in neuroanatomical phenotype, with cerebral ataxia and disruption in the correct layering of cortical and hippocampal neurons, with consequent alterations in their behavioural characteristics [205]. Another fundamental LDLRs ligand is reelin, a secreted glycoprotein that, once bound, promotes an intracellular signalling cascade with the final phosphorylation of disabled-1 (Dab1) protein and Src family kinases, extensively contributing to correct brain development [206]. Hence, the neuroanatomical and behavioural alterations observed *in vivo* in mice lacking apoER2 and VLDLR previously described [205] may result as a combination of the altered reelin signalling and deficient cholesterol supply to neurons.

LDLR is a 160KDa receptor synthesized in ER as a precursor protein, that undergoes maturation in the Golgi apparatus and final translocation onto the cell membrane. Peripheric LDLR expression is ubiquitary, with a high hepatic expression rate and, from a functional point of view, LDLR binds to apoB- and apoE-containing lipoproteins such as LDLs. After LDLR binds to its ligand, it undergoes internalization through endocytosis and separates from its ligand in a pH-dependent process, and recycles to the cell surface, while apoB- and apoE-containing lipoproteins undergo further intracellular metabolization [207]. As follows, different mutations on LDLR encoding gene affecting receptor functionality, either in heterozygosis or homozygosis, often results in familial hypercholesterolemia (FH), an autosomal dominant disease characterized by extremely high LDL-cholesterol levels and high cardiovascular risk [207]. Concerning CNS, due to the presence of BBB that prevents apoB passage from the periphery, LDLR interacts almost exclusively with apoE-containing lipoproteins, thus mediating their cellular internalization [207]. Consistently, mice lacking LDLR are characterized by a strong increase of apoE in CSF and brain tissue, in absence of a significant increase in brain cholesterol levels [208]. LDLR expression is controlled by several transcriptional and post-

transcriptional mechanisms, such as SREBPs and Proprotein Convertase Subtilisin/Kexin type 9 (PCSK9), whose regulating activity will be discussed in paragraph 2.5 [207].

ApoER2 is a 105KDa membrane protein with a 49% of homology with LDLR in its encoding sequence. In peripheral tissues, apoER2 is expressed by ovaries, testis, placenta and platelets, despite its main expression being localized in CNS, specifically in the apical dendrites and cell bodies of the neocortex, in Purkinje cells of the cerebellum, in pyramidal cells of the hippocampus and dentate gyrus, in Schwann cells and radial glial and intermediate progenitor cells (IPCs) [209]. The most relevant function of apoER2 is related to its involvement in the reelin pathway, as mentioned before, thus playing a crucial role in neuronal migration in the cortical area [206]. ApoER2 expression is finely regulated by IDOL, an E3 ubiquitin ligase that promotes its ubiquitination and further lysosomal degradation. In this regard, IDOL overexpression in mice leads to lower apoER2 levels, with consequent impairment in dendritic spine formation, also reflected in defective learning and memory function [210]. In addition, apoER2 expression can be also be post-translationally regulated by PCSK9 [209].

VLDLR is a 161 KDa protein, whose structure is extremely similar to that of LDLR, expressed at high levels in skeletal muscles, heart, adipose tissue, kidney, testis, ovary and lungs [209]. In CNS VLDLR expression has been detected in almost all cerebral regions, with high prevalence in Cajal-Retzius cells, astrocytes, oligodendrocytes and neurons of cerebellum and cortex [209]. VLDLR is localized onto the cell membrane, not associated with lipid rafts [209]. Similarly to apoER2, VLDLR is also involved in the reelin signalling pathway, extremely relevant during neurogenesis [206]. Due to VLDLR ability to bind to apoE, it was initially believed to play a role in lipoprotein homeostasis; however, its absence in pre-clinical experimental models isn't associated with alterations in plasmatic lipoprotein profile, probably because its peripheral function is also exerted by LDLR [211]. Similarly to the above-cited receptors, also VLDLR is a specific target for PCSK9 degrading activity, thus regulating VLDLR expression [209].

LRP1 is a 515 KDa transmembrane protein containing four extracellular ligand-binding domains, together with an extra intracellular YXXL motif near the canonical NPXY sequence, that enables a more rapid endocytotic process [212]. After its translation, LRP1 binds to the molecular chaperone receptor-associated protein (RAP), which enables LRP1 membrane translocation and prevents its premature binding with other molecules; RAP

dissociated from LRP1 only in the late secretory phases, characterized by lower pH [212]. LRP1 is expressed by lungs, liver, gallbladder, vascular system, ovary, testis and connective and soft tissues, while in brain is highly expressed in the cortical tissue and BBB [212]. Interestingly, while in pre-clinical models the absence of LDLR isn't associated with an embryonic lethal phenotype, LRP1 deficiency causes early embryonic lethality in mice [212]. Concerning LRP1 ligands, experimental evidence identified more than 40 molecules, including apoE, α2-macroglobulin and also Aβ, thus suggesting a possible involvement of this receptor in amyloidogenic metabolism [213], which will be furtherly addressed in paragraph 3.3.4. Supporting the ability of LRP1 to bind to apoE, mice lacking LRP1 specifically in the forebrain neurons showed high cerebral apoE levels, while LRP1 overexpression decreases them [214]. Interestingly, LRP1 can be processed and cleaved by secretases, thus producing an intracellular LRP1 segment that seems to act as a transcriptional regulator, able to affect the expression of different genes, such as interferon (IFN)-γ, while its extracellular portion is involved in Aβ metabolization [212]. Similarly to the other LDLRs discussed in the present section, also LRP1 is a target of the degrading activity of PCSK9, hence able to post-translationally regulate its expression [209].

2.4 OXYSTEROLS

Oxidized cholesterol metabolites, namely oxysterols, are bioactive molecules produced by several enzymes able to oxidize cholesterol molecules in its side carbon back-bone chain with higher polar properties compared to cholesterol [215]. Due to their physio-chemical properties, oxysterols fluxes can bypass different bodily membranes, such as BBB [215]. In this regard, the most relevant oxysterols in CNS are 24-OHC, also called cerebrosterol, and 27-OHC, followed by 25-OHC and, interestingly, their levels in plasma and CSF have been extensively used as biomarkers for different neurological and vascular pathologic conditions [215]. Indeed, a specific cerebral enzyme, cholesterol 24-hydroxlase (CYP46A1), particularly expressed in neurons, is able to convert excess cholesterol into 24-OHC, that can furtherly cross BBB through gradient-mediated diffusion and reach peripheric circulation, with a rate of about 4-7 mg every day, to be finally cleared by the liver [216]. As follows, plasmatic 24-OHC levels are almost completely derived from the cerebral metabolism and directly reflect brain cholesterol levels [216]. Cerebral cholesterol, in addition, can also be transformed to 27-OHC by 27-hydroxylase (CYP27A1) and finally converted by oxysterol 7-alpha-hydroxylase (CYP7B1) to 7α-hydroxy-3-oxo-4-cholestenoic acid (7-OH-4-C), even if the cerebral expression of those

enzymes is extremely low [216]. On the other side, 27-OHC is produced in peripheric tissues following cholesterol's metabolization by CYP27A1 enzyme, and about 5 mg per day flow to the brain [217]. Due to their ability to modulate different transcriptional pathways, oxysterols are considered bioactive molecules: as an example, they induce LXRs activation, inhibit SREBPs processing to its active form, and are allosteric modulators of NMDA receptors and G protein-coupled receptors (GPCRs) [215]. Concerning cerebral cholesterol metabolism, as SREBPs inhibitor, 24-OHC acts as a physiological suppressor in cholesterol biosynthesis, as demonstrated in glioblastoma cell line [218]. In addition, by promoting LXRs activation, 24-OHC induces ABCA1, ABCG1 and apoE synthesis in astrocytoma cells [155], thus promoting astrocyte to neuron cholesterol transport. Similar observations also came from proteomic analysis in rat primary cortical neurons [219]. On the other side, 27-OHC function in CNS has not been completely clarified, also due to its levels that in physiological conditions are extremely low. Several experimental evidence obtained in cellular models point to a direct involvement of 27-OHC in cholesterol biosynthesis down-regulation [220], also confirmed by a murine model lacking CYP27A1 expression, characterized by a significant cerebral cholesterol biosynthesis increase [221]. Finally, other than 24-OHC and 27-OHC, also 25-OHC, a peripheral potent regulator of LXRs mediated pathway, is detectable in the brain, despite to date only a few data investigated its function in CNS. Notably, Makoukji and co-workers demonstrated that 25-OHC promotes oligodendrocytes apoptosis and down-regulate myelin production through the LXR/Wnt/β-catenin signalling [222].

2.5 PROPROTEIN CONVERTASE SUBTILISIN/KEXIN TYPE 9

PCSK9 is a 692 amino acid protein encoded by a 22 Kb gene located on chromosome 1p32, composed of 12 exons and 11 introns with a high evolutionary conserved sequence in vertebrates [223]. PCSK9 goes through a non-classical zymogen activation process; indeed, in ER PCSK9 undergoes cleavage of its signal fragment (amino acid 1-30), leading to the release of proPCSK9 zymogen protein (amino acid 31-692), that undergoes further cleavage in $VFAQ_{152}\downarrow SIP$ position, finally releasing the mature enzyme (amino acid 152-692) [223]. Interestingly, PCSK9 is secreted as non-covalently bound to its inhibitory prosegment (amino acid 32-152) that covers the active site of the enzyme, so that PCSK9 exerts its enzymatic activity only following the binding with its targets proteins [223]. Specifically, the active PCSK9's site is located in amino acid 153-421, with Asp_{186}, His_{226}, and Ser_{386} amino acids and the oxyanion hole Asn_{317}; in addition, the

catalytic subunit is linked to the C-terminal region (CHRD), rich in cysteine, through a small hinge region (H), composed by 18 amino acids (from 422 to 439) [223]. Concerning PCSK9 enzymatic activity, as anticipated above, the prosegment-PCSK9 complex can bind to target proteins and convey to specific intracellular organelles, such as lysosomes, to their final degradation [223]. The first identified and most characterized PCSK9 target is LDLR, as PCSK9's catalytic unit binds to its EGF)-A domain [224]. In addition, other LDLR family members, such as VLDLR, apoER2 and LRP1, possess a similar EGF-A domain, that has been demonstrated to be a PCSK9 target as well [224]. Finally, CD36 is another PCSK9 target, despite the absence of the EGF-A domain, suggesting that PCSK9 may act through different binding mechanisms, that still require further investigation [225]. In absence of PCSK9, once LDL-C binds to LDLR, the complex is endocytosed through clathrin-coated vesicles, forming endosome with acid pH, that promotes the allosteric dissociation of LDLR and its subsequent surface recycling for another binding-internalization cycle, while LDL-C is furtherly processed in lysosomes (**Figure 3**) [226]. However, when PCSK9 binds to its target, such as LDLR, the low pH of endosome causes a more tight association between LDLR and LDL-C, thus preventing LDLR recycling into the cell membrane and promoting LDLR - LDL-C complex degradation in lysosome, also with the participation of cyclase-associated protein-1 (CAP-1), despite the exact mechanisms are still not completely characterized [223].

FIGURE 3

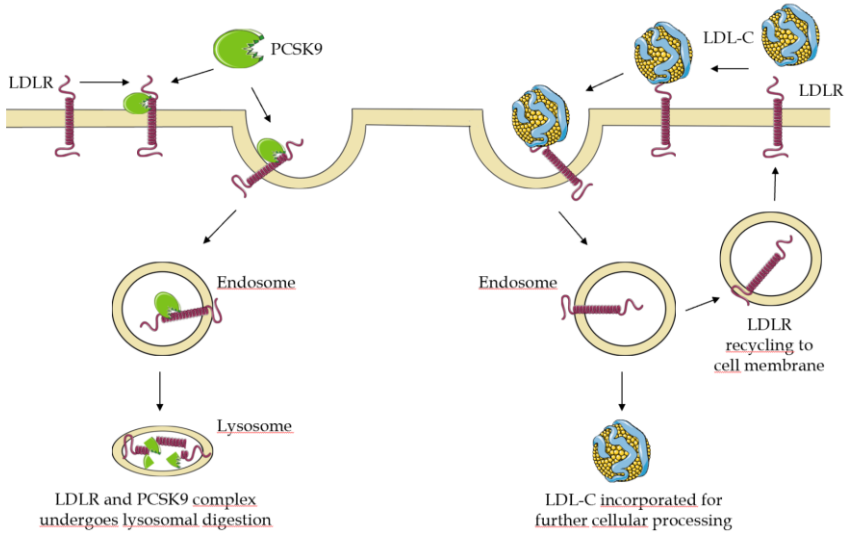

***Figure 3**. Schematic representation of PCSK9 mechanism of action. Pictures have been created by combining images from Smart Servier Medical Art (https://smart.servier.com/). Servier Medical Art by Servier is licensed under a Creative Commons Attribution 3.0 Unported License (https://creativecommons.org/licenses/by/3.0/).*

Furthermore, PCSK9 may exert its biological activity both intracellularly, thus binding LDLR without being secreted, or extracellularly, after its secretion [227]. Interestingly, the absence of the M2 domain in CHRD portion of PCSK9 enables exclusively the intracellular degrading activity, suggesting that two distinct regulatory pathways control PCSK9 intracellular and extracellular functionality [228]. PCSK9 expression is finely regulated through different mechanisms, starting from its transcription. Indeed, mice overexpressing $SREBP_{1a}$ or $SREBP_2$ showed increased PCSK9 mRNA levels [229] and, consistently, statins treatment in human hepatocytes HepG2 cells leads to an upregulation of PCSK9 mRNA levels, as a consequence of the feedback activation of $SREBP_2$ [230]. PCSK9 transcription may be also controlled by ligand-activated nuclear receptors such as peroxisome proliferator-activated receptors (PPARs) and Farnesoid X receptor. In this regard, PPARα agonist fenofibrate, a pharmacological agent used in hypercholesterolemia and hypertriglyceridemia, reduces PCSK9 transcription in primary murine hepatocytes and human HepG2 cells, despite studies in fenofibrate-treated patients showing some confounding evidence [231]. In addition, also the regulation of PCSK9 mRNA stability and final translation contributes to the final PCSK9 activity, despite, to date, the molecular mechanisms of these possible regulatory mechanisms are still unclear, except for the potential binding of microRNA-24 to the 3'-Untranslated Region (UTR) of PCSK9 mRNA, thus possibly interfering with mRNA stability [232].

2.5.1 PCSK9 and plasma cholesterol homeostasis

Since its discovery in 2003 in apoptotic brain cells, PCSK9, initially indeed called neural apoptosis-regulated convertase-1 (NARC-1), was deeply studied to investigate its biological functions. One of the first pieces of evidence related to PCSK9 role in regulating plasmatic cholesterol levels comes from the description of a mutation in the PCSK9 sequence found in families with autosomal dominant FH, in absence of any LDLR and apoB mutations [233]. In addition, the Dallas Heart Study revealed that two nonsense mutations in the PCSK9 encoding sequence (p.Y1422X and p.C679X) retrieved in a multiethnic population composed for its half of Afro-Americans, were associated with extremely low LDL-C levels (-40%) and reduced coronary artery disease (CAD) risk [234]. Since these observations, it has been clearly demonstrated that PCSK9 may be considered one of the main factors regulating plasma cholesterol homeostasis, mainly due to its ability to bind to mainly hepatic LDLR and promote its degradation in lysosome, as described in the previous section, thus preventing LDLR recycling to the cell surface and

the LDLR-mediated removal of circulating LDL-C [233]. Currently, about 250 mutations in the PCSK9 encoding sequence have been identified, distributed in its catalytic domain, in the signal peptide, prodomain and CHRD and can be categorized as Gain of Functions (GOF) and Loss of Function (LOF) mutations, with opposing phenotypes [233]. Subjects with PCSK9 GOF mutations, such as the substitution of amino acid Asp with Tyr (D374Y) are characterized by high LDL-c levels (>500mg/ml) and Lipoprotein(a), thus raising their cardiovascular risk [235]. Conversely, subjects with LOF mutations such as S386A, R46L and S462P, are relatively common, and characterized by extremely high hepatic LDLR and low circulating LDL-C, with an average reduction of 50-86% of their cardiovascular risk [236]. Other than PCSK9 ability to regulate lipoproteins' circulating levels, experimental evidence both *in vitro* and *in vivo* suggest a pro-inflammatory activity by increasing pro-inflammatory cytokines and chemokines, such as IL-1β, IL-6, TNF-α and monocyte chemoattranct protein (MCP)-1 release in macrophages [237]. The relevant role of PCSK9 in atherosclerosis was also confirmed in C57bl/6 mice injected with pAAV/D355Y-mPCSK9, a GOF mutant murine PCSK9 plasmid, resulting in a downregulation of LDLR expression (-90%) and hypercholesterolemia associated with atherosclerosis development [238]. Hence, given the relevant role of PCSK9 in circulating LDL-C and in atherosclerotic plaque burden, and also considering the limited effectiveness of other lipid-lowering drugs such as statins, different pharmacological approaches were developed to inhibit circulating PCSK9. So far, two fully human mAbs, able to prevent the binding of PCSK9 and EGF-A domain of LDLR, were developed: evolocumab (Praluent®) and alirocumab (Repatha®), that are currently approved by FDA, EMA and AIFA for the treatment of hypercholesterolemic subjects with high CV risk, in addition to standard therapies such as statins and ezetimibe [233]. Different Randomized Controlled Trials have been carried out aiming at evaluating both evolocumab and alirocumab safety and efficacy. The Further Cardiovascular Outcomes Research with PCSK9 Inhibition in Subjects with Elevated Risk (FOURIER) enrolled 27564 patients from 49 countries and demonstrated that over 26 months of follow-up, evolocumab treatment added to statin therapy was able to reduce circulating LDL-C by 60%, and by 15% the risk of major adverse cardiovascular events compared to subjects treated with placebo [239]. Similarly, the ODISSEY OUTCOMES study enrolled 18924 patients over 57 countries to test the safety and efficacy of a bi-monthly injection of alirocumab compared to placebo in patients with coronary syndrome already treated with statins, highlighting a 50% reduction of circulating LDL-C and a 15% reduction of major adverse cardiovascular events [240]. Another interesting therapeutic

approach to inhibit PCSK9 comes from RNA interference technology (siRNA), with anti-PCSK9 inclisiran. Specifically, after its injection, inclisiran is rapidly uptaken by hepatocytes, thus excluding any possible off-target adverse effects, and promotes the degradation of PCSK9 mRNA [241]. Inclisiran's safety and efficacy have been tested through the ORION program, which is still ongoing. To date, ORION-9, ORION-10 and ORION-11 phase III randomized controlled studies showed great benefits of a semestral Inclisiran injection compared to placebo in reducing circulating PCSK9 levels (-80%) in patients with high CV risk, and ongoing phase III clinical trials (ORION-4 and ORION-5) will establish the magnitude of the clinical benefits [242]. Currently, new gene-editing techniques to reduce circulating PCSK9 levels, such as *in vivo* Crispr base editing and adenine base editing, are under investigation and some preclinical results on non-human primates showed positive results [233].

2.5.2 PCSK9 and brain cholesterol homeostasis

Despite the great role of PCSK9 in regulating plasma LDL-C levels, PCSK9 exerts also several extra-hepatic effects, being expressed by different tissues, including brain, where it was first identified as an mRNA upregulated during apoptosis in primary cerebellar neurons [243]. Given the high cholesterol content in brain, deciphering the role of PCSK9 in both physiologic and pathologic situations is extremely relevant. PCSK9, due to its inability to cross BBB in normal conditions, is directly synthesized in brain where, differently from peripheric PCSK9, its concentration of about 5 ng/ml is constant through the 24 hours, thus suggesting a different regulation compared to periphery [244]. Several PCSK9 well-described targets are expressed in brain, such as LDLR, apoER2, VLDLR, LRP1 and CD36, thus it's conceivable to assume an interaction with these receptors and PCSK9 also in the cerebral district [245]. In this regard, different experimental evidence supports a direct involvement in several functions in CNS, including neuronal differentiation, apoptosis, neuroinflammation and cholesterol homeostasis. Starting from neuronal development, PCSK9 promotes neuronal differentiation and neurogenesis. In this regard, Seidah and co-workers demonstrated that in mice PCSK9 expression arises concomitantly with telencephalon and cerebellum neurogenesis and, consistently, the overexpression of PCSK9 is associated with an increased amount of proliferating neurons [243]. On the other side, PCSK9 expression in adult zebrafish is mainly restricted to proliferating cerebral areas, such as cortical, intracranial and cerebellar neurons [246]. Mechanistically, PCSK9 involvement in neurogenesis seems to be independent of its

LDLR-binding ability, as murine P19 embryonal cells treated with retinoic acid showed a strong increase in PCSK9 expression, paralleled, however, by constant LDLR levels [246]. In addition, its expression in this developmental phase is not regulated by the typical transcription factors regulating its synthesis, such as $SREBP_2$, as demonstrated in P19 embryonal cells incubated with retinoic acid [246]. Concerning PCSK9 involvement in apoptosis, the currently available results are still controversial. Indeed, as mentioned before, PCSK9 expression was associated with apoptosis in cerebellar granule neurons [243] and in dorsal root ganglion neurons [247]. Specifically, PCSK9 is probably involved in the JNK-mediated apoptotic pathway, as PCSK9 inhibition in apoptotic cerebellar granule neurons is associated with a reduction in phosphorylated c-Jun protein and cleaved caspase-3 [247]. Interestingly, PCSK9 RNA interference in apoptotic cerebellar granule neurons was shown to increase apoER2 expression, suggesting that PCSK9 may exert its pro-apoptotic activity partially by regulating apoER2 levels [247]. On the other side, PCSK9 was also described to promote neuroglioma U251 cell survival: PCSK9 overexpression, indeed, is associated with a decrease in cleaved caspase-3, in intracellular cytochrome c secretion and a decrease of the ratio of Bax/Bcl-2 proteins [248]. However, the currently available *in vivo* experimental evidence is still confusing. Indeed, in rat models of cardiac ischemia/reperfusion injury, the administration of the PCSK9 inhibitor Prep 2-8 wasn't associated with changes in cerebral Bax and Bcl-2 expression, nor in the number of apoptotic cells [249]. As anticipated before, PCSK9 may be involved also in neuroinflammation, as Prep 2-8 PCSK9 inhibitor administration in rats with ischemia/reperfusion injury downregulated NFκB activation, with consequent reduction of activated microglia and astrocytes [249]. Finally, both *in vitro* and i*n vivo* studies highlighted a possible involvement of PCSK9 in brain cholesterol homeostasis, due to its possible degrading activity on lipoprotein receptors. In this regard, Poirier and co-workers showed a substantial reduction of LDLR, apoER2 and VLDLR expression in human embryonic kidney (HEK) 293 cells co-transfected with PCSK9 and lipoprotein receptors compared to those not transfected with PCSK9 [250]. On the other side, cortical and hippocampal LDLR, VLDLR and apoER2 levels were similar in mice with PCSK9 genic deletion or overexpression [251] and, consistently, in $PCSK9^{-/-}$ adult mice, CSF, olfactory bulb and peduncle LDLR and apoER2 expression was similar compared to WT mice [252]. Interestingly, the latter study highlighted a significant increase in LDLR expression in telencephalon at day E12.5 in $PCSK9^{-/-}$ mice compared to WT [252], thus suggesting a possible time- and tissue-specificity for PCSK9 cholesterol regulation.

3. BRAIN CHOLESTEROL METABOLISM IN AD

3.1 CHOLESTEROL HOMEOSTASIS ALTERATIONS

As discussed in paragraph 2.1, several experimental evidence supports a key role for both LXRs and SREBPs in brain cholesterol homeostasis, whose alteration has been demonstrated to be tightly associated with pathological alterations, such as MS, Huntington's Disease, Amyotrophic Lateral Sclerosis (ALS), Niemann-Pick disease type C and AD [140]. Hence, understanding the molecular mechanisms involved in the fine sterol-sensing mechanisms may be helpful for the identification of new possible pharmacological targets.

LXRs involvement in AD has been extensively investigated. The administration of T0-901317 in APP23 mice is associated with a reduction of brain soluble $A\beta_{1-40}$ and $A\beta_{1-42}$ [253]. Consistently, $APP_{swe}/PS1_{\Delta E9}$ Tg mice with genetic ablation of both LXRα and LXRβ showed a strong increase in cerebral amyloid deposits as compared to $APP_{swe}/PS1_{\Delta E9}$ Tg mice, possibly as a consequence of LXRs' ability to dampen the glial response to a pro-inflammatory stimulus such as Aβ [254]. LXRs involvement in microglia anti-inflammatory status has also been addressed in APP/PS1 mice, showing modulation of NF-κB-signaling and an increase in cholinergic neurons, reflected into an ameliorated cognitive function [255]. To date, evidence in humans is still poorly investigated. One of the first pieces of genetic evidence of a connection between LXR and AD comes from the observation that the variability in the NR1H2 locus on the LXRβ-encoding gene may constitute a risk factor for AD, probably as a consequence of its involvement in astrocytes cholesterol homeostasis [256]. Consistently, the C allele of the SNP rs7120118 in the NR1H3 locus on the LXRα-encoding gene seems to be associated with a reduction in CSF tau and phospho-tau protein, together with a reduction in soluble $A\beta_{42}$ [257]. However, despite the lacking of precise association with AD pathogenesis, the available experimental evidence suggests that the pharmacological activation of LXR may represent an interesting pharmacological target for AD.

SREBPs involvement in AD-related degeneration originates from the observation that $A\beta_{42}$ oligomers may exert a detrimental effect upon cholesterol synthesis in neurons [258], paralleled and justified by a reduction in $SREBP_2$ processing and activation [259], probably as a consequence of the $A\beta_{42}$ oligomers-induced reduction of protein kinase B (AKT)

phosphorylation and activation, preventing $SREBP_2$ trafficking to the Golgi. Consistently, APP expression in rat cortical primary neurons is associated with a reduction in endogenous cholesterol biosynthesis, together with a down-regulation of $SREBP_{1a}$, $SREBP_{1c}$ and $SREBP_2$ mRNA expression, while the inhibition of APP expression leads to an increased cholesterol biosynthesis [260]. This evidence highlights the relevant role that brain cholesterol metabolism plays in AD-related degeneration. This strong connection is also remarked by the evidence that SREBPs levels inversely correlate with APP in human brains [261]. Other evidence of involvement of SREBPs in amyloidogenesis derives from the observation that BACE1 expression seems to be directly regulated by $SREBP_2$ and, consistently, its overexpression in APP/PS1 mice is associated with an increase in cognitive functions, Aβ and NFT deposition [262]. In addition, a recent study identifies a SNP in the $SREBP_2$ sequence, rs2269657, that seems to be associated with different clinical and anatomopathological features of LOAD [263]. Finally, Wang and co-workers demonstrated a decrease in $SREBP_2$ activation in pyramidal neurons with NFT deposition [264], suggesting that not only amyloidosis but also tau pathology may be involved in the dysregulation of SREBPs-mediated signalling.

3.2 CHOLESTEROL BIOSYNTHESIS ALTERATIONS

The currently available experimental evidence directly demonstrating a specific alteration in cholesterol biosynthetic pathways in AD are currently limited. However, genic expression of the Dhcr24 enzyme, involved in desmosterol conversion into cholesterol, is strongly reduced in post-mortem AD brain sections compared to those of healthy controls. [265]. In this regard, the investigation of the specific intracellular cholesterol biosynthetic pathways in neurodegenerative diseases may represent an interesting topic for further investigation. Hence, taken together, this experimental evidence suggests that due to the low efficacy of cholesterol biosynthetic activity, adult neurons mostly rely on less-expensive cholesterol provided by astrocytes and, in this regard, the co-culture of neurons with astrocytes is associated with a strong reduction in neuronal squalene synthase activity, an enzyme involved in cholesterol biosynthesis [266]. Thus, the interplay between neurons and glial cells, including astrocytes, represents a fundamental aspect of neuronal homeostasis.

3.3 CHOLESTEROL TRANSPORT ALTERATIONS

3.3.1. Lipoproteins alterations

Recent experimental evidence suggested a dysregulation in CSF lipoprotein metabolism in AD, mainly related to their formation, maturation and to their ability to transport cholesterol. Specifically, two separated studies confirmed that CSF capacity to promote ABCA1- and ABCG1-mediated cholesterol efflux is compromised in patients with AD compared to controls, thus highlighting brain lipoprotein functionality as a possible pathogenetic mechanism in AD [267,268]. A peculiar link between AD-related neurodegeneration and a reduction in neuronal cholesterol providing was also highlighted by the close correlation between brain lipoproteins function and specific neurobiomarkers of AD, such as Aβ and phospho-tau [268]. Concerning lipoprotein remodelling enzymes, Demeester and co-workers highlighted a significant reduction in CSF LCAT activity in AD patients compared to controls [181]. On the other side, CETP involvement in cognitive function is not clear, as some studies reported a SNP (rs5882) in its encoding sequence associated with cognitive decline, which, however, has not been confirmed by other experimental analyses [269,270]. Finally, to date, evidence supporting PLTP involvement in lipoprotein remodelling and maturation are not conclusive, but, interestingly, PLTP expression has been detected in cerebrovascular endothelial cells and its synthesis increases following the *in vitro* LXR activation [271]. In addition, PLTP deficiency is associated with a reduction in BBB functionality and increased permeability [272] and, consistently, analysis on PLTP concentration in CSF of AD subjects showed a significant increase in its expression, thus furtherly supporting the evidence of dysregulation of brain lipid metabolism [273].

3.3.2. Apolipoproteins alterations

Investigating how CNS apolipoproteins may influence brain physiology, also given the relevant association between apoE Ɛ4 isoform and LOAD pathogenesis [7], may help in the investigation of novel disease-associated mechanisms and novel therapeutic targets.

Concerning apoA-I, several pre-clinical studies, P/PS1 mice overexpressing human apoA-I showed an improvement in cognitive functions and memory, paralleled by a decrease in Aβ deposition, glial activation and pro-inflammatory cytokines secretion [274] and,

accordingly, apoA-I deficiency was associated with worsened cognitive performances [275]. Interestingly, apoA-I seems to be involved in APP processing by either enhancing cellular cholesterol efflux, thus increasing the non-amyloidogenic pathway, or by directly binding to APP and preventing its internalization and cleavage [276]. Moreover, apoA-I seems to be involved also in Aβ clearance and, in this regard, both HDL and apoA-I, due to their affinity, were able to promote Aβ clearance through BBB [180]. Concerning epidemiological studies, the relevance of apoA-I in AD was highlighted by the observation that AD patients from a French cohort were characterized by lower levels of circulating apoA-I levels compared to controls, and the levels inversely correlated with the severity of the disease [277]. Furthermore, a recent study observed a reduction in CSF apoA-I levels in AD subjects [278]. However, in this unclear context, a phase II clinical trial showed that the 12 weeks infusion of RXV-208, able to induce apoA-I genic transcription, was associated with increased circulating Aβ levels, possibly suggesting an increased cerebral clearance [195]. Another protective effect of apoA-I seems to be related to its anti-inflammatory activity; in this regard, APP/PS1 mice lacking apoA-I showed increased Aβ deposition compared to apoA-I-expressing littermates, together with a strong increase in neuroinflammation-related markers such as IL-1β [279].

Several experimental evidence supports the direct involvement of apoE in AD pathogenesis through different mechanisms, such as Aβ metabolism, tau-mediated neurodegeneration, and cholesterol homeostasis alteration. Indeed, apoE is able to bind to Aβ, leading to the formation of complexes that alter its clearance and promote Aβ plaques formation: at this regard, apoE Ɛ4 isoform showed a stronger binding ability, with subsequent Aβ oligomerization and deposition [280]. The negative impact of apoE Ɛ4 isoform on Aβ clearance may be also due to its competition for LRP1 binding, as suggested by the observation through immunostaining on human AD brains that LRP1 positively correlated with Aβ, and this correlation was furtherly increased in apoE Ɛ4 carriers [281]. Concerning tau-related neurodegeneration, P301S tau Tg mice overexpressing or not the three human apoE isoforms revealed that those overexpressing apoE Ɛ4 were characterized by increased brain atrophy with reduced neuronal viability, the release of proinflammatory cytokines such as TNF-α and tau hyperphosphorylation, with faster disease progression [282]. Furthermore, a study conducted upon 1056 post-mortem brains of AD subjects and matched controls revealed a positive correlation between the presence of the apoE Ɛ4 isoform and the frequency of NFT tangles, which is an index of tauopathy,

probably as a consequence of apoE ε4-induced hyperphosphorylation [283]. Interestingly, the treatment of cultured neurons with astrocyte-derived apoE ε4 is associated with subsequent hyperexcitability, leading to an excessive and imbalanced neuronal activity [284]. Despite these possible relevant mechanisms linking apoE to AD pathogenesis, one of the main functions of apoE is the regulation of brain cholesterol homeostasis by contributing to the delivery of newly-synthesized cholesterol from astrocytes to neurons [187], as described in paragraph 2.3. Hence, correct apoE lipidation plays a fundamental role in brain cholesterol homeostasis. Interestingly, nondenaturing gel electrophoresis in human CSF samples with different apoE genotypes showed that apoE ε4 complexes were smaller compared to those of individuals with apoE ε3 and, above all, apoE ε2 [285]. These observations suggest a limited lipidation of ε4 isoform compared to ε3, while ε2 isoform seems to be more prone to bind cholesterol and form apoE-containing lipoproteins. ApoE lipidation occurs following its interaction with the ABCA1 transporter and, in this regard, Rawat and colleagues observed a reduction in apoE ε4 ability to interact with ABCA1, resulting in a reduction of *in vitro* cholesterol efflux from astrocytes and apoE lipidation compared to apoE ε3 isoform [286]. In this regard, our research group previously demonstrated a reduction in ABCA1- and ABCG1-mediated cholesterol efflux of CSF from AD subjects compared to controls [268], suggesting the impaired lipidation of apoE-containing lipoproteins as a possible disease pathogenetic mechanism. Disruption in brain cholesterol homeostasis may also occur in its last step, namely the interaction between neuronal apoE-binding receptors and apoE-containing lipoparticles. In this regard, one of the main possible pathogenetic mechanisms may be related to the degrading activity of the PCSK9 enzyme. Interestingly, a study conducted in our research group revealed increased PCSK9 levels in CSF of AD patients compared to non-AD subjects, also highlighting that CSF PCSK9 concentration was higher in those bearing the apoE ε4 isoform with respect to non-carriers [287]. Another possible involvement of apoE ε4 in AD pathogenesis may be related to its well-described ability to disrupt BBB integrity, which is a typical hallmark of the disease [288]. Indeed, Montagne and co-workers recently demonstrated that carriers of apoE ε4, either in heterozygous or homozygosis, showed BBB hippocampal breakdown, possibly contributing to cognitive decline [289]. Concerning neuroinflammation, several pieces of evidence support a possible involvement of apoE ε4 in the inflammatory cascade, as demonstrated by an increased release of proinflammatory cytokines such as IL-6 and TNF-α in the brain of transgenic mice expressing human apoE ε4 allele, compared to those bearing the apoE ε3 gene, after the administration of

lipopolysaccharides (LPS) [290]. Finally, also oxidative stress seems to be influenced by apoE and, consistently, in an isoform-dependent fashion. In this regard, post-mortem analysis in the hippocampus of AD patients highlighted that apoE Ɛ4 carriers were characterized by enhanced oxidative stress compared to non-carriers [291]. The possible relevant pathogenic role of apoE Ɛ4 is highlighted by Xiong and colleagues, that demonstrated that the immunotherapy with the infusion of anti-human apoE antibody HAE-4 in 5XFAD apoE $Ɛ4^{+/+}$ mice is associated with a reduction in Aβ deposition and cerebrovascular dysfunction, together with a reduction in neuroinflammatory-related parameters [292].

ApoJ involvement in LOAD has been highlighted by different experimental evidence. As an example, two GWAS studies demonstrated that SNPs in its encoding sequence are one of the most common genetic risk factors and, among them, the apoJ variant rs331896 is highly associated with AD risk and dementia [293]. The relevance of apoJ in AD is also highlighted in several experimental pieces of evidence. ApoJ may be involved, indeed, in the amyloid aggregation process: in this regard, an *in vitro* study using single-molecule fluorescence, revealed that apoJ is able to act as a chaperone molecule and bind to different oligomeric aggregates of Aβ peptides, thus leading to the formation of complexes [294]. Consistently, the infusion of apoJ in hippocampal tissue was found to be associated with a reduction in Aβ-induced toxicity and better cognitive performances in rats [295]. Concerning the evidence in humans, Sheperd and co-workers recently demonstrated that brain apoJ levels were higher in AD patients compared to controls [296]. Taken together, these observations suggest that apoJ is involved in Aβ clearance, but in presence of extremely high Aβ levels compared to those of apoJ, the amyloidogenic pathway is enhanced.

3.3.3. Transporters alterations

ABCA1 involvement in AD-related neurodegeneration is testimonied by several experimental evidence. For instance, APP Tg mice lacking ABCA1 showed an increased Aβ deposition and lower apoE and apoA-I levels compared to APP littermates [297]. Interestingly, APP Tg mice with ABCA1 haplodeficiency showed a significant worsening of memory deficits only in those expressing human apoE Ɛ4 compared to those expressing apoE Ɛ3 [298]. In addition, it has been recently demonstrated that after brain injury, astrocytes become reactive and with a pronounced phagocytic activity that requires ABCA1 upregulation [299]. Despite the available pre-clinical studies pointing to a protective

role of ABCA1 in brain cholesterol homeostasis and AD pathogenesis, the picture is not completely defined, as the available human studies present many confounders factors, including the sample size and different genetic background. As an example, the SNPs rs2230806 and rs1800977 identified in 71 AD patients were not associated with increased cerebellar Aβ deposition compared to 81 healthy controls [300]. On the other side, Nordestgaard and co-workers identified in a large cohort an ABCA1 LOF mutation, N1800H, present in about 1:500 subjects, associated with low plasmatic apoE concentration ad high AD risk [301]. Remarkably, despite the ABCA1 sequence wasn't identified as a disease-susceptible gene in recent GWAS [61], it is currently enlisted among the encoding sequences that require particular attention. As an example, fibroblasts isolated from patients with the N935S mutation, characterized by extremely low HDLs, showed an aberrant response to LXR agonist T0901317 by releasing Aβ, thus confirming the involvement of ABCA1 in amyloid processing [253].

Several experimental evidence suggests a possible involvement of ABCG1 in the pathophysiology of AD through different mechanisms, mainly related to its involvement in cholesterol metabolism homeostasis and to ABCG1 ability to transport Aβ. Specifically, Kim and co-workers observed a significant reduction in Aβ production in CHO cells expressing ABCG1 [200]. In contrast, in Human Embryonic Kidney (HEK) 293 cells carrying the human APPsw mutation, characterized by higher Aβ production, ABCG1 transfection is associated with an even more increased Aβ release [302]. The reasons for this apparently contrasting evidence are probably related to the difference in the experimental cell models and the APP encoding sequence. However, ABCG1 possibly limits the production of wild-type APP, while mutant APP escapes the ABCG1-mediated regulation. ABCG1 involvement in Aβ metabolism has been addressed using APP with the specific familial AD mutation overexpressing ABCG1, showing that its overexpression is not linked to an alteration in Aβ production, cholesterol efflux and apoE secretion, neither in cognitive functions [303]. Another evidence, yet indirect and contrasting, comes from the observation that APP/PS1 Tg - LXRα/β $^{-/-}$ mice were characterized by a strong decrease in ABCA1 and ABCG1 expression, that was associated with a significant reduction in Aβ deposition compared to LXRα/β-expressing littermates [254]. Concerning human studies, a SNP in ABCG1 encoding sequence has been associated with AD risk in a Polish and Swiss cohort, which, however, wasn't confirmed in other European populations [304].

Concerning ABCG4 involvement in AD pathogenesis, Uehara and co-workers demonstrated for the first time a close co-localization of *Abcg4* mRNA in microglia near senile plaques of post-mortem brain tissues of AD patients [305]. More recently, ABCG4 $^{-/-}$ mice showed reduced Aβ clearance due to lower export through BBB, together with a reduced desmosterol transport. Hence, ABCG4 ligand desmosterol may antagonize Aβ clearance [306].

3.3.4. Receptors alterations

Several experimental evidence from *in vitro* or *in vivo* studies, together with some evidence on humans from genetic studies helped in deciphering a possible involvement of lipoprotein receptors, mainly LDLR, VLDLR, apoER2 and LRP1 in AD pathogenesis.

LDLR involvement in AD pathogenesis has been extensively investigated. Cao and co-workers generated a Tg2576, LDLR $^{-/-}$ mouse model, highlighting that the absence of the receptor was associated, as expected, with hypercholesterolemia, but also with cerebral Aβ deposition, accompanied with hyperactivity, memory and spatial learning disabilities compared to Tg2576 mice expressing LDLR [307]. Consistently, LDLR overexpression in mice is associated with a strong reduction in Aβ aggregation and higher Aβ clearance, accompanied by a reduction in neuroinflammatory biomarkers [308]. Indeed, using primary murine astrocytes Basak and co-workers demonstrated that LDLR can directly bind Aβ, thus mediating its uptake and clearance through lysosomal degradation [309]. Another physiological mechanism to degrade Aβ is through the BBB-mediated transport: at this regard, LRP1 involvement in BBB clearance has been extensively studied and will be reviewed in the next paragraph. Concerning LDLR, using a murine model expressing Aβ only in brain and investigating the brain efflux index, Castellano and co-workers revealed that also LDLR participates in the Aβ elimination from brain to blood [310]. In this context, evidence on humans are more conflicting: despite some case-control studies revealing some SNPs in LDLR encoding sequence associated with increased AD risk, other studies failed in confirming such association. Recently, however, an association between haplotype GTT and SNP rs688 and AD onset was found in females and males, respectively [311].

ApoER2 involvement in the AD pathogenetic process has been highlighted by a preliminary observation of its overexpression in activated astrocytes near Aβ plaques [312]. In addition, the protein F-spondin seems to mediate the extracellular interaction between

the central domain of APP and the reeler domain of apoER2 [313]. In this regard, the overexpression of apoER2 is associated with an increase in retained APP, which mainly localizes into lipid rafts, suggesting that apoER2 possibly influences APP processing by promoting their shift to membrane areas rich in lipid rafts, where BACE1 and γ-secretase are mainly expressed [16,314]. In addition, apoER2 may impact APP metabolism by competing for protease binding: indeed, α-secretase can cleave apoER2, producing a soluble fragment that is furtherly cleaved by γ-secretase [315]. Hence, apoER2 may limit the availability of proteases involved in APP processing. Another possible connection between apoER2 and APP metabolism comes from the observation that the cytoplasmatic protein disabled-1 (Dab1) is able to bind to both NPxY sequence of apoER2 and to APP intracellular domain, negatively affecting their metabolism [316]. Interestingly, primary neurons treated with exogenous apoER2 ligand reelin showed an increased interaction of apoER2 and APP, thus highlighting a possible involvement of Dab1 in response to exogenous ligands in apoER2 and APP metabolization [316].

To date, the direct experimental evidence supporting an alteration of VLDLR functionality in AD is still limited and mostly related to its involvement in the reelin signalling pathway, crucial for neuronal migration, synaptic plasticity and dendritic spine formation [206]. Interestingly, using *in vitro* biochemical assays, it has been demonstrated that apoE ε4 tends to aggregate with Aβ, thus diverting the direct binding of the aggregate with LRP1 to VLDLR, able to internalize apoE ε4-Aβ complex more slowly and efficiently compared to LRP1 [317].

LRP1 involvement in AD pathogenesis has been investigated in several studies, either in pre-clinical *in vitro* and *in vivo* models and also in humans. One of the first pieces of evidence of direct involvement of LRP1 in amyloidogenesis comes from the observation that in H4 cells expressing human APP the inhibition of LRP1 results in an increase in APP and lower Aβ production [318]. In contrast, neuronal cell lines overexpressing LRP1 showed a reduction in Aβ processing and deposition as a consequence of the competition with APP for its processing [319]. However, LRP1 major involvement in Aβ metabolism is related to its endocytic activity with consequent lysosomal degradation. Experiments conducted upon APP/PS1 mice lacking LRP1 confirmed a direct involvement of astrocytic and neuronal LRP1 in Aβ uptake and clearance [320]. In addition, LRP1 mediates the active transport from brain tissue to periphery through BBB [321] and, noteworthy, also a peripheral expression of LRP1 may be involved in central Aβ processing. Indeed, as

explained by the "peripheral sink hypothesis", peripheric and cerebral Aβ pools coexist in a peculiar equilibrium, where hepatic LRP1 binds and removes a large amount of plasmatic Aβ, that probably derives from the brain through BBB: at this regard, hepatic LRP1 overexpression in mice leads to reduced cerebral Aβ accumulation [212]. However, despite the direct role of LRP1 in amyloid clearance, some experimental evidence suggested that excessive Aβ internalization is associated with cellular apoptosis, thus accelerating the neurodegeneration in AD [322]. These observations clearly demonstrate the involvement of LRP1 in Aβ processing, despite further studies are still needed to clarify its role. Concerning evidence in humans, different studies identified a SNP in the LRP1 encoding sequence (C766T) that is significantly associated with AD risk [323]. Interestingly, the same polymorphism is associated with Aβ deposition and CAA[323]. Furthermore, a neuropathological study first observed an increased expression of LRP1 near Aβ plaques in AD brain compared to controls [324]. Interestingly, in post-mortem analysis, LRP1 expression was found to be decreased in neurons, paralleled by an increase in astrocytes and vessels near Aβ plaques in the hippocampus [325]. An extremely relevant aspect concerns whether the variation of LRP1 expression occurs during the preclinical stage of AD, in parallel with the strong Aβ accumulation typical of this stage of the disease. In this regard, post-mortem brains of subjects with MCI revealed that hippocampal LRP1 expression was lower compared to controls [326], thus suggesting a possible pathogenetic-related mechanism of LRP1 involvement in AD.

3.4 OXYSTEROLS BALANCE ALTERATIONS

Given the important role of cholesterol in several processes involved in AD pathogenesis, and considering the relevant bioactivity of oxysterols as signalling molecules, it's not surprising that oxysterol homeostasis has been found to be altered during AD development. One of the main pieces of evidence originates from the observation of a significant reduction in 24-OHC, paralleled by an increase in 27-OHC and 25-OHC in post-mortem brain of AD patients compared controls, accompanied by a reduction of CYP46A1 and increase of CYP27A1 enzymes [327]. In addition, AD patients are characterized by an increase in plasmatic 24-OHC during the early phase of the disease, which progressively decreases with AD progression, together with an increase in CSF 24-OHC and 27-OHC content, thus possibly representing novel disease biomarkers [328]. So far, four SNPs in the intron 2 of CYP46A1 encoding sequence (rs754203, rs49000442, rs7157609 and rs4900442) leading to lower CSF 24-OHC concentration have been associated with

increased AD risk and associated with apoE ε4, despite the mechanism is still not clarified [329]. Noteworthy, several experimental evidence suggests a possible involvement in CYP46A1 in ageing and memory function; in this regard, CYP46A1 $^{-/-}$ mice, characterized by lower 24-OHC, showed impaired learning ability due to deficient long-term potentiation (LTP) [330]. The relevance of CYP46A1 is also highlighted by the extremely toxic consequences of its inhibition, leading to excessive neuronal cholesterol loading and apoptosis, with subsequent tissue atrophy in mice [331]. Concerning Aβ metabolism, CYP46A1 activation with the subsequent 24-OHC formation in SH-SY5Y cells modulated APP processing, with an increase in the non-amyloidogenic pathway [332] and, consistently, in AD mice the intra-hippocampal injection of AAV containing CYP46A1 encoding sequence is associated with a reduction in Aβ plaques and with amelioration of learning and memory ability [333]. Hence, this experimental evidence supports a possible involvement of CYP46A1 and its metabolite 24-OHC in cognition preservation and anatomopathological ameliorations in pre-clinical AD models, thus reinforcing the role of 24-OHC as a disease-biomarker and possible pharmacological target. Focusing on 27-OHC, different studies highlighted an association between alterations in its levels, cognitive deficits and AD [334]. In this regard, CYP27A1 $^{-/-}$ mice fed with a high-fat diet showed amelioration in the altered memory functions induced by the diet, suggesting that 27-OHC may be one of the main sterols involved in the well documented cognitive impairment related to dietary cholesterol [335]. One possible explanation of this observation may be related to the impact of high levels of 27-OHC in dendritic spine density depletion, as observed both *in vitro* in primary cortical neurons isolated from rats as well as in CYP27A1 overexpressing mice [336] and, interestingly, dendritic spine alterations have been well documented in AD [29]. In this regard, marked accumulation of 27-OHC has been measured in CSF and brain parenchyma of patients with the $APP_{670/671}$ Swedish mutation, typical of EOAD [337]. In addition, post-mortem analyses on AD brains confirmed an increased CYP27A1 activity compared to non-AD subjects, thus suggesting a specific disease-related increased 27-OHC production [327]. The molecular mechanisms of these observations are still under investigation; in this regard, SH-SY5Y neuroblastoma cells treated with 27-OHC displayed an increased Aβ production and tau phosphorylation [338], together with ER stress [339]. Intriguingly, a recent study showed a possible involvement of 27-OHC also in glucose neuronal hypometabolism, a typical AD feature [121], highlighting that in mice 27-OHC is able to affect brain Insulin-regulated aminopeptidase (IRAP)/Glut4 and Renin-Angiotensin system (RAS), thus altering several relevant

cerebral functions such as memory, Spatio-temporal leaning, emotional responses and sensory information, together with glucose uptake [340]. Hence, considering the relevance of oxysterols, mainly 24-OHC and 27-OHC, in pre-clinical models of AD and human studies, several pharmacological approaches targeting both CYP46A1 and CYP27A1 are currently under investigation. As an example, anastrozole, able to inhibit CYP27A1 is able to reduce 27-OHC levels in rats, and CYP46A1 enhancing agent efavirenz was associated with a reduction in Aβ deposition and neuroinflammation in 5XFAD mice, together with amelioration in rodents' cognitive functions [334].

3.5 PCSK9 INVOLVEMENT IN AD

As described in chapter 2.5.2, PCSK9 may modulate several relevant processes for brain homeostasis, thus being possibly involved also in neurodegenerative processes of AD, despite, to date, still limited and controversial evidence being available. PCSK9 role in modulating neuronal apoptosis has been highlighted by several *in vitro* and *in vivo* studies [245]. Interestingly, Zhao and co-workers observed that hippocampal neuronal apoptosis occurring in hypercholesterolemic apoE$^{-/-}$ mice subjected to a high-fat diet was paralleled by a concomitant increase in PCSK9 expression [341]. Similarly, in mice with brain ischemia and subsequent cerebral damage, the inhibition of PCSK9 expression through sh-RNA is associated with a lower neuronal apoptotic rate, possibly through apoER2-mediated signalling [342]. Conversely, a possible anti-apoptotic activity of PCSK9 may be related to its involvement in Aβ generation process. Indeed, an increased brain BACE1 expression and Aβ deposition have been observed in PCSK9 $^{-/-}$ mice and, consistently, its overexpression was associated with reduced cerebral BACE1 levels [343]. Recently, however, Apaijai and co-workers demonstrated that PCSK9 inhibitor administration in rats before the induction of cardiac ischemic/reperfusion injury and consequent brain damage is associated with a reduction in Aβ formation, dendritic spine loss and microglial activation [249]. Another possible mechanism by which PCSK9 may be involved in AD-related neurodegeneration is due to its ability to target several cholesterol-related genes already studied for their link with AD. In this regard, a degrading activity of PCSK9 on LRP1 has been well-documented on hepatocytes and vascular cells [227]. Since LRP1 expression has been reported in several cerebral cell types, such as neurons, astrocytes, brain vascular cells [212], it's conceivable to hypothesize a PCSK9-mediated regulation of LRP1 levels also in these districts. LDLR is another well-described PCSK9 target and, in this regard, LDLR$^{-/-}$ mice are characterized by a reduction in proliferating hippocampal

neurons as well as in the number of active presynaptic boutons and impaired neurites outgrowth compared to WT mice, accompanied by an impairment in memory and learning functions [344]. PCSK9 is also able to increase scavenger receptor CD36 expression, as observed in mouse peritoneal macrophages [345]. Noteworthy, CD36 in microglial cells and astrocytes is able to bind and mediate the clearance of Aβ fibrils; at this regard, Stewart and co-workers demonstrated that CD36 can be considered as a co-receptor in toll-like receptors (TLRs) 4 and 6 heterodimerizations, fundamental to propagate the neuroinflammatory cascade involved in neurodegeneration [86]. Despite the available evidence on the pre-clinical model pointing to a possible involvement of PCSK9 in AD-related neurodegeneration, to date, the available studies conducted in humans are more ambiguous. Indeed, PCSK9 was first listed among different cholesterol-related genes associated with AD in the AlzGene dataset [346], despite, to date, LOF mutations rs11583680, InsLEU and R46L in PCSK9 encoding sequence weren't associated with AD risk in different cohorts of Japanese and French Canadian patients, respectively [347,348]. Similarly, in Afro-American participants of the Reasons for Geographic and Racial Differences in Stroke (REGARDS) carrying or not the LOF PCSK9 variants C697X and Y142X, no differences were retrieved in neurocognitive functions [349]. On the other side, studies conducted in 111194 patients from the Copenhagen City Heart Study with GOF PCSK9 mutation rs505151 excluded an increased AD risk [350]. Recently, it was shown that only female subjects with the rs499718 and rs4927193 PCSK9 variants are characterized by an increased risk for LOAD onset [351], that, however, still need to be deeply investigated. A study conducted in our laboratory highlighted increased PCSK9 concentrations in CSF of AD subjects compared to controls, in which, interestingly, apoE ε4 carriers showed the highest PCSK9 values [287]. Additionally, Picard and co-workers observed an increase in PCSK9 expression in post-mortem LOAD patients compared to controls specifically in the frontal cortex brain area [351].

Finally, given the high efficacy of the currently available anti-PCSK9 mAbs evolocumab and alirocumab in reducing circulating PCSK9 and LDL-C [239,240], some concerns were raised about some possible neurological side effects. In this regard, the Ebbinghaus study followed for 19 months 1204 patients receiving either evolocumab or placebo, which didn't highlight significant differences in neurocognitive functions [352]. A similar result was recently confirmed in 2086 patients treated with alirocumab or placebo, with a follow-up of 96 weeks [353]. An extension of the FOURIER trial, with a 5-year follow-up, is

currently ongoing, possibly clarifying the long-term effect of PCSK9 mABs on cognitive functions (ClinicalTrials.gov Identifier: NCT02867813). One possible explanation of the absence of neurocognitive effects derived from PCSK9 mABs administration may be related to the presence of BBB that, if intact, limits plasmatic LDL-C, PCSK9 and PCSK9 mABs passage to the CNS. However, so far no alterations in cognitive functions in evolocumab-treated patients with diabetes, a disease that induces alterations in BBB, have been observed [352]. Hence, investigating the impact in neurocognition of small, lipophilic PCSK9 inhibitors able to cross BBB would be of great interest.

AIM OF THE STUDY

AD represents the most common form of dementia and constitutes one of the most lethal and burdening pathological condition, with an estimated prevalence of about 50 million people worldwide, which is expected to furtherly increase in the next years [4,5]. Different studies focused on the etiopathological processes concurring to the AD development, currently considered a multifactorial disease, but, to date, the underlying causes are not fully defined. Different coexisting hypotheses describe the pathological alterations that characterize AD, and, among them, the Aβ deposition [12,13], the tau hyperphosphorylation with consequent NFT formation [37,38], neuroinflammation [75–77] and several mutations on specific AD-related genes [14,53–55] are worth noting. In addition, recent GWAS studies identified several variants of genes involved in lipid metabolism that are associated with AD [61]. Among these, it has been estimated that about 40% of AD patients carry the ε4 isoform of the apoE encoding gene, thus highlighting that apoE ε4 represents a strong risk factor for AD [60]. Interestingly, apoE plays a key role in brain homeostasis, being involved in different processes including the maintenance of synaptic plasticity, the regulation of Aβ aggregation process, together with its relevant involvement in cerebral lipid metabolism [60]. This evidence thus markedly support the hypothesis of possible involvement of lipid metabolism, and mainly of cholesterol, in AD pathogenesis.

Specifically, CNS is considered the most cholesterol-enriched bodily compartment [126], and indeed cholesterol plays a fundamental role in its homeostasis, being involved in neuronal development, in neurite outgrowth, synaptogenesis, plasticity and in the repair of damaged membranes [130]. As follows, brain cholesterol homeostasis alterations are associated with different neurodegenerative diseases, including AD [133,137,138,140]. In particular, brain relies on *in situ* cholesterol synthesis, due to its inability to overcome BBB [126,167]. While neuronal cholesterol biosynthesis rate is high during the early phases of development [169], it greatly decreases in adult neurons, that thus strongly depend on cholesterol synthesized by astrocytes for their cholesterol needs [170]. Brain cholesterol transport represents therefore a fundamental aspect of cerebral homeostasis and relies on the cooperation of specific molecules, transporters and receptors. Briefly, cholesterol synthesized from astrocytes is complexed with astrocyte-secreted apoE, thus originating apoE-containing lipoparticles, through the interaction with ABCA1, ABCG1 and ABCG4 transporters and remodelling enzymes [186]. Those particles furtherly interact with LDLR, LRP1, VLDLR and apoER2 on of neurons [187], thus supplying their cholesterol need. In this context, the protein PCSK9, beyond its well-known ability to modulate plasma LDL-C levels, also exerts several extra-hepatic effects, being expressed by different tissues,

including brain, where it was first identified [243]. Different pre-clinical evidence supports a direct involvement of PCSK9 in several relevant processes in CNS, including the promotion of neuronal differentiation [243,246], apoptosis (despite its role is still unclear) [247–249], neuroinflammation [249] and also cholesterol homeostasis, as lipoprotein receptors may be sensitive to the degrading activity of brain PCSK9, as in peripheral tissues [250–252,344,345]. To date, the available studies conducted in humans are however more ambiguous. Indeed, PCSK9 was first listed among different cholesterol-related genes associated with AD in the AlzGene dataset [346], despite, to date, different identified LOF or GOF mutations in PCSK9 encoding sequence weren't found to be associated with AD risk [347–350].

Particularly, the present research work stems from the previous observation derived from a study conducted in our laboratory, that demonstrated increased PCSK9 concentrations in CSF of AD subjects compared to controls [287]. Interestingly, PCSK9 levels were higher in apoE ε4 carriers [287]. A similar observation was also reported by others, highlighting an increased PCSK9 expression in post-mortem AD cerebral tissues compared to controls [351]. The available data, although still controversial, overall suggest a possible link between PCSK9 and AD.

This research project is aimed at investigating and clarifying the potential involvement of PCSK9 in AD pathogenesis, by exploring the possible mechanisms by which it may interfere with brain cholesterol homeostasis and thus identifying PCSK9 as a new possible pharmacological target for the development of future therapies.

To this aim, a translational study has been carried out by following three experimental approaches, involving *in vitro* and *ex vivo* studies.

The first part of the study aims at investigating the possible deleterious influence of PCSK9 on the key steps of brain cholesterol transport from astrocytes to neurons, based on the possible degrading effect on lipoprotein receptors. Specifically, PCSK9 impact on the most relevant processes involved in brain cholesterol metabolism, including the endogenous cholesterol biosynthesis, the efflux from astrocytes and the final cholesterol uptake by neurons, has been evaluated through *in vitro* models of astrocytes and neurons. Furthermore, the incubation with $A\beta_{1-42}$ fibrils simulated *in vitro* the typical pathological alterations retrieved in AD. In addition, with this specific experimental setting, PCSK9 impact on neuronal viability has been assessed, as neuronal loss is extremely relevant for AD pathogenesis.

Secondly, the study explored the impact of PCSK9 on plasma and brain lipid levels in transgenic mice model of AD lacking PCSK9, specifically generated within this project. In

particular, an *ex vivo* study has been set up, aiming at evaluating the main sterol-related parameters, such as cholesterol and hydroxysterols levels, in serum and brain specimens. The main objective of these analyses is therefore to explore and clarify the possible interaction between PCSK9, AD and lipid metabolism, and to investigate if the possible functional alteration of brain cholesterol transport observed through *in vitro* studies may be reflected also in a pre-clinical model of the disease. Indeed, while cholesterol homeostasis alterations have been widely described in AD [137,139], disease-linked variations of hydroxysterols balance have been postulated only recently in pre-clinical studies [327–329]. Hydroxysterols, mainly 24- and 27-OHC, are indeed considered bioactive molecules due to their ability to modulate different transcriptional pathways, linked to either cholesterol homeostasis [155,220,221,327,336] but also to apoptosis [331] and Aβ metabolism [332,333].

Finally, in the last part of the present research project, a case-control study has been performed by recruiting subjects with different degrees of cognitive impairment. In particular, PCSK9, cholesterol and hydroxysterols were measured in CSF and serum of the above-mentioned subjects, to investigate a possible association between PCSK9 measurements, lipid-related parameters and the specific neurobiomarkers normally adopted for AD diagnosis, as well as with patients' apoE genotype.

The results of this translational study, articulated through three approaches including *in vitro* studies as well as *ex vivo* analyses of samples from both animal and humans specimens will help to define the role of PCSK9 in cerebral cholesterol homeostasis, thus offering the bases to clarify its potential involvement in AD pathogenesis. Furthermore, understanding the molecular mechanisms involved in the possible PCSK9-derived disturbance of cerebral lipid homeostasis may pave the way for the identification and development of specific promising pharmacological approaches.

MATERIALS AND METHODS

1. INFLUENCE OF PCSK9 ON CHOLESTEROL HOMEOSTASIS: *IN VITRO* EVIDENCE

1.1 GENERAL PROCEDURES

The *in vitro* studies were conducted upon two human immortalized cell lines: human astrocytoma U373 cells and human neuroblastoma SH-SY5Y cells, as cellular models of astrocytes [354] and neurons [355], respectively.

1.1.1 Cell cultures

Cell culture analyses were carried out in sterile conditions inside an incubator (Euroclone, Italy), which guarantees the optimal culturing conditions (37°C and 5%CO_2). For cell manipulation, a laminar flow biological safety cabinet (Angelantoni Life Science, Italy) was used, together with sterile disposable plastics (adhesion flasks suitable for cell culture, serological pipettes, tips, plastic tubes and plates).

Human U373 astrocytoma cells were identified and validated through the Cell Line Authentication Test (CLA; Eurofins Genomics Europe Applied Genomics GmbH, Germany) before the start of the experiments. Briefly, DNA isolation was carried out from cell pellet and the genetic characteristics were determined by PCR-single-locus-technology, confirming a 100% correspondence with the original American Type Culture Collection (ATCC) certified DNA and our cytogenetic analysis (**Table 1**). U373 cells were cultured in Dulbecco's Modified Eagle Medium (DMEM; Euroclone, Italy), supplemented with 2% v/v of L-Glutamine (Thermo Fisher Scientific, MA, USA), 1% of an antibiotic solution composed by Penicillin/Streptomycin (Thermo Fisher Scientific, MA, USA) and 10%v/v of heat-inactivated Fetal Calf Serum (FCS; Euroclone, Italy). U373 cells were sub-cultivated twice per week, using sterile Phosphate Buffer Saline solution (PBS; Euroclone, Italy) before the incubation with a sterile trypsin-EDTA solution (Thermo Fisher Scientific, MA, USA) for about 2-3 minutes to detach cells. U373 were centrifuged for 5 minutes at 1500 revolutions per minute (rpm) and then resuspended in a fresh cultured medium.

Human control and PCSK9-overexpressing SH-SY5Y neuroblastoma cells were specifically generated for this research project in collaboration with Professor N. Ferri from the University of Padua. Specifically, SH-SY5Y cells were retrovirally transduced to overexpress human PCSK9 and, in particular, retroviral expression plasmid has been

constructed using the pBM-IRES-PURO, expressing the puromycin resistance gene as a selectable second cistron gene. Human PCSK9-FLAH tag cDNA was kindly provided by Professor P. Tarugi from the University of Modena and Reggio Emilia, and subcloned into retroviral expression plasmid by blunt-end ligation [356]. Similarly to U373 cells, control and PCSK9-overexpressing SH-SY5Y cells were identified and validated through CLA (Eurofins Genomics Europe Applied Genomics GmbH, Germany) before starting the experiments. With the same experimental procedure previously described, a 100% correspondence with the original ATCC certified DNA and our cytogenetic analysis was confirmed in both the two analysed SH-SY5Y cell lines (**Table 1**). SH-SY5Y control and PCSK9-overexpressing cells were cultured in Dulbecco's Modified Eagle Medium (DMEM; Euroclone, Italy), supplemented with 2% v/v of L-Glutamine (Thermo Fisher Scientific, MA, USA), 1% of an antibiotic solution composed by Penicillin/Streptomycin (Thermo Fisher Scientific, MA, USA) and 20%v/v of heat-inactivated FCS (Euroclone, Italy). SH-SY5Y cells were sub-cultivated twice per week, using sterile PBS (Euroclone, Italy) before the incubation with a sterile trypsin-EDTA solution (Thermo Fisher Scientific, MA, USA) for about 2-3 minutes to detach cells. U373 were centrifuged for 3 minutes at 1000 rpm and then resuspended in a fresh cultured medium. Before each experimental procedure, SH-SY5Y cells were plated and terminally differentiated to neurons with 10μM all-trans retinoic acid (ATRA) for 6 days in DMEM supplemented with 1% v/v FCS, adding fresh medium every two days [357]. Control and PCSK9-overexpressing SH-SY5Y cells were previously characterized for their PCSK9's gene and protein expression, as well as for the secretion of PCSK9 enzyme in culture media. RT-PCR, Western Blot and ELISA assays, indeed, confirmed a marked increase in PCSK9 gene and protein expression ($p<0.001$ and $p<0.01$, respectively), together with a strong increase in PCSK9 release in culture medium as compared to control SH-SY5Y ($p<0.0001$), in which the enzyme was barely detectable. Similarly, the expression of the main lipoprotein receptors has been evaluated in SH-SY5Y cells, confirming a significant reduction in both LDLR and apoER2 in PCSK9-overexpressing SH-SY5Y as compared to controls (-60% and -37.5%, respectively; data not shown).

TABLE 1

Markers	U373 Cell line authentication	SH-SY5Y CTRL Cell line authentication	SH-SY5Y PCSK9 Cell line authentication
Amelogenin	X,Y	X,X	X,X
CSF1PO	11,12	11,11	11,11
D13S317	10,11	11,11	11,11
D16S539	12,12	8,13	8,13
D5S818	11,12	12,12	12,12
D7S820	10,12	7,10	7,10
TH01	9.3, 9.3	7,10	7,10
TPOX	8,8	8,11	8,11
vWA	16,18	14,18	14,18
D8S1179	13,15	15,15	15,15
D21S11	29,30	31, 31.2	31, 31.2
D3S1358	16,17	15,16	15,16
D2S1338	22,24	17,19	17,19
D19S433	13,15	13,14	13,14
D18S51	13,13	13,16	13,16
FGA	21,25	23.2, 24	23.2, 24

***Table 1**. Authentication of U373, SH-SY5Y CTRL AND SH-SY5Y PCSK9 cell lines.* DNA isolation was carried out starting from cells pellet and the genetic characteristics were determined by PCR-single-locus-technology, confirming a 100% correspondence with the original American Type Culture Collection (ATCC) for all the three considered cell lines.

1.1.2 $A\beta_{1-42}$ oligomers and fibrils preparation

The $A\beta_{1-42}$ oligomers and fibrils preparation procedure was carried out in sterile conditions under the laminar flow biological cabinet, following a protocol previously used in literature [358]. The commercial $A\beta_{1-42}$ peptide (Cayman Chemical, MI, USA) was resuspended in Hexafluoroisopropanol (HFIP; Merck, Germany) to a final concentration of 1mg/ml. This initial passage is fundamental to resuspend and monomerize the random pre-existing dried $A\beta_{1-42}$ aggregates. HFIP was then allowed to evaporate under a nitrogen stream and the resulting dried peptide film was resuspended in DMSO, with a final

concentration of 5mM. The obtained solution was then water-bath sonicated for 10 minutes to completely dissolve the eventually present random aggregates.

The $A\beta_{1-42}$ oligomers (2–3 nm diameter) were prepared starting from bath-sonicated $A\beta_{1-42}$ monomers, by diluting the 5mM DMSO solution in a 7.4 pH buffer, composed by 50mM phosphate buffer and 150mM NaCl, to a final 100µM concentration. The obtained solution was incubated at 4°C for 24 hours, then stored at -20°C until use.

The $A\beta_{1-42}$ fibrils (3–4 nm diameter) were prepared starting from bath-sonicated $A\beta_{1-42}$ monomers, by diluting the 5mM dimethyl sulfoxide (DMSO) solution in HCl 10mM with pH 2 to a final 100µM concentration. The obtained solution was incubated at 37°C for 72 hours, then stored at -20°C until use. Finally, Atomic Force Microscopy (AFM) was used to verify the actual and correct formation of the $A\beta_{1-42}$ fibrils, in collaboration with the Institute of Materials for Electronics and Magnetism (IMEM) of the Consiglio Nazionale delle Ricerche of Parma. Briefly, one drop of freshly-prepared $A\beta_{1-42}$ fibrils at a concentration of 10µM were incubated on a freshly—cleaved mica disk for 1-2 minutes, then the excess water was removed, the disks were dried under a nitrogen stream, and finally analyzed. As shown in **Figure 1**, the fibrillar preparation was extremely aggregated near the centre of the analyzed drop (right panel) and more diluted in the marginal zones of the drop. Importantly, the shape and size of the obtained $A\beta_{1-42}$ fibrils were similar to images previously reported in literature [358,359].

FIGURE 1

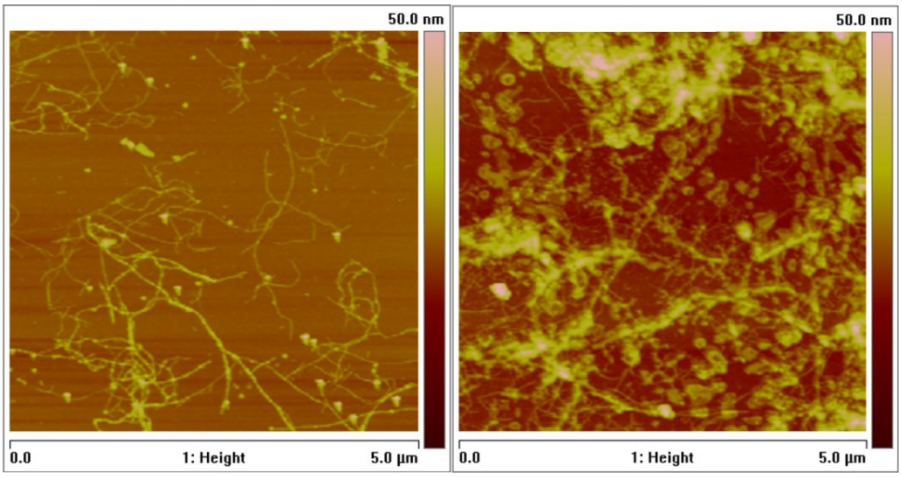

***Figure 1**. $A\beta_{1-42}$ fibrils visualization through AFM.* A drop containing $A\beta_{1-42}$ fibrils with a final concentration of 10 µM in H_2O was incubated on freshly-cleaved mica disks for about 1-2 minutes. Excess H_2O was then removed and the disks were dried under a nitrogen stream. The samples were then visualised through AFM. The figure on the left refers to $A\beta_{1-42}$ fibrils located on the marginal zone of the analyzed drop, while the right figure refers to more aggregated $A\beta_{1-42}$ fibrils in the centre of the drop.

1.1.3 rHDL-apoE preparation

Reconstituted HDL (rHDL) containing apoE, similar to the HDL-like particles retrieved in the human CSF, able to mediate *in vitro* cholesterol transport between astrocytes and neurons, were prepared following a protocol previously published [360]. Specifically, rHDL-apoE were prepared with the cholate dialysis procedure, using a Tris-HCl buffer solution composed of 10mM Tris-HCl, 140mM NaCl and 1mM EDTA, with a verified pH of 7.4. rHDL liposomes contained apoE/lecithin/cholesterol with a molar ratio of 1:100:2 and were prepared starting from a lipid mixture of unlabeled cholesterol (Merck, Germany), lecithin (Merck, Germany) and [1-2^{3}H]Cholesterol (Perkin Elmer, MA, USA), with an activity of 1mCi/ml, if needed by the experimental protocol. The mixture was further dried under a nitrogen stream. Then, the proper amount of apoE (Peprotech EC, UK) dissolved into Tris-HCl buffer with a concentration of 1mg/ml was added to the dried components, thus reaching the final concentration of apoE of 10μM. A final volume of 0.7 ml was then reached by adding Tris-HCl buffer. Then, a sodium cholate solution with a concentration of 725 nM, was added, following a molar ratio of lecithin : sodium cholate [1:8], to promote the formation of liposomes. The suspension was mixed for 2 minutes at room temperature, until reaching a clear solution. Then, the mixture was incubated for additional 2 hours at room temperature under a mild shaking and then extensively dialyzed for 48 hours at 4°C with Tris-HCl buffer, in order to remove the excess cholate. Finally, the obtained dialysate solution containing liposomes was brought to the final volume (e.g: 1ml) and then filtered to sterilize the preparation. To evaluate the non-apoE-mediated uptake of rHDL-contained cholesterol, a parallel identical solution, without apoE, was prepared. Furthermore, to evaluate cholesterol efflux from U373 cells, an identical preparation not containing [1-2^{3}H]Cholesterol was prepared. Protein concentration was detected through the Lowry colourimetric Assay as described in section 1.4.1.

rHDL-apoE liposomes were preliminarily tested by evaluating their ability to promote cholesterol efflux through the specific membrane transporters. Indeed, following the above-mentioned experimental protocol, rHDL-apoE should be characterized by an average size of about 9nm [360], similarly to spherical and mature HDLs, known to promote cholesterol efflux by interacting with ABCG1 transporter and through the aqueous diffusion process [361]. As expected, rHDL-apoE [10μM] were able to efficiently promote ABCG1-mediated cholesterol efflux as well as the aqueous diffusion process. On the other

side, as expected, rHDL-apoE ability to promote ABCA1-mediated cholesterol efflux was extremely low (data not shown).

1.2 CHOLESTEROL METABOLISM ASSAYS

The impact of PCSK9 on different cholesterol-related parameters in human U373 astrocytoma cells as well as in human neuroblastoma cells overexpressing or not PCSK9 was carried out through *in vitro* assays, aimed at evaluating the possible functional alterations, with radioisotopic and fluorometric techniques. For the most relevant parameters, the molecular analysis of the expression of specific receptors and transporters was performed.

1.2.1 Endogenous cholesterol biosynthesis

Endogenous cholesterol biosynthesis was evaluated by monitoring and quantifying the incorporation of a radioactive precursor (^{14}C-acetate) in the intracellular cholesterol synthetic process, adopting a protocol previously used in our laboratory to quantify cholesterol synthesis in cultured macrophages [362]. In particular, U373 cells were seeded with a density of 200000 cells/well in 12-well plates (Corning, MA, USA). After 24 hours, cells were treated, based on the specific experimental protocol, with DMEM supplemented either with 1% v/v (referred to as "basal") or 5%v/v and PCSK9 [5μg/ml] or activated simvastatin [10μM] for additional 24 hours. On the other side, SH-SY5Y control or PCSK9-overexpressing neuroblastoma cells were seeded in 12-well plates (Corning, MA, USA) with a density of 300000 cells/well. After the 6 days incubation with ATRA as previously described, cells were treated with a solution composed of DMEM supplemented with 1% v/v FCS (referred to as "Basal") or 5%v/v and $A\beta_{1-42}$ fibrils [1μM] or activated simvastatin [10μM], based on the specific experimental conditions, for 24 hours. Subsequently, both U373 and SH-SY5Y cells were incubated for other 24 hours with a solution of DMEM supplemented with 0.5% v/v of sodium acetate (with an initial concentration of 8mg/ml), 0,2% v/v ^{14}C-Acetate (with a radionuclide activity of 1mCi/ml), 0,4% v/v of FCS and, based on the specific experimental conditions with human recombinant PCSK9 [5μg/ml], $A\beta_{1-42}$ fibrils [1μM] or activated simvastatin [10μM]. The supernatant was then removed and the cell monolayer was washed with PBS, to remove any culture medium leftover.

The cell monolayer was then incubated overnight at 4 °C with 1ml/well of NaOH 0.1M, which promotes cell lysis and the release of cellular content in the suspension. Then, lipid extraction was carried out in a glass tube, previously cleaned with 0.2ml of a Methanol and Chloroform [1:2] solution for 2h at 60°C, until the complete evaporation. Specifically, 850µl of cell lysate, 400µl of an aqueous solution of KOH 50%w/v, 10µl of a solution of 2mg/ml of unlabeled cholesterol (Merck, Germany) dissolved in Ethanol, 10µl of a solution of [1-2^{3}H]Cholesterol (Perkin Elmer, MA, USA), containing a total of 10^{5} counts per minutes, and 2ml of ethanol were added into the previous-mentioned glass tube and incubated at 60°C for 1h, mixing each glass tube for 15'' every 15 minutes. Once cooled, the lipid extraction was then carried out by adding to each glass tube 2ml of ethanol, 400µl of deionized H_2O and 3ml of Petroleum Ether 40°-60°. Tubes were vortexed for 30'' and then the upper organic phase was collected with a glass Pasteur pipette and placed into a new glass tube. The operation was repeated with other 2ml of Petroleum Ether 40°-60°. Finally, the obtained organic solution containing the cellular lipid content was allowed to dry under a nitrogen stream.

The extracted and dried lipid phase was then resuspended into 65µl of Hexane and vortexed for 30'' to fully resuspend the sample; then 40µl of the so-obtained solution were seeded onto a thin liquid chromatography (TLC) glass plate. This latter is placed in the TLC tank, saturated with 50 ml of a mixture of Petroleum Ether 40°-60°, Diethyl ether and Acetic acid with a volume ratio of [70:30:1] for about one hour, then furtherly transferred into a new tank saturated with Iodine (I_2) that binds to the specific regions of the TLC plate in which free cholesterol is embedded, visualised thanks to the yellowish colour. Finally, using a scalpel, the specific regions of the TLC plate containing cholesterol were scratched and collected in specific vials suitable for radioactive quantification, as the newly-synthesized cholesterol corresponds to the ^{14}-C quantification in the isolated free cholesterol region of the TLC plate. Results were then expressed as total ^{14}C cpm on the total protein content of each sample.

The total amount of proteins in each cell monolayer was quantified after cell lysis using the Pierce Bicinconinic Acid (BCA) Assay (Thermo Fisher Scientific, MA, USA), as described in section 1.4.2.

1.2.2 Lipoprotein receptors expression

Lipoprotein receptors LDLR and apoER2 expression have been evaluated through Western Blot analyses in collaboration with Professor N. Ferri from the University of Padua. Specifically, U373 cells were plated in a 6-wells plate (Corning, MA, USA) with a density of 500000 cells/well and, 24 hours later, cells were treated with a solution composed of DMEM supplemented with 1% FCS (referred to as "Basal") and human recombinant PCSK9 [5μg/ml] for additional 48 hours, the last 24 of which with additional $A\beta_{1-42}$ fibrils [1μM] in the required conditions. Cell monolayers were then incubated for 5' in ice with the Ripa Buffer solution supplemented with a Protease Inhibitor Cocktail (Merck, Germany), followed by a vigorous scraping to fully promote cell lysis. The cell suspension was then centrifuged in 1.5ml tubes (VWR, PA, USA) at 10000 rpm, 4°C for 10 minutes and the supernatant was finally collected.

Total protein content was then quantified through the Pierce Bicinconinic Acid (BCA) Assay (Thermo Fisher Scientific, MA, USA), as described in section 1.4.2.

Subsequently, 40μg of each sample were loaded in precast sodium dodecyl sulphate-polyacrylamide gel electrophoresis (SDS-PAGE; BioRad, CA, USA) with a density gradient of 4-12%, enriched with 6.5μl of Sample Buffer (Thermo Fisher Scientific, MA, USA) as a sample dye. The SDS-PAGE gel was then soaked in the electrophoresis tank, filled with a specific Tris/Glycine/SDS Running Buffer (BioRad, CA, USA) and a voltage of 100V for about 1.5 hours was applied to separate proteins based on their molecular weight. The gel was then removed from the electrophoresis apparatus and soaked in Tris/Glycine/Methanol Transfer Buffer for about 10'. Subsequently, a "sandwich" was assembled by combining the SDS-PAGE with a polyvinylidene-fluoride membrane (PVDF; BioRad, CA, USA) previously activated in methanol, two layers of filter papers and two sponges, removing any air bubble eventually present. The so-formed sandwich was placed into the transfer tank, filled with Transfer Buffer and a voltage of 100V was applied for 2 hours, to allow the protein embedded in the SDS-PAGE to transfer into the PVDF membrane. PVDF membrane was then incubated for 1 hour at room temperature in a solution composed of TrisHCl, NaCl and TritonX-100 (TBS-T) supplemented with a 5% w/v of non-fat dried milk (BioRad, CA, USA). The membrane was then rinsed 3 times (about 15 minutes each) with TBS-T solution and subsequently incubated for 18 hours at 4°C with the primary antibody solution, composed by TBS-T buffer supplemented with

1% w/v of non-fat dried milk and the diluted primary antibody (LDLR and apoER2 from Novus Biological, MN, USA, and housekeeping protein β-Actin from Merck, Germany). The optimal dilution was obtained following the manufacturer's instructions. The membrane was then rinsed 3 times (about 10 minutes each) with the TBS-T solution and furtherly incubated with the secondary antibody solution, composed by TBS-T supplemented with 1% w/v of non-fat dried milk and the diluted secondary antibody (VWR, PA, USA), able to recognize the specific epitope upon the primary antibiotic. Finally, the membrane was rinsed again as previously described, to get rid of any antibody residual, and freshly reconstituted ECL reagent (Thermo Fisher Scientific, MA, USA) was incubated at dark for 1-5 minutes. The membrane was then analyzed using ChemiDoc (BioRad, CA, USA) chemiluminescent imaging system and protein quantification was finally obtained by measuring the pixels in each band through ImageJ Fiji software [363].

1.2.3 rHDL-apoE-mediated cholesterol internalization

Cholesterol internalization was evaluated by measuring the radioactivity in cell monolayers following the incubation with rHDL-apoE containing radiolabelled cholesterol. Briefly, U373 cells were seeded in a 24-wells plate (Sarstedt, Germany), with a density of 100000 cells/well and treated with human recombinant PCSK9 [5μg/ml] for 48 hours. On the other side, SH-SY5Y control and PCSK9-overexpressing neuroblastoma cells were seeded in a 24-well plate (Sartsted, Germany) with a density of 300000 cells/well and incubated for 6 days with DMEM supplemented with 1% FCS and All Trans-Retinoic Acid (ATRA) [10μM], adding fresh medium every two days, to allow SH-SY5Y to revert their phenotype into fully-differentiated neurons [357]. Both U373 and SH-SY5Y cells were treated with a solution composed of DMEM supplemented with 5% v/v of LPDS for 48 hours, the last 24 of which with additional $A\beta_{1-42}$ fibrils [1μM] in the required conditions. Then, DMEM supplemented with either rHDL-apoE [10μg/ml] or rHDL not containing apoE, prepared as described in section 1.1.3, and containing a small amount of [1-2^{3}H] Cholesterol, was incubated for 4hours at 37°C, to allow reconstituted HDL particles to interact with lipoprotein receptors, if expressed, being thus internalized into astrocytes. Cell monolayers were washed with PBS, to remove any possible residue of culture medium, and then incubated for 18 hours at 4°C with 300μl/well of NaOH 1N, to promote cellular lysis [157]. An aliquot of 100μl for each sample was finally collected to quantify the radioactivity inside the cell monolayers, which is proportional to the apoE-

mediated cholesterol internalization, while another aliquot of 25µl was used to quantify the total protein content in cell monolayers through BCA assay, as described in section 1.4.2. Results were finally expressed as cpm on total protein content.

1.2.4 Intracellular cholesterol content

Intracellular cholesterol content was evaluated through its quantification in cell monolayers with a commercially available kit. Specifically, U373 cells were seeded in a 24-wells plate (Sarstedt, Germany), with a density of 100000 cells/well. After 24 hours, cells were treated with a solution composed of DMEM supplemented with 1% v/v of FCS (referred to as "Basal") and human recombinant PCSK9 [5µg/ml] for other 48 hours, the last 24 of which with additional $A\beta_{1-42}$ fibrils [1µM] in the required conditions. Cell monolayers were then incubated for 18h at 4°C with 250µl of a solution composed of Sodium chloride 0.05M, Cholic acid 5mM and TritonX-100 0.1% v/v and 50U/ml of Deoxyribonuclease I from bovine pancreas (Merck, Germany) to promote cell lysis. 62.5µl of Reaction Buffer provided by the commercial kit Amplex® Red Cholesterol assay (Thermo Fisher Scientific, MA, USA) were then added to each well and incubated for an additional 30'. Cell lysis was furtherly promoted through mechanical homogenization, then samples were transferred to 1.5ml tubes (VWR, PA, USA), bath-sonicated for 30' and incubated for other 30' at 60°C. The cholesterol content of each sample was finally quantified through the fluorescent Amplex® Red Cholesterol assay kit following the manufacturer's instructions. Briefly, following the incubation for 30' of a small sample aliquot (50µl) with 50µl of the Amplex Red solution (300 µM Amplex® Red fluorescent dye, 2U/ml Cholesterol oxidase, 0.2U/ml Cholesterol esterase and 2U/ml Horseradish Peroxidase, all dissolved in Reaction buffer), fluorescence was recorded after 20 minutes using an excitation wavelength of 535nm and an emission wavelength of 590nm. Cholesterol concentration in each sample was finally derived by interpolating the absorbance of each sample on the linear response curve derived from the standard scale, with cholesterol concentrations ranging from 3µg/µl to 0µg/µl. Data were expressed as µg of cholesterol over mg of the proteins contained in cell monolayer, determined through the Pierce Bicinconinic Acid (BCA) Assay (Thermo Fisher Scientific, MA, USA), as described in section 1.4.2.

1.2.5 Membrane cholesterol content

Membrane cholesterol content was quantified based on a radioisotopic assay widely used in our laboratory on macrophages cell line [364], based on the utilization of the specific cholesterol oxidase enzyme, able to oxidate cholesterol specifically localized in the cell membrane. In particular, U373 cells were seeded in a 12-well plate (Corning, MA, USA) with a density of 200000 cells/well. Cells were then incubated for 24 hours with a solution composed of DMEM supplemented with 1% FCS, 3µCi/ml of [1-2^{3}H]Cholesterol (Perkin Elmer, MA, USA), and an ACAT-inhibitor compound (Sandoz; Merck, Germany) at a concentration of 2 µg/ml. Then, human recombinant PCSK9 [5µg/ml] dissolved in DMEM and supplemented with 1% FCS was added for 24 hours as a pre-treatment. Cells were subsequently treated with a solution composed of DMEM supplemented with 0.2% w/v of BSA (referred to as "Basal") or with LXR/RXR agonists 22-OHC/9cRA at a final concentration of [5µg/ml] and [10µM], respectively, for 18 hours. Human recombinant PCSK9 [5µg/ml] and $A\beta_{1-42}$ fibrils [1µM] were added in the specific required experimental conditions. Probucol [10µM], a compound that was previously demonstrated to reduce membrane cholesterol content [364], was added for 2 hours. Finally, Cholesterol oxidase from *Streptomyces* (1U/ml) dissolved in PBS was incubated for 2 hours, then cell monolayers were dried for the following lipid extraction phase.

Lipids were then extracted from the cell monolayer by adding 0.6ml of isopropanol to each well for 18 hours; isopropanol containing the total cellular lipid content was then transferred in clean glass tubes (VWR, PA, USA) and a nitrogen stream was applied to promote the solvent's evaporation. Dried samples were then resuspended in 30µl of a solution composed of free cholesterol [20mg/ml] (Merck, Germany) and oleate cholesterol [10mg/ml] (Merck, Germany), dissolved in Chloroform : Methanol [1:1]. 25µl of the resuspended sample were finally seeded into a TLC plate. 25µl of a solution of Cholest-4-en-3-one [2mg/ml] (Merck, Germany) dissolved in Chloroform : Methanol [1:1] were additionally seeded into each TLC lane. Finally, TLC plate was placed in the TLC tank, previously saturated with 100 ml of a mixture of 90ml of Hexane, 10ml of Diethyl ether and 1ml of Methanol for about one hour, then furtherly transferred into a new tank saturated with Iodine (I_2) that binds to the specific regions of the TLC plate in which free cholesterol, oxidate cholesterol (Cholest-4-en-3-one) and cholesterol ester (oleate cholesterol) is embedded, visualized thanks to the yellowish colour. Finally, using a

scalpel, the specific regions of the TLC plate were scratched and collected in specific vials suitable for radioactive quantification.

Results were expressed by calculating the percentage of oxidate cholesterol, derived from the incubation with Cholesterol oxidase enzyme and index of membrane cholesterol content, upon the total cell cholesterol content, calculated as the total cpm of free, oxidate and esterified cholesterol.

1.2.6 Cholesterol efflux

Cholesterol efflux from U373 astrocytoma cells has been evaluated through a radioisotopic technique widely used in our laboratory to evaluate cholesterol efflux from cultured macrophages [365]. Specifically, U373 cells were seeded in a 96-well plate (Corning, MA, USA) with a density of 18000 cells/well. Subsequently, cells were radiolabelled with a solution composed of DMEM supplemented with 1% FCS, 2µCi/ml of [1-^{2}^{3}H]Cholesterol (Perkin Elmer, MA, USA), and an ACAT-inhibitor compound (Sandoz; Merck, Germany) at a concentration of 2 µg/ml, together with $A\beta_{1-42}$ fibrils [1µM] where specifically required by the experimental protocol. After 24 hours, a solution containing DMEM supplemented with 0,2% BSA, the ACAT-inhibitor compound and human recombinant PCSK9 [5 µg/ml], where required, was added to each well for 32 hours. Subsequently, cells were treated with a solution composed of DMEM supplemented with 0.2% BSA and the ACAT-inhibitor compound alone (Basal, non-stimulated cells) or with a solution composed of DMEM supplemented with 0.2% BSA, the ACAT-inhibitor and LXR/RXR agonists 22-OHC/9cRA at a final concentration of [5µg/ml] and [10µM], respectively (LXR/RXR stimulated cells). Again, human recombinant PCSK9 [5 µg/ml] was added in the specific required conditions. Finally, cells were incubated for 6 hours with two different solutions of DMEM supplemented with cholesterol acceptors human recombinant lipid-free apoE [10µg/ml] and rHDL-apoE [10µg/ml], able to promote ABCA1- and ABCG1-mediated cholesterol efflux, respectively [360,366]. Specifically, rHDL-apoE were prepared as described in section 1.1.3 and they only contained unlabelled free cholesterol. The cellular medium was then collected and the radioactivity was quantified in each sample supernatant. A set of cell monolayers were washed with PBS before the incubation with cholesterol acceptors, to evaluate the cholesterol amount inside the cells before the efflux phase. These specific samples were subjected to lipid extraction with 200µl of isopropanol for 18 hours. Then, the extracts were transferred into a clean glass

tube (VWR, PA, USA) and brought to dryness under a nitrogen stream. The lipid extracts were then resuspended in 500µl of toluene, from which 200µl were taken and the inner radioactivity was finally quantified. Cholesterol efflux was indeed calculated as the percentage of radioactivity released into the medium compared to the radioactivity incorporated by the cells before the addition of the acceptors.

1.2.7 ABCA1 transporter expression

ABCA1 transporter expression has been quantified through Western Blot analyses. To this aim, U373 cells were plated in a 6-wells plate (Corning, MA, USA) with a density of 500000 cells/well and, 24 hours later, cells were treated with a solution composed of DMEM supplemented with 1% FCS, an ACAT-inhibitor compound (Sandoz; Merck, Germany) at a concentration of 2µg/ml, together with $A\beta_{1\text{-}42}$ fibrils [1µM] where specifically required by the experimental protocol. After 24 hours, a solution containing DMEM supplemented with 0,2% BSA, the ACAT-inhibitor compound and human recombinant PCSK9 [5µg/ml], where required, was added to each well for 32 hours. Subsequently, cells were treated with a solution composed of DMEM supplemented with 0.2% BSA and the ACAT-inhibitor compound alone (Basal, non-stimulated cells) or with a solution composed of DMEM supplemented with 0.2% BSA, the ACAT-inhibitor and LXR/RXR agonists 22-OHC/9cRA at a final concentration of [5µg/ml] and [10µM], respectively (LXR/RXR stimulated cells). Again, human recombinant PCSK9 [5µg/ml] was added in the specific required conditions. Cell monolayers were then incubated for 5' in ice with the Ripa Buffer solution supplemented with a Protease Inhibitor Cocktail (Merck, Germany), followed by a vigorous scraping to fully promote cell lysis. The cell suspension was then centrifuged in 1.5ml tubes (VWR, PA, USA) at 10000 rpm, 4°C for 10 minutes and the supernatant was finally collected.

Total protein content was then quantified through the Pierce Bicinchoninic Acid (BCA) Assay (Thermo Fisher Scientific, MA, USA), as described in section 1.4.2.

Western Blot analyses were carried out as specifically described in section 1.2.2, using as primary antibody the anti-human ABCA1 (Novus Biological MN, USA) with an optimal dilution obtained following manufacturer's instructions.

1.3 CELLULAR VIABILITY ASSAY

Cell viability was quantified through the MTT assay, based on the ability of the cell's mitochondrial enzyme succinate dehydrogenase to reduce the tetrazolium yellow dye MTT (-(4,5-dimethylthiazol-2-yl)-2,5-diphenyltetrazolium bromide; Merck, Germany) to its insoluble salt, formazan. Briefly, U373 cells were seeded in 96-well plates (Corning, MA, USA) with a density of 18000 cells/well. After 24 hours, cells were treated with a solution of DMEM supplemented with 1% FCS and human recombinant PCSK9 [5µg/ml], together with increasing concentrations of $A\beta_{1-42}$ oligomers and fibrils ([1µM] and [10µM]) for 48 hours. On the other side, SH-SY5Y control and PCSK9-overexpressing neuroblastoma cells were seeded in 48-well plates (Corning, MA, USA) with a density of 120000 cells/well and treated for 6 days with ATRA to revert their phenotype to fully differentiated neurons, as previously described. To evaluate the impact of cholesterol depletion or excess on neuronal viability in the presence or absence of PCSK9, cells were treated for 48 hours with a solution composed by DMEM supplemented wither with 1% FCS v/v (referred to as "Basal"), BSA 0.2% w/v or cholesterol [25µM]. Conversely, to evaluate the impact of $A\beta_{1-42}$ aggregates at different concentrations in the presence or absence of PCSK9, cells were treated for 48 hours with $A\beta_{1-42}$ oligomers and fibrils, both at the increasing concentrations of [1µM], [5µM] and [10µM].

MTT assay was performed by incubating cells for 2 hours at 37°C with a solution of cell culture medium DMEM supplemented with 1% FCS and MTT [1mg/ml]. Since MTT salt is a photosensitive dye, the incubation was carried out away from any light sources. The supernatant was then removed and 300µl of DMSO were added to each well to solubilize the newly-formed purple formazan. An aliquot of the suspension was then collected and the absorbance was quantified through the spectrophotometer at 570nm. Cell viability of each experimental condition was then calculated by comparing the absorbance of the specific sample with the absorbance of the non-treated cells (basal) and expressed as percentage viability as compared to basal.

1.4 PROTEIN DETERMINATION ASSAYS

1.4.1 Lowry assay

Protein concentration in rHDL-apoE particles was detected through the Lowry colourimetric Assay, which allows to quantify the protein content in lipoparticles, due to the presence of the anionic detergent sodium dodecyl sulphate (SDS). Briefly, 10µl of filtered rHDL-apoE were incubated for 10 minutes at 37°C with 13µl of SDS, 187µl of Tris-HCL and 1ml of a mixture of Reagent A (7mM NaK tartrate, 0.81M sodium carbonate and 0.5N NaOH) and Reagent B (70 mM Na-K tartrate, 40 mM copper sulfate) with a volume ratio of [50:1]. Afterwards, 100µl of a solution composed of Folin-Cicolteau (Merck, Germany) and H2O with a volume ratio of [1:1] was added to each sample and furtherly incubated for 20 minutes at 37°C. An aliquot of 300µl was then collected and the absorbance at 550nm was recorded. Protein concentration was then determined by interpolating the absorbance of the sample with the absorbance of a standard scale with known protein concentration, ranging from 0µg/µl to 100µg/µl.

1.4.2 Bicinchoninic acid (BCA) assay

Total protein content was indeed quantified through the Pierce Bicinconinic Acid (BCA) Assay (Thermo Fisher Scientific, MA, USA), following the manufacturer's instructions. This assay is based on the biuret reaction, in which the reduction of Cu^{2+} to Cu^{+} by protein with the following complexation with BCA produces a purple colour that is proportional to the protein concentration in each sample. Briefly, 25µl of each sample were incubated with 200µl of a solution composed of Reagent A (BCA/tartrate in alkaline carbonate buffer) and Reagent B (4% CuSO2 · 5H2O) [50:1] for 20' at RT. The absorbance of each sample was then measured at 550nm using a spectrophotometer. A standard scale containing a known protein concentration, ranging from 0µg/ml to 100µg/ml, and protein concentration was derived by interpolating the absorbance of each sample on the linear response curve derived from the standard scale.

2. *EX VIVO* STUDIES ON AD TRANSGENIC MICE MODELS AND HUMANS

Cholesterol and its main oxidised metabolites, hydroxysterols, have been evaluated through *ex vivo* studies on biological samples isolated from both transgenic mice, specifically generated within the present research project, and a population of subjects with different degrees of cognitive impairment.

2.1 ANIMAL MODELS

A new transgenic mouse has been generated in collaboration with Professor D. Giuliani from the University of Modena and Reggio Emilia. Specifically, PCSK9$^{-/-}$ (PCSK9^{ko}) mice purchased from the Jackson Laboratories (B6;129S6-Pcsk9^{tm1Jdh}/J) were crossed with 5XFAD$^{+/-}$ (5XFAD^{he}) mice. 5XFAD^{he} mice are characterized by the expression of human APP and PSEN1 transgenes, carrying five mutations associated with familial AD: Swedish (K670N/M671L), London (V7171) and Florida (I716V) on APP gene and M146L and L286V on PSEN1 gene. Hence, 5XFAD^{he} mice have an early and aggressive presentation of several AD-related phenotypes, such as Aβ plaques deposition, gliosis and neuronal loss, together with a plethora of cognitive as well as motor deficits [367]. The above-mentioned mice were bred in the Specific Pathogen Free (SPF) animal facility of the University of Modena and Reggio Emilia (CSSI) following the ministerial approval (511/2019-PR, 19-07-2019). Mice were grown in rooms with a stable temperature of 21°C and humidity of 60%, with lights/dark cycles of 12 hours. The specific breeding scheme is reported in **Figure 2**, and the experimental analyses were performed upon 10 months-old mice belonging to the second filial generation (F2).

FIGURE 2

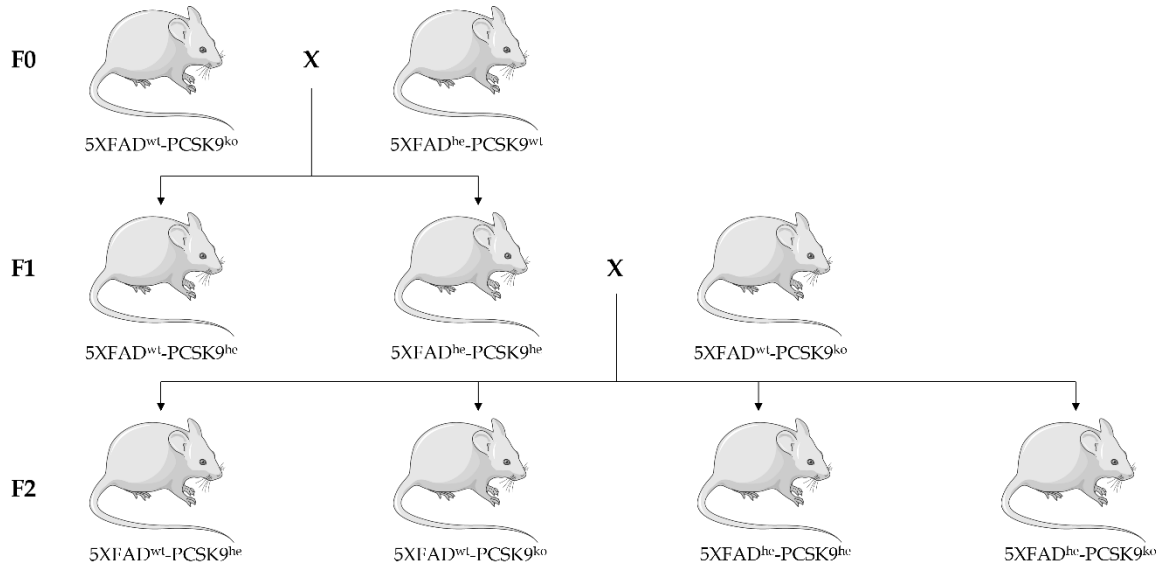

***Figure 2**. Breeding scheme of the newly generated transgenic mouse model.* 5XFAD^{wt}-PCSK9^{ko} and 5XFAD^{he}-PCSK9^{wt} mice (F0) were crossed to obtain either 5XFAD^{wt}-PCSK9^{he} and 5XFAD^{he}-PCSK9^{he} mice; these latter were furtherly crosse with 5XFAD^{wt}-PCSK9^{ko} mice (F1), to finally obtain the F2 generation (5XFAD^{wt}-PCSK9^{he}, 5XFAD^{wt}-PCSK9^{ko}, 5XFAD^{he}-PCSK9^{he} and 5XFAD^{he}-PCSK9^{ko}), upon which the reported analyses have been performed.

Finally, the four experimental groups belonging to the F2 generation were furtherly compared to WT and 5XFAD^{he} mice, both carrying two WT PCSK9 alleles, to investigate a possible gene-dependent effect of PCSK9 presence, and, specifically, WT – PCSK9^{wt} and 5XFAD^{he} – PCSK9^{wt} mice.

2.2 PATIENTS POPULATION

In collaboration with Professor M. Bertolotti of the Center for Cognitive Neurology of the Modena City Hospital and University of Modena and Reggio Emilia, a cohort of 83 patients followed between 2011 – 2017 were recruited and a case-control study was set up. Specifically, patients were followed for the early diagnosis and differential diagnosis of cognitive disorders. During the first visit, patients were subjected to clinical, neuropsychological, neuroradiological (brain CT or MRI) evaluations, and blood analyses, as well as CSF analyses, were carried out. A clinical follow-up was then maintained. Based on the obtained clinical parameters, patients were classified into three different groups:

- Patients with a diagnosis of MCI, with a stable clinical behaviour at follow-up (MCI; n= 28);

- Patients with a diagnosis of MCI, whose clinical picture at follow-up furtherly degenerated and was compatible with a diagnosis of AD (MCI-AD; n=27);

- Patients with an established diagnosis of AD at the initial clinical evaluation (AD, n=28).

All patients gave written informed consent, previously approved by the local Ethics Committee.

2.3 CHOLESTEROL QUANTIFICATION

Total cholesterol quantification was achieved through a commercially available fluorometric assay, by slightly modifying the manufacturer's instructions based on the required experimental procedure.

2.3.1 Cholesterol quantification in serum and CSF

Peripheral blood was collected in Vacutainer tubes after the sacrifice from 10 months-old mice and in patients after 1-night fasting; serum was immediately isolated by centrifuging tubes at 2000 g for 10' at 4°C and collecting the resulting supernatant into a new tube. Serum was then immediately stored at -80°C until use. CSF was isolated through lumbar puncture for the clinical diagnosis of patients and immediately stored at -80°C.

The fluorometric Amplex® Red Cholesterol assay (Thermo Fisher Scientific, MA, USA) was then used to quantify serum and CSF cholesterol content, following the manufacturer's instruction, also described in section 1.2.4. Several analyses were performed to optimize the correct dilution factor for each biological matrix. Hence, serum, both from mice and humans was diluted 1:200, while CSF was tested with a 1:2 dilution factor.

2.3.2 Cholesterol quantification in brain

Brain was collected after mice's sacrifice and immediately soaked in liquid nitrogen, to ensure rapid freezing, then stored at -80°C until use. To quantify brain cholesterol content, the right hemisphere was collected and weighted, then shredded with the help of a ceramic pestle and the obtained brain homogenate was intensively shaken and placed into a glass tube, furtherly incubated for 2 hours with 0.5ml of PBS. Then, 5ml of the Folch Solution, composed of Chloroform and Methanol in a [2:1] v/v ratio, were added to each sample and furtherly incubated for 24 hours. This extraction phase is crucial to separate non-polar lipids from the polar compounds in the cerebral tissue. Then, 2ml of PBS were furtherly added to each sample to better visualize the polar (upper) and the non-polar lipid-rich phase (lower), and the tube was finally centrifuged for 10 minutes at 2000 rpm. The non-polar phase was then collected and placed into a clean glass tube and the solvent was brought to dryness under a nitrogen stream.

The lipid extract was then resuspended in Reaction Buffer, composed of 0.5 M potassium phosphate, 0.25 M NaCl, 25 mM cholic acid and 0.5% Triton X-100, bath-sonicated for 30' and furtherly incubated for other 30' at 60°C, to facilitate the complete sample resuspension. The fluorometric Amplex® Red Cholesterol assay (Thermo Fisher Scientific, MA, USA) was then used to quantify brain cholesterol content, following the manufacturer's instruction, also described in section 1.2.4. Brain samples were diluted before testing, with an optimal dilution of 1:500, obtained based on preliminary analyses and were expressed as μg of cholesterol over mg of tissue.

2.4 HYDROXYSTEROLS QUANTIFICATION

The quantification of the three main hydroxysterols in mice's sera and brains and patients sera and CSF was achieved by liquid chromatography-tandem mass spectrometry (LC-MS/MS), by adopting and optimizing some previously published experimental protocols [221,368,369].

2.4.1 Alkaline hydrolysis

Sera and CSF were allowed to gently thaw in ice, then, a small aliquot of 0.2ml of serum, both for mice and humans, and an aliquot of 0.5ml of CFS were collected and placed into a clean glass tube, together with Butylated hydroxytoluene [0.1μg/μl] as an antioxidant agent, and 1ml of a solution composed of NaOH 1M dissolved in Ethanol

90%. With respect to mice's brains, left hemispheres were weighed, homogenized and underwent Folch extraction as described in section 2.3.2. Then, 1ml of NaOH 1M dissolved in Ethanol 90% and Butylated hydroxytoluene [0.1µg/µl] were added to the dried lipid extract. Alkaline hydrolysis was then carried out at 60°C for 2 hours. Once the samples were cooled, 1 ml of 0.9% w/v was added to each glass tube, together with 2ml of Petroleum Ether 40°-60°. Glass tubes were then vigorously mixed and the upper phase containing the extracted lipids was collected with a glass Pasteur pipette and placed into a new glass tube. The same operation was repeated by adding 1 additional ml of Petroleum Ether 40°-60°, then the extracted lipid phase was brought to dryness under a nitrogen stream.

2.4.2 Solid phase extraction

Solid Phase Extraction (SPE) was carried upon the lipid extract to remove its cholesterol content and to finally purify the hydroxysterols. Lipid extracts from serum, CSF and brain were indeed resuspended in 2 ml of a solution composed of deionized H_2O supplemented with 5% v/v of Methanol and mixed vigorously to allow the complete resuspension of the dried samples. SPE was performed through SPE Cartridges C18 (Waters, MA, USA), by loading the silica cartridges columns with the following experimental procedure:

- 2ml of Methanol. The eluate was discarded;
- 2ml of deionized H_2O supplemented with 0.1% v/v of Formic acid. The eluate was discarded;
- 2ml of the lipid extract resuspended as previously described: the elution flow was maintained extremely slow to facilitate the binding of the sterol fraction to the silica cartridges. The eluate was again discarded;
- 1ml of deionized H_2O supplemented with 0.1% v/v of Formic acid. The eluate was discarded;
- 1ml of Hexane. The eluate, which contains cholesterol, was discarded;
- 2ml of Ethyl Acetate. The eluate, which contains the hydroxysterols fraction of the biological sample was finally collected into a 2ml plastic tube (VWR, PA, USA) and brought to dryness using a nitrogen stream.

2.4.3 LC-MS/MS analysis

24-, 25- and 27-OHC quantification in serum, CSF and brain specimens was achieved by LC-MS/MS analysis, in collaboration with Professor L. Elviri from the University of Parma. Once the extracts were dried, 100µl of Methanol enriched with 1µg/µl of 24-, 25 and 27-deuterated OHC, used as internal standards, were added to each sample. Each tube was vigorously shaken and water-bath sonicated for 10 minutes, to ensure the complete sample resuspension, and finally centrifuged for 10' at 15000rpm. The supernatant was then collected and placed into specific vials suitable for LC-MS/MS analyses. Samples were eluted using a column C18 Synergi Hydro-RP (150mm x 3mm, 80A, 4µm particles; Phenomenex, CA, USA), equipped with a C18 pre-filtering column. The mobile phase was composed of Methanol : acetonitrile : H_2O [14:1:0.6], added with 0.1% v/v formic acid. The elution was isocratic at a flow rate of 200µl/min for 50 minutes, the injection volume was 20µl and each sample was injected in duplicate.

The analysis was carried out using an Agilent HP 1200 chromatographic system (Agilent Technologies, CA, USA), equipped with a 100-vial capacity sample tray and coupled with a QTRAP 4000 triple quadrupole mass spectrophotometer (ABSCIEX, CA, USA), equipped with a pneumatically assisted ESI interface. Nitrogen (99.99% of purity) was used as a sheat gas and the auxiliary gas was delivered at flow rates of 45 and 5 arbitrary units, respectively. Optimized conditions of the interface were the following:

- ESI voltage 5.5 kV;
- Desclustering potential (DP) 35V;
- Entrance potential (EP) 10V;
- Collision exit potential (CXP) 10V;
- Capillary temperature 350°C.

Experiments were performed under positive ion-selected reaction monitoring conditions, using nitrogen as a collision gas (pressure of 2.1 x 10-3 mbar). The analytical method performed was initially set up by using 24-, 25- and 27-OHC spiked with 1µg/µl of the respective deuterated internal standard. The quantification of the analytes in serum, CSF and brain was performed through calibration curves with a known concentration of the standards dissolved in Methanol, with concentrations ranging from 0.5µg/µl to 5µg/µl.

2.5 PCSK9 QUANTIFICATION

Human PCSK9 was quantified in serum and CSF specimens obtained from the above-mentioned patient's population using a commercially available ELISA assay kit (R&D System, MN, USA), following the manufacturer's instructions.

3. STATISTICAL ANALYSES

Statistical analyses have been performed using Prism 7 software (GraphPad Software, CA, USA). *In vitro* studies have been performed in triplicate and each experiment has been repeated twice; the reported values are expressed as mean ± standard deviation (SD). The *ex vivo* evaluations have been performed in duplicate, reporting the mean value of each quantification. The Kolmogorov-Smirnov test was used to determine the normality of the distribution and skewed variables were compared by the Kruskal-Wallis test, using Dunnett's post-hoc test for multiple comparisons. Continuous variables were reported as mean ± standard deviation (SD) for normal distributions or as median (interquartile range [IQR] defined as the 25th percentile – 75th percentile) for skewed distribution. Statistically significant differences among the mean values of each experimental group were investigated using the one-way or two-way analysis of variance (ANOVA), based on the specific experimental requirements, for normally distributed data, while skewed variables were compared by the Kruskal-Wallis test. The post-doc Tuckey's multiple comparison test was used to compare each experimental condition in one-way ANOVA analyses, while the post-hoc Sidak's multiple comparison test was used in two-way ANOVA analyses.

RESULTS

1. INFLUENCE OF PCSK9 ON CHOLESTEROL HOMEOSTASIS: *IN VITRO* EVIDENCE

The possible influence of PCSK9 on the key steps of brain cholesterol transport from astrocytes to neurons was evaluated through *in vitro* studies, using human cultured cell models of astrocytes and neurons. The most relevant cholesterol-related parameters were evaluated and, to simulate *in vitro* an experimental picture similar to the *in vivo* anatomopathological alteration typical of AD, most of the parameters have been evaluated in cells incubated with $A\beta_{1-42}$ fibrils.

1.1 INFLUENCE OF PCSK9 ON CHOLESTEROL HOMEOSTASIS IN HUMAN ASTROCYTOMA CELLS

The impact of human recombinant PCSK9 was first evaluated in a human astrocytoma cell line, in order to analyse the first step of brain cholesterol transport. To this aim, human astrocytoma cells U373 were incubated with exogenous PCSK9 and different aspects contributing to cellular cholesterol homeostasis and viability were evaluated.

1.1.1 Impact of PCSK9 on cell viability in presence of $A\beta_{1-42}$

The impact of exogenous recombinant PCSK9 on U373 astrocytoma cell viability was initially investigated. Furthermore, to identify the optimal aggregation form and concentration of $A\beta_{1-42}$, the impact of $A\beta_{1-42}$ oligomers and fibrils at [1µM] and [10µM] was evaluated either in the presence or absence of exogenous PCSK9. As shown in **Figure 1**, the treatment with exogenous PCSK9 [5µg/ml] didn't produce any changes in cell viability as compared to the basal condition, in absence of PCSK9. Focusing on the impact of $A\beta_{1-42}$ oligomers, as seen in **Figure 1A**, a dose-dependent reduction of cellular viability was observed, with a decrease of about 11% ($p<0.05$) and 44% ($p<0.0001$) compared to the basal condition with oligomers at 1µM and 10µM, respectively. In these conditions, PCSK9 incubation didn't further modify cellular viability, since in presence of $A\beta_{1-42}$ oligomers, both at 1µM and 10µM, a similar reduction of viability was observed in cells exposed or not to exogenous PCSK9.

FIGURE 1

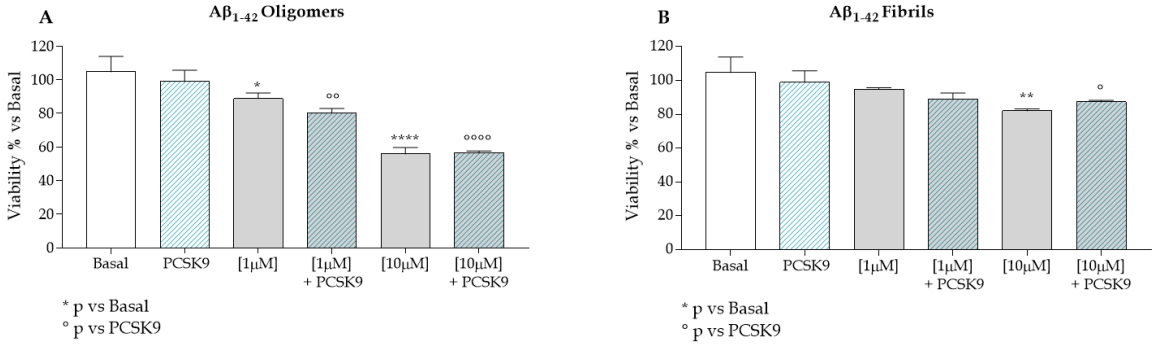

Figure 1**. Impact of PCSK9 on cell viability in presence of Aβ1-42 oligomers (**A**) and fibrils (**B**) in cultured human U373.* U373 astrocytoma cells were treated for 48h with different concentrations of $A\beta_{1-42}$ oligomers or fibrils and subsequently exposed (striped bars) or not (plain bars) to human recombinant PCSK9 [5μg/ml] for the following 24 hours. Cell viability was then assessed through the MTT colourimetric assay. Data were performed in triplicate and expressed as mean ± standard deviation. Statistical analyses were performed using the one-way ANOVA test, with the post-hoc Tuckey's multiple comparison test. A value of $p<0.05$ was considered statistically significant. * refers to Basal and ° to PCSK9-treated cells. * and ° $p<0.05$; ** and °° $p<0.01$; * and °°°° $p<0.0001$.

Finally, as shown in **Figure 1B**, in absence of any cytotoxic effect of PCSK9, the incubation with $A\beta_{1-42}$ fibrils led to a minimal reduction of cell viability, that becomes statistically significant only at 10μM, with a reduction of about 17% ($p<0.01$) and 13% ($p<0.05$) compared to basal and PCSK9-treated cells, respectively.

Thus, $A\beta_{1-42}$ fibrils at 1μM were selected to perform the experiments described in the following paragraphs, in order to investigate the impact of PCSK9 on cholesterol-related parameters in AD-like conditions, but in absence of any cytotoxic effect induced by the incubation of this latter factor. Furthermore, $A\beta_{1-42}$ fibrils represent the most common neuropathological aggregation form retrieved in brain sections of AD patients [370].

1.1.2 Impact of PCSK9 on endogenous cholesterol biosynthesis

The first cholesterol-related parameter analysed was the impact of PCSK9 on endogenous cholesterol biosynthesis in U373 astrocytoma cells. To this aim, the experimental conditions were first set up by adopting a protocol that has been previously used by our group to evaluate endogenous cholesterol biosynthesis in cultured macrophages [362]. The obtained results clearly indicated that also in U373 astrocytoma cells, endogenous cholesterol synthesis was detectable and modulable. Indeed, in U373 cells cultured with 1% v/v of FCS, the incubation with simvastatin [10μM] for 48 hours, known to inhibit HMG-CoA reductase enzyme and therefore to downregulate the cholesterol biosynthetic pathway [371], led to a significant reduction of endogenous

cholesterol biosynthesis compared to basal cells (-30%, $p<0.01$). Interestingly, a similar reduction in endogenous cholesterol synthesis rate (-32%, $p<0.001$) was observed in cells cultured with 5% v/v of FCS, probably as a consequence of a reduced need for synthesizing cholesterol (data not shown). Once set the optimal experimental conditions, the impact of PCSK9 on astrocytes cholesterol biosynthesis was assessed. As reported in **Figure 2A**, the effect of increasing concentrations of PCSK9, ranging from [2.5µg/ml] to [10µg/ml], was tested first, showing that, starting from [5µg/ml], PCSK9 significantly increased endogenous cholesterol biosynthesis in astrocytes ($p<0.01$ vs basal), with an even more pronounced effect at [10µg/ml] ($p<0.001$ vs basal, r^2 for dose-response=0.8816). Thus, the minimal effective PCSK9 concentration of [5µg/ml] was selected to evaluate endogenous cholesterol biosynthesis, confirming the previously described increase of cholesterol synthesis rate induced by the enzyme (**Figure 2B**). In this context, the endogenous cholesterol biosynthetic pathway wasn't affected by the concomitant incubation with $A\beta_{1-42}$ fibrils [1µM], neither in the absence or presence of PCSK9.

FIGURE 2

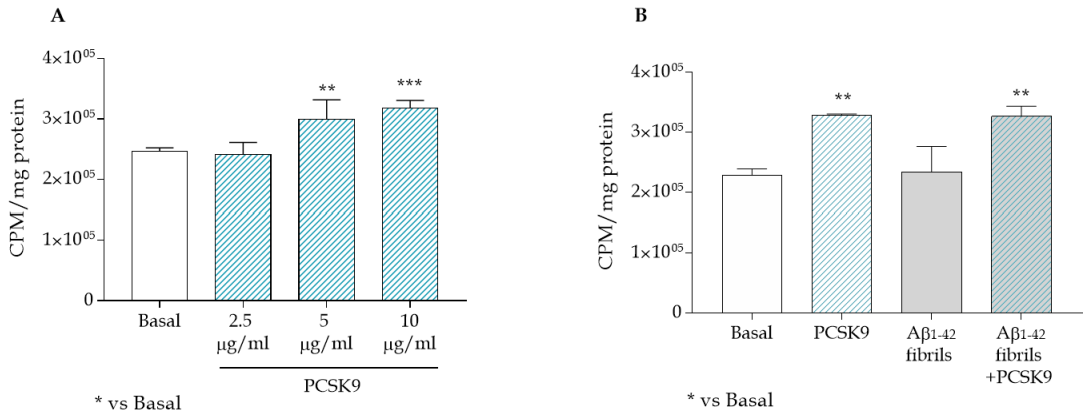

Figure 2**. Impact of PCSK9 on endogenous cholesterol biosynthesis in cultured human U373. **(A) U373 astrocytoma cells were treated for 48h with increasing concentrations of human recombinant PCSK9, ranging from [2,5 µg/ml] to [10 µg/ml] (striped bars), then endogenous cholesterol biosynthesis was evaluated. ***(B)*** U373 astrocytoma cells were treated with human recombinant PCSK9 [5µg/ml] (striped bars) for 48 hours, the last 24 of which with the addition of $A\beta_{1-42}$ fibrils [1µM] (grey bars), then endogenous cholesterol biosynthesis was evaluated. Data were performed in triplicate and expressed as mean ± standard deviation. Statistical analyses were performed using the one-way ANOVA test, with the post-hoc Tuckey's multiple comparison test. A value of $p<0.05$ was considered statistically significant. ** $p<0.01$; *** $p<0.001$.

1.1.3 Impact of PCSK9 on lipoprotein receptors expression

Subsequently, having observed a dose-dependent increase in endogenous cholesterol biosynthesis following the incubation with human recombinant PCSK9, the expression of lipoprotein receptors involved in exogenous cholesterol internalization, such as LDLR and apoER2, was analysed. Indeed, similarly to its hepatic effect, PCSK9 may act by degrading the receptors responsible for cholesterol internalization [245] also in astrocytes, thus activating a feedback mechanism that stimulates the endogenous cholesterol synthesis. As demonstrated in **Figure 3A**, LDLR expression was dramatically decreased following the incubation with exogenous recombinant PCSK9 [5µg/ml] for 48 hours (-82%; $p<0.001$); consistently, a more moderate, but still significant reduction of apoER2 expression (-36%, $p<0.01$) was observed following PCSK9 treatment (**Figure 3B**). As expected, for both LDLR and apoER2, the incubation with $A\beta_{1-42}$ fibrils [1µM] wasn't able to affect the expression of the analysed receptors, neither alone nor with the simultaneous treatment of PCSK9 (**Figure 3A** and **3B**).

FIGURE 3

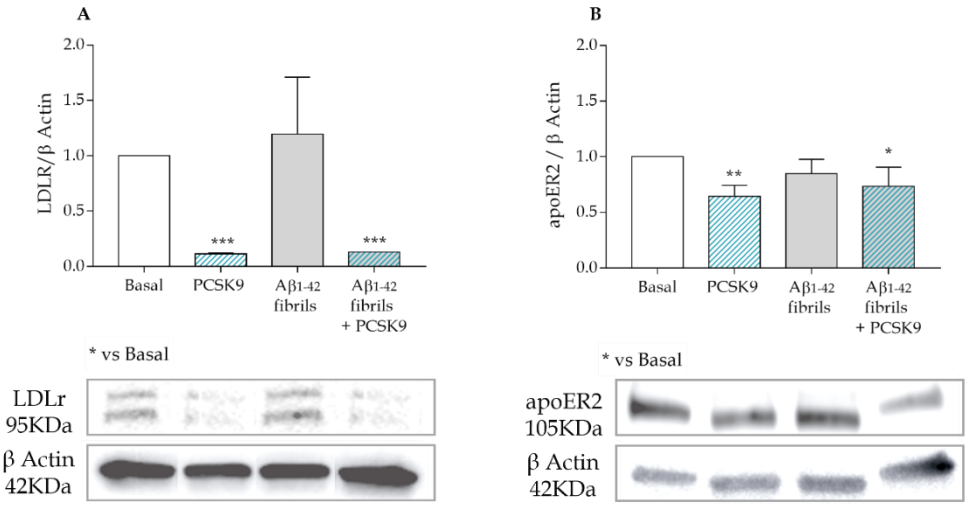

***Figure 3**. Impact of PCSK9 on LDLR (**A**) and apoER2 (**B**) expression in cultured human U373 astrocytoma cells.* U373 cells were treated with human recombinant PCSK9 [5µg/ml] (striped bars) for 48 hours, the last 24 of which with the addition of $A\beta_{1-42}$ fibrils [1µM] (grey bars), then protein expression was analysed through WB analyses and furtherly quantified through ImageJ Fiji software. Data were performed in triplicate and expressed as mean ± standard deviation. Statistical analyses were performed using the one-way ANOVA test, with the post-hoc Tuckey's multiple comparison test. A value of $p<0.05$ was considered statistically significant. * $p<0.05$; ** $p<0.01$; *** $p<0.001$.

The PCSK9-mediated decrease of LDLR and apoER2 expression was functionally demonstrated by evaluating the uptake of rHDL-apoE [10µg/ml] containing radiolabelled cholesterol, prepared as described in the Methods section [360]. Specifically, those synthetic liposomes were used since they share a similar structure, shape and protein content with the HDL-like particles found in CSF [185]. As reported in **Figure 4**, U373 cells incubated with human recombinant PCSK9 [5µg/ml] for 48 hours are characterized by a significant and well-pronounced reduction of rHDL-apoE-mediated cholesterol internalization as compared to control cells (-36.3%, $p<0.0001$). As expected, the pre-treatment with $A\beta_{1-42}$ fibrils [1µM] for 24 hours wasn't able to affect cholesterol internalization into astrocytes, showing a similar reduction of apoE-mediated cholesterol uptake in PCSK9-treated U373 cells as compared to controls (-35%, $p<0.0001$). The specific degrading effect of PCSK9 on lipoprotein receptors was also confirmed by the evidence that when rHDL particles not containing apoE were used as cholesterol donors, an extremely moderate rate of radiolabelled cholesterol internalization was detected as compared to the process mediated by rHDL-apoE. Furthermore, in this case, no significant differences were observed following the treatment with human recombinant PCSK9.

FIGURE 4

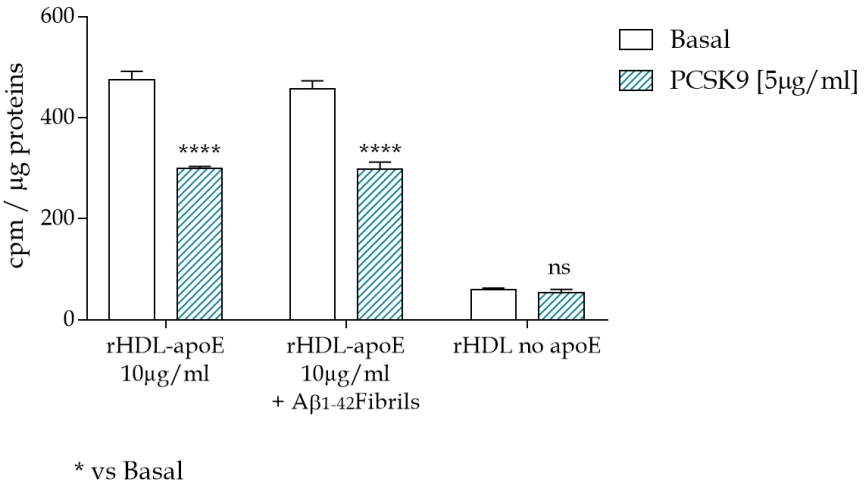

***Figure 4**. Impact of PCSK9 on rHDL-apoE-mediated cholesterol internalization in cultured human U373 astrocytoma cells.* U373 cells were treated with human recombinant PCSK9 [5µg/ml] (striped bars) for 48 hours, the last 24 of which with the addition of $A\beta_{1-42}$ fibrils [1µM] (grey bars), then exposed to radiolabelled rHDL containing or not apoE. Radioactivity was then quantified in cell monolayers. Data were performed in triplicate and expressed as mean ± standard deviation. Statistical analyses were performed using the two-way ANOVA test, with the post-hoc Sidak's multiple comparison test. A value of $p<0.05$ was considered statistically significant. **** $p<0.0001$.

1.1.4 Impact of PCSK9 on intracellular cholesterol content

The impact of PCSK9 on total intracellular cholesterol content was then investigated, as it's the results of different processes, including cholesterol biosynthesis and cholesterol uptake from the extracellular milieu. As shown in **Figure 5**, the treatment with PCSK9 [5µg/ml] for 48 hours determined a significant reduction in total cholesterol content as compared to the basal condition (-20%; $p<0.05$). Furthermore, even the incubation with $A\beta_{1-42}$ fibrils [1µM] for 24 hours was associated with a significant reduction in cellular cholesterol content as compared to the basal condition (-24%; $p<0.01$). Interestingly, the simultaneous incubation of both PCSK9 [5µg/ml] and $A\beta_{1-42}$ fibrils [1µM] led to an even more marked reduction in total cholesterol content in astrocytes (-37%; $p<0.001$ compared to the basal condition and $p<0.05$ compared to PCSK9 alone).

FIGURE 5

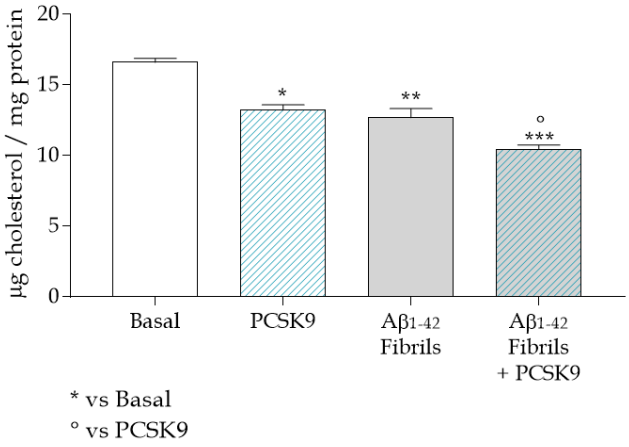

***Figure 5**. Impact of PCSK9 on intracellular cholesterol content in cultured human U373 astrocytoma cells.* U373 cells were treated with human recombinant PCSK9 [5µg/ml] (striped bars) for 48 hours, the last 24 of which with the addition of $A\beta_{1-42}$ fibrils [1µM] (grey bars), then intracellular cholesterol content was quantified through Amplex® Red cholesterol fluorometric assay and protein content through BCA assay. Data were performed in triplicate and expressed as mean ± standard deviation. Statistical analyses were performed using the one-way ANOVA test, with the post-hoc Tuckey's multiple comparison test. A value of $p<0.05$ was considered statistically significant. * refers to basal and ° to PCSK9-treated cells. * and ° $p<0.05$; ** $p<0.01$; *** $p<0.001$.

1.1.5 Impact of PCSK9 and Aβ1-42 on membrane cholesterol content

One of the main and most relevant cellular pools of free cholesterol is represented by the plasma membrane, playing an extremely relevant role due to its involvement in cholesterol efflux and in mediating cellular functions in CNS [372]. Thus, the impact of PCSK9 on cholesterol content distribution specifically localized in the plasma membrane of U373 astrocytoma cells was analysed. First, the experimental conditions were set up by adopting a protocol that has been previously used by our group to evaluate plasma membrane cholesterol content in cultured macrophages [364]. The obtained results clearly indicated that also in U373 astrocytoma cells, membrane cholesterol content was detectable and modulable (data not shown). Specifically, following the incubation of U373 with LXR/RXR agonists 22-OHC/9cRA ([5µg/ml] and [10µM], respectively), known to up-regulate ABCA1 and ABCG1-mediated pathway [155,186], a 2-fold increase in plasma membrane cholesterol content was observed ($p<0.001$ as compared to non-stimulated cells). Interestingly, the treatment of LXR-RXR-stimulated U373 cells with Probucol [10µM], which we previously demonstrated to reduce membrane cholesterol content in macrophages [364], was associated with a significant reduction in plasma membrane cholesterol content (-19% compared to 22-OHC/9cRA stimulated cells; $p<0.05$). In these established experimental conditions, the effect of PCSK9 has been investigated.

FIGURE 6

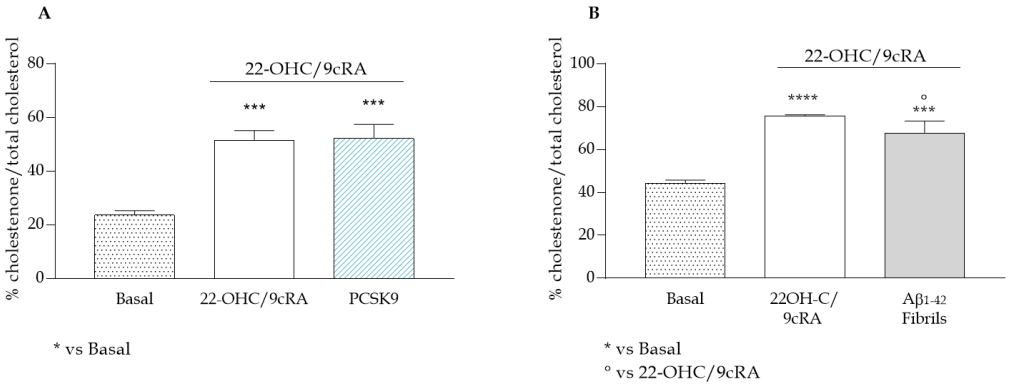

***Figure 6**. Impact of PCSK9 (**A**) and Aβ1-42 fibrils (**B**) on intracellular cholesterol content in cultured human U373 astrocytoma cells. (**A**)* U373 cells were radiolabelled and treated with human recombinant PCSK9 [5µg/ml] (striped bars) for 48 hours, in the absence (dotted bars) or presence (plain bars) of LXR/RXR agonists 22-OHC/9cRA. (**B**) U373 cells were radiolabelled and treated with Aβ1-42 fibrils [1µM] (grey bars) for 24 hours, in the absence (dotted bars) or presence (plain bars) of LXR/RXR agonists 22-OHC/9cRA. Cells were then treated with or without 1U/ml of cholesterol oxidase enzyme for 2 hours at 37°C. Data were performed in triplicate and expressed as mean ± standard deviation. Statistical analyses were performed using the one-way ANOVA test, with the post-hoc Tuckey's multiple comparison test. A value of $p<0.05$ was considered statistically significant. * refers to basal and ° to 22-OHC/9cRA-treated cells. ° $p<0.05$; *** $p<0.001$; **** $p<0.0001$.

As shown in **Figure 6A**, 22-OHC/9cRA treatment in U373 cells confirmed a significant increase in membrane cholesterol content as compared to non-stimulated cells ($p<0.001$); however, PCSK9 [5μg/ml] incubation wasn't able to significantly affect this parameter. Interestingly, as seen in **Figure 6B**, in 22-OHC/9cRA-stimulated U373 cells, the incubation with $A\beta_{1-42}$ fibrils [1μM] for 24 hours was associated with a significant decrease in plasma membrane cholesterol content (-11%; $p<0.05$ as compared to 22-OHC/9cRA-stimulated U373 cells), which is mostly dependent on ABCA1 transporter [364].

1.1.6 Impact of PCSK9 and $A\beta_{1-42}$ on cholesterol efflux

Cellular cholesterol efflux represents the first step of cholesterol transport from astrocytes towards neurons, in which cellular cholesterol is actively transported by ABCA1 and ABCG1 transporters to extracellular acceptors. Hence, the impact of PCSK9 on this relevant process has been evaluated. Lipid-free apoE, as well as synthetic reconstituted HDL particles containing apoE (rHDL-apoE), resembling HDL-like particles identified in CSF, were used as extracellular cholesterol acceptors, due to their ability to promote cholesterol efflux preferentially mediated by ABCA1 and ABCG1 transporter, respectively [366,373]. First, the experimental conditions were set up by adopting a protocol that has been previously used by our group to evaluate cholesterol efflux in cultured macrophages [365]. The obtained results clearly demonstrated that cholesterol efflux was detectable and modulable also in the considered astrocytoma cell line (data not shown). Once established the optimal experimental conditions, the impact of PCSK9 on cholesterol efflux from astrocytes was investigated. In non-stimulated cells, human recombinant PCSK9 incubation affected cholesterol efflux neither to apoE nor to rHDL-apoE as extracellular acceptors (data not shown). As reported in **Figure 7,** the treatment of U373 cells with LXR/RXR agonists 22-OHC/9cRA ([5μg/ml] and [10μM], respectively), was associated with a significant increase in cholesterol efflux to both acceptors, with a more pronounced effect occurring in U373 cells exposed to lipid-free apoE [10μg/ml] (8-fold increase, $p<0.0001$ vs non-stimulated cells) rather than with rHDL-apoE [10μg/ml] (3-fold increase, $p<0.0001$ vs non-stimulated cells). In this context, the incubation with exogenous PCSK9 didn't alter either cholesterol efflux to apoE (**Figure 7A**) or to rHDL-apoE (**Figure 7B**). This observation suggests that the enzyme doesn't impact on ABCA1- and ABCG1-mediated cholesterol efflux process.

Interestingly, in U373 cells stimulated with 22-OHC/9cRA, $A\beta_{1-42}$ fibrils [1µM] incubated for 24 hours were able to significantly reduce ABCA1-mediated cholesterol efflux (-14%, $p<0.001$ as compared to 22-OHC/9cRA-treated cells), both in the absence or presence of human recombinant PCSK9 (**Figure 7A**). This observation is in accordance with the $A\beta_{1-42}$ fibrils-mediated reduction of membrane cholesterol content previously described (**Figure 6B**).

FIGURE 7

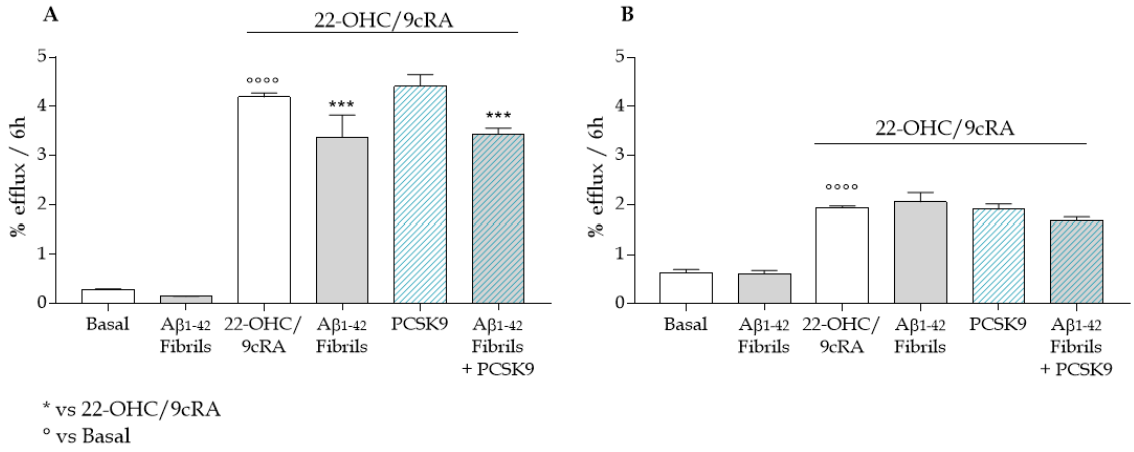

***Figure 7**. Impact of PCSK9 and $A\beta_{1-42}$ fibrils on cell cholesterol efflux in cultured human U373 astrocytoma cells.* U373 cells were radiolabelled and treated with human recombinant PCSK9 [5µg/ml] (striped bars) for 48 hours, in the absence (dotted bars) or presence (plain bars) of LXR/RXR agonists 22-OHC/9cRA, the last 24 hours of which with the co-incubation of $A\beta_{1-42}$ fibrils [1µM] (grey bars). Exogenous apoE [10µg/ml] and rHDL-apoE [10µg/ml] were then added for 6 hours as cholesterol acceptors for ABCA1- and ABCG1-mediated cholesterol efflux, respectively (Panel **A** and panel **B**). Data were performed in triplicate and expressed as mean ± standard deviation. Statistical analyses were performed using the one-way ANOVA test, with the post-hoc Tuckey's multiple comparison test. A value of $p<0.05$ was considered statistically significant. ° refers to basal and * to 22-OHC/9cRA-treated cells. *** $p<0.001$; °°°° $p<0.0001$.

1.1.7 Impact of PCSK9 and $A\beta_{1-42}$ on ABCA1 expression

Having observed a reduction both in membrane cholesterol content (**Figure 6B**) and in ABCA1-mediated cholesterol efflux (**Figure 7A**) in presence of $A\beta_{1-42}$ fibrils [1µM], ABCA1 protein expression was assessed in cultured U373 cells incubated with exogenous PCSK9 and $A\beta_{1-42}$ fibrils [1µM], then furtherly stimulated with 22-OHC/9cRA. As shown in **Figure 8**, a marked increase in ABCA1 expression was confirmed in 22-OHC/9cRA-treated U373 cells as compared to basal. In stimulated cells, the incubation of PCSK9 wasn't associated with any changes in ABCA1 protein expression. On the other side, consistently with the functional observations previously described, $A\beta_{1-42}$ fibrils [1µM] led to a slight, but significant, reduction in ABCA1 expression ($p<0.05$). These observations

suggest an interfering effect with the ABCA1-mediated process occurring in $A\beta_{1-42}$ fibrils-treated cells, either in the absence or presence of PCSK9.

FIGURE 8

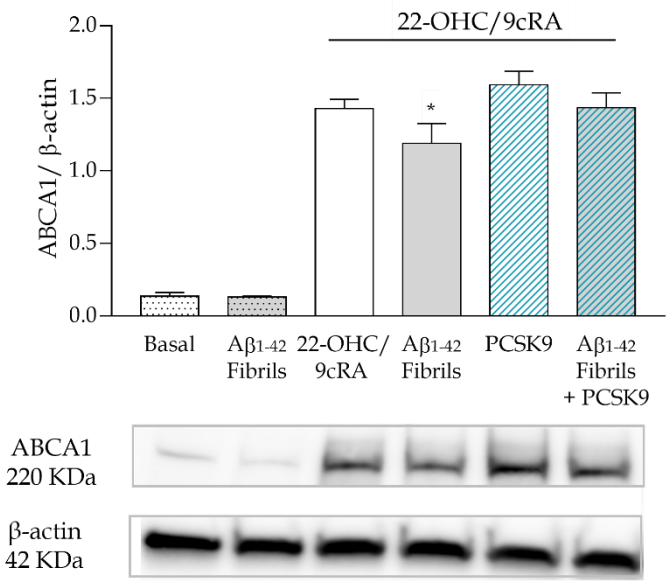

***Figure 8**. Impact of PCSK9 and $A\beta_{1-42}$ fibrils on ABCA1 expression in cultured human U373 astrocytoma cells.* U373 cells were incubated with human recombinant PCSK9 [5µg/ml] (striped bars) for 48 hours, in the absence (dotted bars) or presence (plain bars) of LXR/RXR agonists 22-OHC/9cRA, the last 24 hours of which with the co-incubation of $A\beta_{1-42}$ fibrils [1µM] (grey bars). Protein expression was analyzed through WB analyses and furtherly quantified through ImageJ Fiji software. Data were performed in triplicate and expressed as mean ± standard deviation. Statistical analyses were performed using the one-way ANOVA test, with the post-hoc Tuckey's multiple comparison test. A value of $p<0.05$ was considered statistically significant. * $p<0.05$.

1.2 INFLUENCE OF PCSK9 ON CHOLESTEROL HOMEOSTASIS IN HUMAN NEUROBLASTOMA CELLS

Cholesterol secreted from astrocytes and assembled with apoE in HDL-like particles is finally delivered and incorporated into neurons by interacting with apoE-receptors [185]. Hence, the potential influence of PCSK9 in this last step of brain cholesterol transport has been evaluated. To this aim, human neuroblastoma cell line SH-SY5Y has been specifically retrovirally transfected to overexpress human PCSK9, as deeply described in the Materials and Methods section. Then, different aspects contributing to neuronal cholesterol homeostasis and viability were evaluated.

1.2.1 Impact of PCSK9 on apoE-mediated cholesterol internalization

Cholesterol internalization in SH-SY5Y neuroblastoma cells has been evaluated first, being one of the most important processes that guarantee the maintenance of the optimal intracellular cholesterol pool in adult neurons [185]. As previously described in the Materials and Methods section, the reduction in LDLR and apoER2 expression in PCSK9-overexpressing SH-SY5Y cells has previously been verified through molecular assays including gene and protein expression analyses.

The uptake of radioactive cholesterol was indeed evaluated after the exposure of PCSK9-overexpressing and of control SH-SY5Y cells to rHDL-apoE [10µg/ml] for 4 hours. As reported in **Figure 9**, PCSK9-overexpressing cells were characterized by a significant reduction of cholesterol internalization as compared to control cells (-41%; $p<0.001$). As expected, the preliminary treatment with $A\beta_{1-42}$ fibrils [1µM] for 24 hours wasn't able to affect cholesterol internalization into neurons, showing a reduction in rHDL-apoE-containing radioactive cholesterol internalization of about 39% in SH-SY5Y PCSK9-overexpressing cells compared to SH-SY5Y control neuroblastoma cells ($p<0.001$).

FIGURE 9

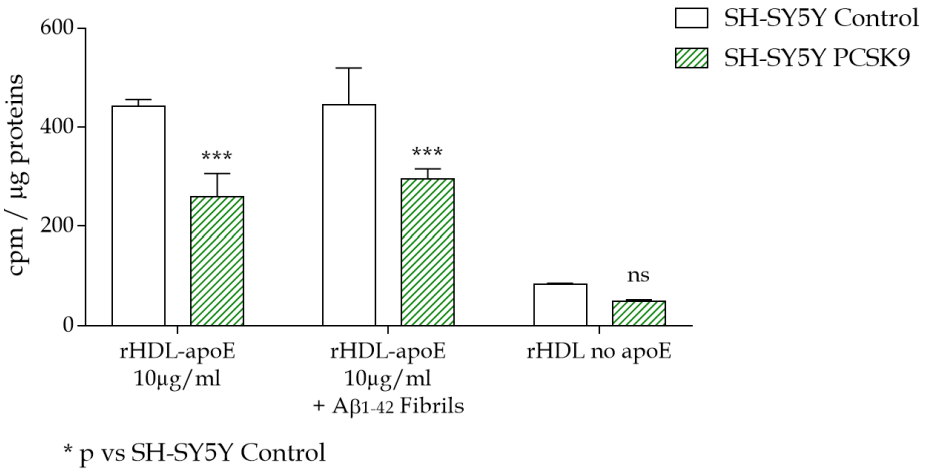

***Figure 9**. rHDL-apoE-mediated cholesterol internalization in cultured human SH-SY5Y neuroblastoma cells controls (plain bars) or overexpressing PCSK9 (striped bars).* Differentiated SH-SY5Y cells were treated with or without $A\beta_{1-42}$ fibrils [1µM] for 24 hours, then exposed for 4 hours to radiolabelled rHDL containing or not apoE. Radioactivity was then quantified in cell monolayers. Data were performed in triplicate and expressed as mean ± standard deviation. Statistical analyses were performed using the two-way ANOVA test, with the post-hoc Sidak's multiple comparison test. A value of $p<0.05$ was considered statistically significant. ***$p<0.001$.

However, when rHDL particles not containing apoE were used as cholesterol donors, an extremely modest rate of cholesterol internalization was detected as compared to the

process mediated by rHDL-apoE particles in both SH-SY5Y controls and PCSK9-overexpressing cells, with no significant differences between the two considered cell lines.

This observation clearly suggests that PCSK9, through its degrading activity on receptors such as LDLR and apoER2, may act by counteracting the cholesterol internalization process in neurons, which is specifically mediated by apoE. This experimental evidence was also confirmed in a similar experimental model, by evaluating cholesterol internalization mediated by rHDL-apoE in *Wild Type* SH-SY5Y neuroblastoma cells exposed to exogenous recombinant PCSK9 [5µg/ml] for 48h. Interestingly, the incubation of WT SH-SY5Y cells with human recombinant PCSK9 [5µg/ml] resulted in a significant reduction of rHDL-apoE-mediated cholesterol uptake as compared to non-treated WT SH-SY5Y cells (-16%, $p<0.05$; data not shown).

1.2.2 Impact of PCSK9 on endogenous cholesterol biosynthesis

The impact of PCSK9 overexpression on endogenous cholesterol biosynthesis was evaluated. Indeed, the endogenous biosynthetic pathway represents the other cellular mechanism, together with exogenous cholesterol uptake, that provides the adequate cholesterol pool, despite its rate and efficiency being extremely low in adult neurons [172]. Similarly to what was previously described in astrocytes, the experimental conditions to evaluate endogenous cholesterol biosynthesis in neuroblastoma cells were first set up. The obtained results clearly indicated that also in cultured SH-SY5Y cells cholesterol biosynthetic pathway was detectable and modulable by different amounts of exogenous cholesterol content, experimentally represented by different percentages of FCS (data not shown). Indeed, in SH-SY5Y cells cultured with 5% v/v of FCS, the endogenous cholesterol synthesis rate was reduced as compared to SH-SY5Y cells cultured with 1% v/v of FCS (-38%, $p<0.001$). Once set the optimal experimental conditions, the effect of PCSK9 overexpression on endogenous cholesterol biosynthesis was then investigated. As reported in **Figure 10**, in neuroblastoma cells the overexpression of PCSK9 was associated with a significant reduction of cholesterol synthesis (-25% as compared to control SH-SY5Y cells, $p<0.01$). This experimental observation was peculiar, as PCSK9 incubation in astrocytes was associated with the opposite effect (**Figure 2**), leading to a significant increase in their cholesterol biosynthetic rate. However, similarly to what was previously observed in U373 astrocytoma cells, the incubation with $A\beta_{1-42}$ fibrils [1µM] for 24 hours

showed no impact on endogenous cholesterol biosynthesis (**Figure 10**) both in SH-SY5Y controls and PCSK9-overexpressing cells.

FIGURE 10

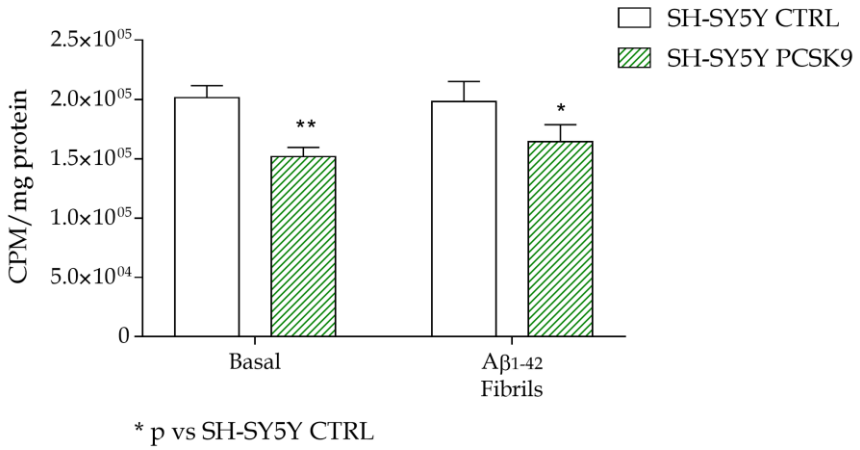

***Figure 10**. Endogenous cholesterol biosynthesis in cultured human SH-SY5Y controls (plain bars) and SH-SY5Y-overexpressing PCSK9 (striped bars) neuroblastoma cells.* Differentiated SH-SY5Y neuroblastoma cells were treated with or without $A\beta_{1-42}$ fibrils [1μM] for 24 hours, then cholesterol biosynthesis was evaluated by incubating cells with ^{14}C acetate and monitoring its incorporation into newly-synthesized cholesterol. Data were performed in triplicate and expressed as mean ± standard deviation. Statistical analyses were performed using the two-way ANOVA test, with the post-hoc Sidak's multiple comparison test. A value of $p<0.05$ was considered statistically significant. *$p<0.05$; **$p<0.01$.

1.2.3 Impact of PCSK9 and cholesterol excess or depletion on cell viability

Additionally, the impact of PCSK9 overexpression on cell viability in neuroblastoma cells exposed to either cholesterol depletion or its excess was investigated. Indeed, sterols levels in neurons requires a fine regulation, as both cholesterol deficiency, as well as its excess, has been described to negatively affect neuronal development and functions [133,137–139]. Specifically, the basal condition was represented by cell culture medium enriched with 1% v/v of FCS, with a concentration of cholesterol similar to that retrieved in CNS [267]. On the other side, cholesterol deficiency and its excess were simulated by incubating cells with a culture medium enriched in 0.2% w/v of BSA or 25 μM of cholesterol, respectively.

FIGURE 11

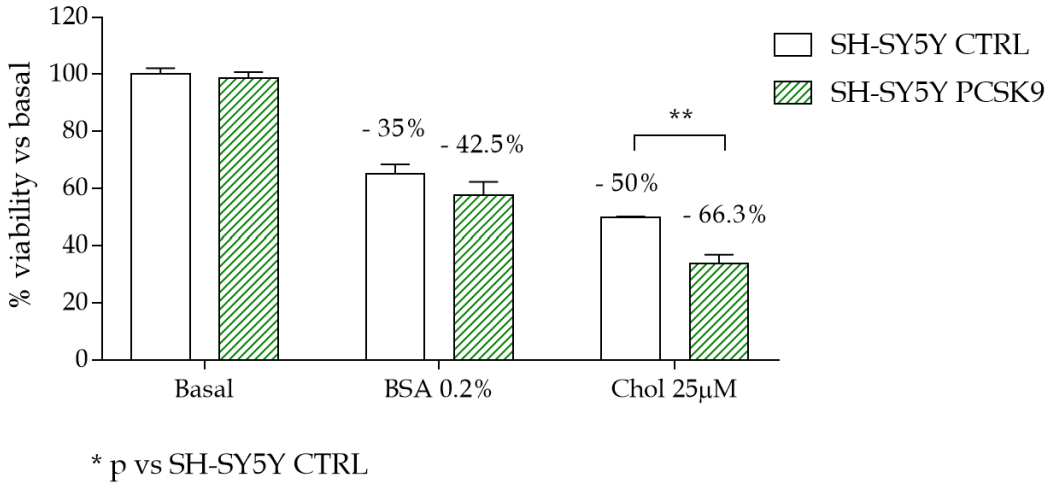

***Figure 11**. Cell viability in cultured human SH-SY5Y controls (plain bars) and SH-SY5Y-overexpressing PCSK9 (striped bars) neuroblastoma cells incubated with different concentrations of exogenous cholesterol.* Differentiated SH-SY5Y neuroblastoma cells were treated for 48 hours with a culture medium supplemented with 1% v/v of FCS (Basal) or 0.2% w/v of BSA, representing a condition of cholesterol depletion, or supplemented with 25µM of cholesterol, representing a condition of cholesterol excess. Cell viability was then assessed through MTT assay. Data were performed in triplicate and expressed as mean ± standard deviation. Statistical analyses were performed using the two-way ANOVA test, with the post-hoc Sidak's multiple comparison test. A value of $p<0.05$ was considered statistically significant. **$p<0.01$.

As shown in **Figure 11**, in basal conditions PCSK9 overexpressing SH-SY5Y cells were characterized by similar viability as compared to SH-SY5Y controls. On the other hand, as expected, both cholesterol depletion and excess caused a reduction of neuroblastoma viability. Specifically, cholesterol-depleted SH-SY5Y control neuroblastoma cells were characterized by a reduction of their viability of about 35% as compared to the basal condition. A similar trend was retrieved also in cholesterol-depleted PCSK9-overexpressing SH-SY5Y (-42.5% as compared to the basal condition), with a more pronounced reduction in cell viability as compared to control SH-SY5Y neuroblastoma cells, however not reaching the statistical significance. Cholesterol excess induced an even more evident reduction of neuronal viability in SH-SY5Y control cells (-50% as compared to the basal condition), which is more pronounced in PCSK9-overexpressing SH-SY5Y neuroblastoma cells (-66.3% as compared to the basal condition). In this context, the overexpression of PCSK9 in SH-SY5Y was associated with a pronounced and significant reduction of neuronal viability as compared to SH-SY5Y control cells exposed to the same cholesterol loading ($p<0.01$ vs SH-SY5Y control).

1.2.4 Impact of PCSK9 on cell viability in presence of $A\beta_{1-42}$

Finally, as performed for astrocytoma cells, the potential cytotoxic effect of the enzyme was analysed in PCSK9-overexpressing SH-SY5Y neuroblastoma as compared to SH-SY5Y cells in presence of increasing concentrations of $A\beta_{1-42}$ (**Figure 12**) at different degrees of aggregation: oligomers and fibrils. As reported in **Figure 12A**, the incubation of SH-SY5Y control cells with $A\beta_{1-42}$ oligomers negatively affected cellular viability only when incubated at [10μM] ($p<0.0001$ vs SH-SY5Y control cells not incubated with $A\beta_{1-42}$ oligomers; r^2 for dose-dependency=0.9). On the other side, $A\beta_{1-42}$ fibrils (**Figure 12B**) were able to affect neuronal viability already at [1μM] ($p<0.0001$ vs SH-SY5Y control cells not incubated with $A\beta_{1-42}$ fibrils), which becomes more pronounced at [5μM] and [10μM], in a dose-dependent manner ($p<0.0001$ vs SH-SY5Y control cells not incubated with $A\beta_{1-42}$ fibrils for both; r^2 for dose-dependency=0.66). Interestingly, PCSK9 overexpression was able to significantly affect neuronal viability in cells treated with both $A\beta_{1-42}$ fibrils and oligomers. Indeed, as reported in **Figure 12A**, PCSK9-overexpressing cells treated with $A\beta_{1-42}$ oligomers [1μM] were characterized by a reduction of 19% of cell viability as compared to SH-SY5Y controls exposed to the same oligomeric concentration ($p<0.0001$), while PCSK9-overexpressing cells incubated with $A\beta_{1-42}$ oligomers [5μM] were characterized by a reduction of 24% of cell viability as compared to controls ($p<0.0001$). Finally, PCSK9 overexpressing cells treated with $A\beta_{1-42}$ Oligomers [10μM] displayed a reduction and about 11% as compared to controls ($p<0.05$). Concerning the impact of PCSK9 in cells incubated with $A\beta_{1-42}$ fibrils, as reported in **Figure 12B**, PCSK9-overexpressing SH-SY5Y cells were characterized by a more neurotoxic effect with respect to SH-SY5Y control cells, showing a reduction of about 16% of cellular viability in presence of $A\beta_{1-42}$ Fibrils [1μM] ($p<0.001$ compared to SH-SY5Y controls exposed to the same $A\beta_{1-42}$ Fibrils concentration), that becomes less pronounced in cells exposed to $A\beta_{1-42}$ Fibrils [5μM] and [10μM] (-10%, $p<0.05$ for both).

FIGURE 12

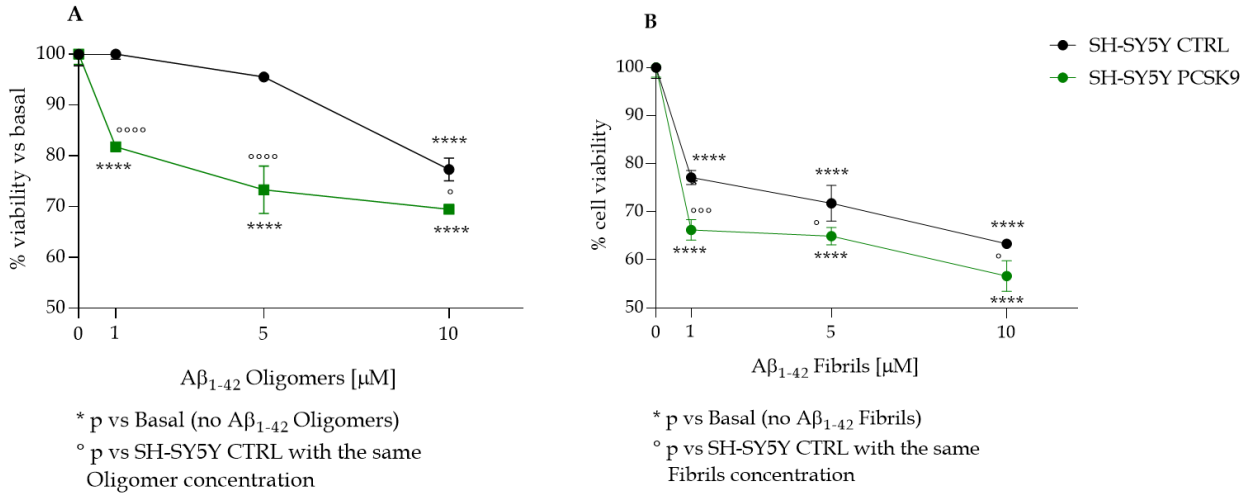

Figure 12**. Cell viability in cultured human SH-SY5Y controls (black line) and SH-SY5Y-overexpressing PCSK9 (green line) neuroblastoma cells incubated with different concentrations of $A\beta_{1-42}$ oligomers (**A**) and $A\beta_{1-42}$ fibrils (**B**).* Differentiated SH-SY5Y neuroblastoma cells were treated for 48 hours with concentrations of $A\beta_{1-42}$ oligomers and $A\beta_{1-42}$ fibrils ranging from [1μM] to [10μM]. Cell viability was then assessed through MTT assay. Data were performed in triplicate and expressed as mean ± standard deviation. Statistical analyses were performed using the two-way ANOVA test, with the post-hoc Sidak's multiple comparison test. A value of $p<0.05$ was considered statistically significant. * refers to the Basal condition and ° refers to SH-SY5Y CTRL cells treated with the same concentration of oligomers or fibrils. ° $p<0.05$; *** $p<0.001$; * and °°°° $p<0.0001$.

2. INFLUENCE OF PCSK9 ON CHOLESTEROL PARAMETERS: *EX VIVO* EVIDENCE FROM AD TRANSGENIC MODELS

Having previously observed through *in vitro* studies a potential negative impact of PCSK9 on both astrocytic and neuronal cholesterol metabolism, with a possible compromising of brain cholesterol transport, this second part of the study aimed to investigate the potential PCSK9-derived effect on specific cholesterol-related parameters in *ex vivo* samples from animal models. To this purpose, a new transgenic mouse has been generated, in collaboration with the University of Modena and Reggio Emilia, as widely described in the Material and Method section. Briefly, 5XFAD^{he} mice, expressing five mutations associated with familial AD, were bred with PCSK9^{ko} mice, thus generating a new mouse model that recapitulates the major behavioural and anatomopathological features of AD, lacking also PCSK9. This specific mouse model was compared to specific controls as follows:

- WT – PCSK9^{he} mice (n=14)
- WT – PCSK9^{ko} mice (n=10)
- 5XFAD^{he} – PCSK9^{he} mice (n=13)
- 5XFAD^{he} – PCSK9^{ko} mice (n=12)

Additionally, the four above-listed experimental groups were compared with WT and 5XFAD^{he} mice, both carrying two WT PCSK9 alleles, in order to investigate a possible gene-dependent effect of PCSK9 presence, and specifically:

- WT – PCSK9^{wt} mice (n=3)
- 5XFAD^{he} – PCSK9^{wt} mice (n=4)

Within this experimental setting, cholesterol and its main oxidised metabolites, 24-, 25- and 27-hydroxysterols (OHC) were analysed in the isolated brain and sera specimens.

2.1 IMPACT OF PCSK9 ON SERUM CHOLESTEROL LEVELS

The first parameter analysed was total cholesterol level in serum of the above-mentioned experimental setting. As shown in **Figure 13**, in WT mice, not carrying the five mutations associated with familial AD, a gene-dependent reduction (r^2 for gene-dependency=0.581; p<0.0001) of circulating total cholesterol levels was observed in mice carrying a heterozygous PCSK9 mutation (****p<0.0001 vs $PCSK9^{wt}$) and in mice carrying a homozygous PCSK9 mutation (****p<0.0001 vs $PCSK9^{wt}$). Interestingly, $5XFAD^{he}$ mice, independently on their PCSK9 genotype, were characterized by lower serum total cholesterol levels (***p<0.001 for $PCSK9^{wt}$ and ****p<0.0001 for $PCSK9^{he}$ and $PCSK9^{ko}$ vs WT-$PCSK9^{wt}$ mice). Also in mice with a $5XFAD^{he}$ background, a gene-dependent reduction of circulating cholesterol levels was observed based on the heterozygous or homozygous PCSK9 deletion (r^2 for gene-dependency=0.262; p=0.005).

FIGURE 13

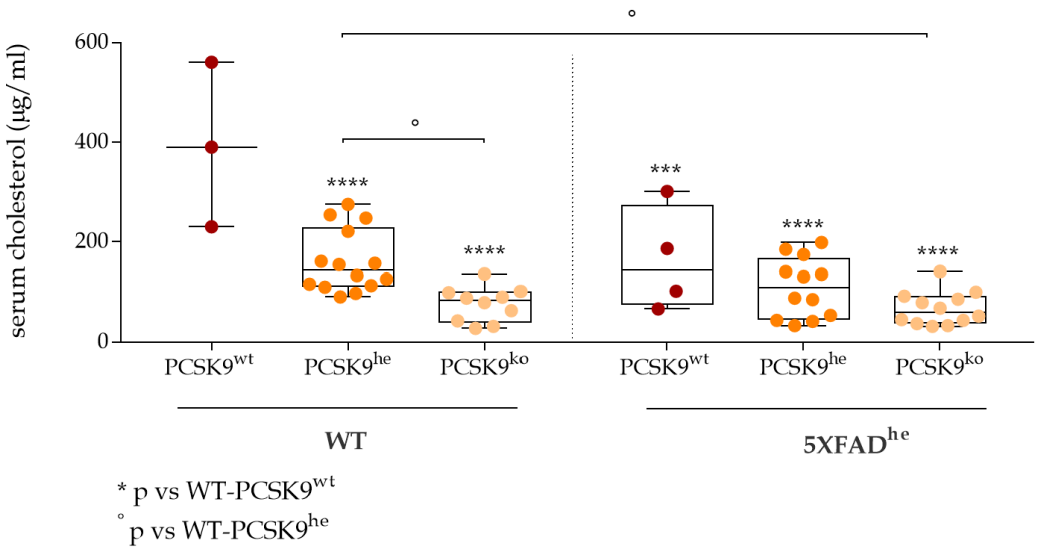

***Figure 13**. Serum cholesterol levels of WT or $5XFAD^{he}$ mice with homozygous or heterozygous PCSK9 mutation.* After sacrifice, a small aliquot of blood was collected, serum was isolated and then conserved at -80°C until use. Each point of the scatter plot represents the mean value of duplicate serum cholesterol quantification. The Kolmogorov-Smirnov test was used to determine the normality of the distribution. To compare the six experimental groups the one-way ANOVA test was performed for data normally distributed, while skewed variables were compared by the Kruskal-Wallis test. The Dunnett's post-hoc test was performed for multiple comparisons. A value of p<0.05 was considered statistically significant. * refers to WT-$PCSK9^{wt}$ and ° to WT-$PCSK9^{he}$. ° p<0.05; *** p<0.001 and ****p<0.0001.

2.2 IMPACT OF PCSK9 ON SERUM HYDROXYSTEROLS LEVELS

Cholesterol metabolites, mainly oxidative products such as hydroxysterols (OHC), have been suggested as possibly altered in different neurodegenerative diseases, including AD [327,334], and have been proposed as new disease biomarkers. To this aim, three of the main hydroxysterols, 24-, 25- and 27-OHC have been quantified in serum of the analysed experimental groups through LC-MS/MS, as deeply described in the Material and Method section.

FIGURE 14

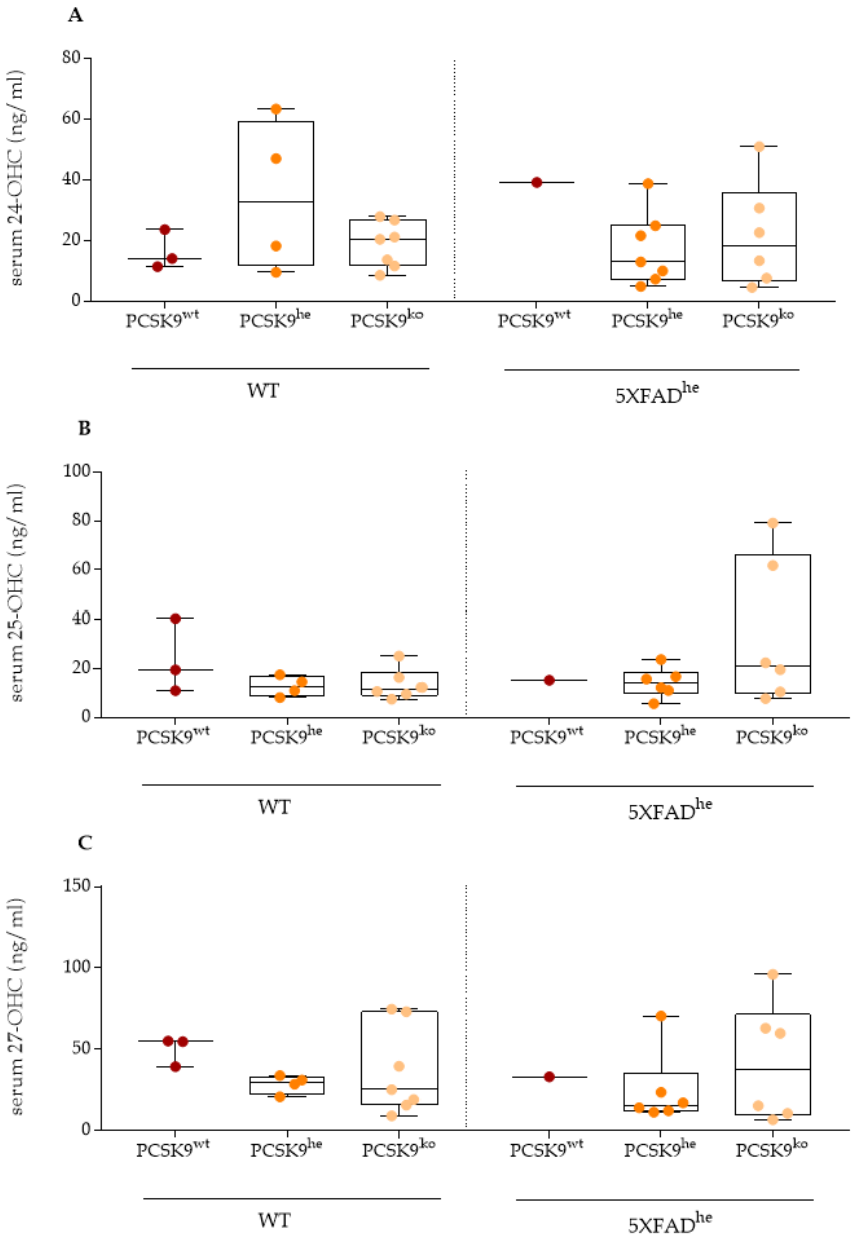

***Figure 14**. Serum levels of 24-OHC (**A**), 25-OHC (**B**) and 27-OHC (**C**) in WT or 5XFAD^{he} mice with homozygous or heterozygous PCSK9 mutation.* Each point of the scatter plot represents the mean percentage of duplicate quantification of serum. The horizontal, solid line represents the mean of each group. The Kolmogorov-Smirnov test was used to determine the normality of the distribution. The one-way ANOVA was performed for data normally distributed, while skewed variables were compared by the Kruskal-Wallis test. The Dunnett's post-hoc test was performed for multiple comparisons.

As reported in **Figure 14A**, no differences were detected in 24-OHC levels between the six analysed animal groups, with no changes nor between mice with a WT or 5XFAD^{he} genetic background, nor based on the presence of two fully functioning PCSK9 alleles or their heterozygous or homozygous deletion. A similar picture was also observed for 25-OHC (**Figure 14B**) and 27-OHC (**Figure 14C**) levels in all the six considered animal groups. However, these observations are possibly affected by the small number of samples in both WT-PCSK9^{wt} and 5XFAD^{he}-PCSK9^{wt} experimental groups, which will be furtherly implemented.

2.3 IMPACT OF PCSK9 ON BRAIN CHOLESTEROL LEVELS

Subsequently, in the above-mentioned animal models, brain cholesterol levels were quantified. As the brain represents the most sterol-enriched bodily organ, before cholesterol quantification, the cerebral tissue of each animal was carefully weighed, to express the analytical cholesterol concentration obtained corrected for brain weight of each animal. As reported in **Table 1**, no significant differences were found in mice brains' weight based on their specific genotype.

TABLE 1

GENOTYPE	Brain weight (mg)
WT-PCSK9^{wt}	470 (460 - 482.4)
WT-PCSK9^{he}	477 (466.5 - 479.2)
WT-PCSK9^{ko}	482 (462.4 - 490.5)
5XFAD^{he}-PCSK9^{wt}	462.2 (440.2 - 524.1)
5XFAD^{he}-PCSK9^{he}	491.3 (482.7 - 494.9)
5XFAD^{he}-PCSK9^{ko}	486.7 (480 - 494.4)

***Table 1**. Median brain weight of the six studied experimental murine models.* The Kolmogorov-Smirnov test was used to determine the normality of the distribution. Continuous variables were reported as median (interquartile range [IQR] defined as the 25th percentile – 75th percentile) for skewed distribution. To compare the three groups, the one-way ANOVA test was performed for data normally distributed, while skewed variables were compared by the Kruskal-Wallis test. Dunnett's post-hoc test was performed for multiple comparisons.

Then, total cholesterol was quantified in the right hemisphere. As reported in **Figure 15**, no differences were detected in brain cholesterol levels of WT mice, even if a trend towards the gene-dose dependency reduction was detected based on the PCSK9 genotype (r^2 for gene-dependency=0.231; p=0.017). Interestingly, in 5XFAD^{he} mice, a general reduction in brain cholesterol content was detected as compared to the WT ones, reaching the statistical significance in 5XFAD^{he}-PCSK9^{wt} and 5XFAD^{he}-PCSK9^{he} mice (*p<0.05 vs WT-PCSK9^{wt} mice). In this experimental group, no differences in cholesterol levels were detected in mice's brains based on their PCSK9 allelic background, probably as a consequence of the already low cholesterol levels induced by the heterozygous 5XFAD mutations.

FIGURE 15

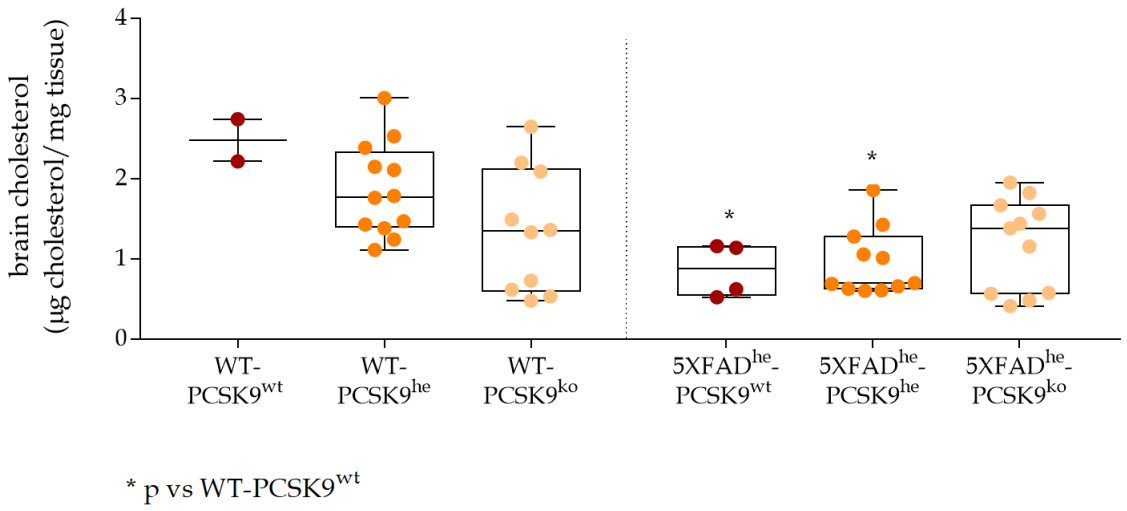

***Figure 15**. Brain cholesterol levels of WT or 5XFAD^{he} mice with homozygous or heterozygous PCSK9 mutation.* After sacrifice, brain was isolated and then conserved at -80°C until use; cholesterol was quantified through Amplex® Red Cholesterol Assay kit performed upon the right hemisphere. Each point of the scatter plot represents the mean value of duplicate serum cholesterol quantification. The Kolmogorov-Smirnov test was used to determine the normality of the distribution. To compare the six experimental groups, skewed variables were compared by the Kruskal-Wallis test. The Dunnett's post-hoc test was performed for multiple comparisons. A value of p<0.05 was considered statistically significant. * refers to WT-PCSK9^{wt}. * p<0.05.

2.4 IMPACT OF PCSK9 ON BRAIN HYDROXYSTEROLS LEVELS

Finally, in parallel with serum analyses, the most relevant cholesterol oxidised products were quantified also in animals' brain. As reported in **Figure 16**, only 24-OHC and 27-OHC were detectable in brain tissue. Similarly to serum, both 24-OHC and 27-OHC levels were comparable among the six considered experimental groups (**Figure 16A** and **16B**, respectively).

FIGURE 16

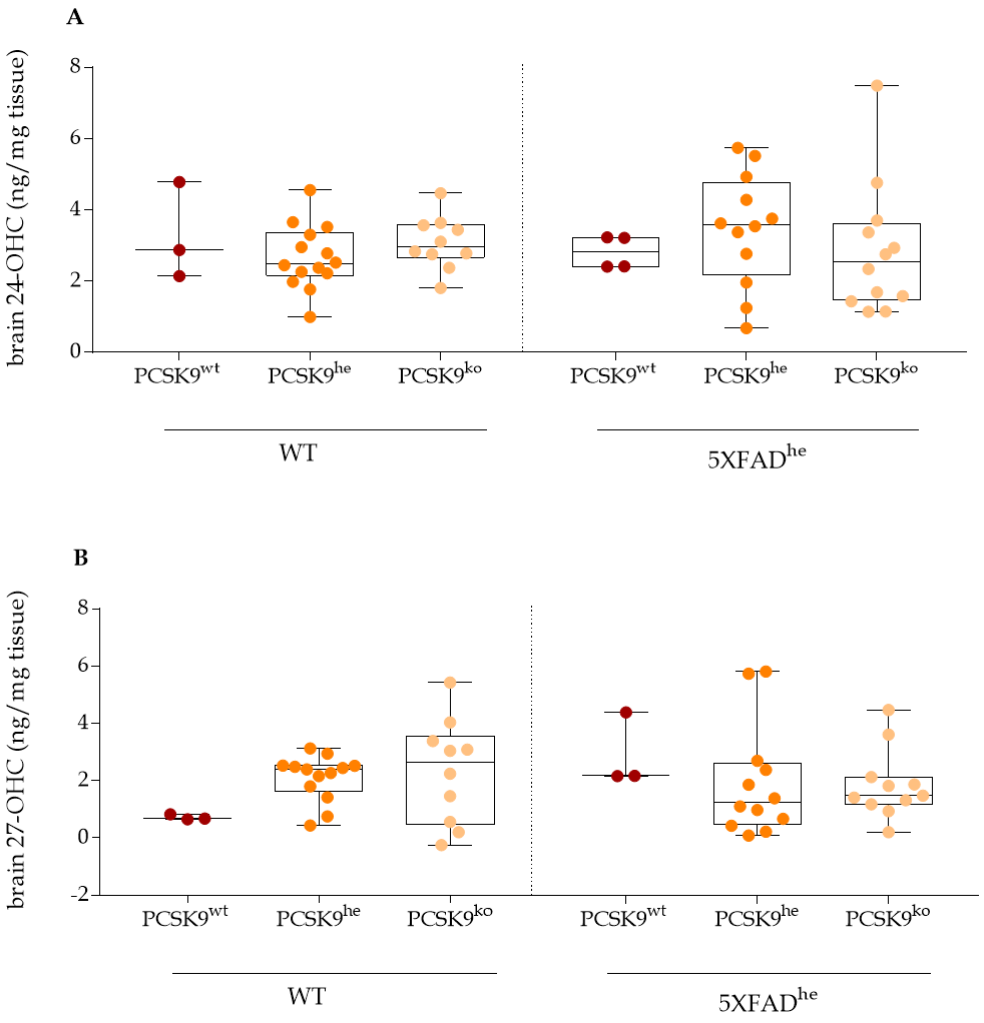

***Figure 16**. Brain levels of 24-OHC (**A**) and 27-OHC (**B**) in WT or 5XFAD^{he} mice with homozygous or heterozygous PCSK9 mutation.* Each point of the scatter plot represents the mean percentage of duplicate quantification of cerebral tissue. The horizontal, solid line represents the mean of each group. The Kolmogorov-Smirnov test was used to determine the normality of the distribution. To compare the three groups, the one-way ANOVA was performed for data normally distributed, while skewed variables were compared by the Kruskal-Wallis test. The Dunnett's post-hoc test was performed for multiple comparisons.

3. INFLUENCE OF PCSK9 ON CHOLESTEROL PARAMETERS: *EX VIVO* EVIDENCE FROM HUMAN SAMPLES

The possible relevance of PCSK9 in cholesterol homeostasis alterations occurring in AD pathogenesis was finally investigated through an *ex vivo* study conducted upon biological samples isolated from patients with different degrees of cognitive alteration. In particular, in collaboration with the Department of Biomedical, Metabolic ad Neural Sciences of the University of Modena and Reggio Emilia and with the University Hospital of Modena, a case-control study was set up, aiming at evaluating the role of PCSK9 as a possible disease-linked biomarker. Indeed, PCSK9 quantification was performed in CSF and serum samples, and its association with apoE genotype and the neurobiomarkers normally evaluated in AD diagnosis was performed, together with the analysis of some of the most relevant sterol-related parameters such as cholesterol and oxidised cholesterol metabolites 24-, 25- and 27-OHC.

Specifically, 83 patients were recruited by the Center of Cognitive Neurology of the Modena City Hospital and underwent clinical, neuropsychological and neuroimaging investigation, with a subsequent follow-up. As widely described in the Material and Method section, the recruited patients were furtherly divided into 3 experimental groups:

- Patients with a diagnosis of MCI (MCI; n= 28);
- Patients with MCI furtherly degenerated to AD (MCI-AD; n=27);
- Patients with an established diagnosis of AD (AD, n=28).

The main demographic and clinical characteristics of the considered population are reported in **Table 2**, as well as their apoE genotype. Concerning the main demographic parameters, MCI-AD subjects were slightly older compared to MCI subjects (* p=0.0235), with a median age of 67 (60-70) as compared to median age of 61.5 (54-66.75) in MCI subjects. Furthermore, MCI subjects were composed of a lower female percentage as compared to AD (46% MCI vs 75% AD, * p=0.0286). No differences were retrieved in the schooling years of the subjects of each group, with a median of 8 (5-13) years for both MCI and AD subjects and 13 (5-13) for MCI-AD patients.

TABLE 2

	MCI (n=28)	**MCI-AD (n=27)**	**AD (n=28)**	**p-value**
Demographic parameters				
Age	61.5 (54-66.75)	**67 (60-70)**	65 (62-69.75)	0.0235 (MCI-AD vs MCI)
Female (%)	**46**	63	75	0.0286 (MCI vs AD)
Schooling (years)	8 (5-13)	13 (5-13)	8 (5-13)	ns
apoE Genotype				
apoEε4 non-carriers (%)	68	**20**	48	0.0005 (MCI-AD vs MCI) 0.033 (MCI-AD vs AD)
apoE ε4 heterozygous (%)	32	**60**	33	0.042 (MCI-AD vs MCI) 0.005 (MCI-AD vs AD)
apoE ε4 homozygous (%)	**0**	20	19	0.017 (MCI vs MCI-AD) 0.013 (MCI vs AD)
Diagnostic parameters				
MMSE	28 (27-29)	27 (24-28)	**21.5 (16.5-25.75)**	<0.0001 (AD vs MCI) 0.0007 (AD vs MCI-AD)
ADL	6 ± 0	6 ± 0	**5.54 ± 1.14**	0.006 (AD vs MCI) 0.007 (AD vs MCI-AD)
IADL	8 (0)	8 (0)	**6 (1.75)**	<0.0001 (AD vs MCI) <0.0001 (AD vs MCI-AD)
$A\beta_{1-42}$ (pg/ml)	889.8 ± 303	**437 ± 90.2**[a]	**416.6 ± 111**[b]	[a] and [b] <0.0001 vs MCI
Total-Tau (pg/ml)	242 (156.8 – 300.8)	**495 (334-699)**[a]	**509.5 (344 – 847)**[b]	[a] and [b] <0.0001 vs MCI
Phospho-Tau (pg/ml)	47.50 (37.25 – 66)	**76 (62-98)**[a]	**72.5 (60.75 – 117)**[b]	[a] 0.0002 vs MCI [b] <0.0001 vs MCI

***Table 2**. Demographic and clinical characteristics of the studied subjects population.* The Kolmogorov-Smirnov test was used to determine the normality of the distribution. Continuous variables were reported as mean ± standard deviation (SD) for normal distribution or median (interquartile range [IQR] defined as the 25th percentile – 75th percentile) for skewed distribution. To compare the three groups, the one-way ANOVA test was performed for data normally distributed, while skewed variables were compared by the Kruskal-Wallis test. Dunnett's post-hoc test was performed from multiple comparisons. The Chi-square test was used to compare categorical data presented as percentages. Statistically significant values are reported in bold.

Concerning the frequency of the apoE Ɛ4 genotype, the MCI group showed the highest percentage of apoE Ɛ4 non-carriers (68%) as compared to MCI-AD (20%) and AD (48%). On the other hand, the MCI-AD group was characterised by the highest percentage of heterozygous apoE Ɛ4 carriers (60%), significantly higher compared to MCI (32%; * p=0.042) and AD (33%; **p=0.005). Finally, the percentage of homozygous apoE Ɛ4 carriers was similar in MCI-AD and AD patients (20% and 19%, respectively), while, interestingly, no patients in the MCI group was homozygous for the apoE Ɛ4 allele (*p=0.017 vs MCI-AD and *p=0.013 vs AD). Concerning the main AD diagnostic parameters, the AD group, as expected, was characterized by a clinical picture with poorer cognitive performances and difficulties in facing the daily activities, as reflected in lower MMSE, ADL and IADL scores as compared to MCI-AD and MCI subjects. Moreover, both AD and MCI-AD patients displayed increased and similar pathological CSF biomarkers as compared to MCI subjects: $A\beta_{1-42}$ was indeed higher (****p<0.0001 vs MCI group), as well as total-tau (****p<0.0001 vs MCI group) and phospho-tau (***p=0.0002 for MCI-AD vs MCI group and ****p<0.00001 for AD vs MCI group).

3.1 CSF AND SERUM PCSK9 CONCENTRATION

The first analysed parameter was PCSK9 concentration in both CSF and serum (**Figure 17**). As shown in **Figure 17A**, no significant differences among the three groups were detected in the CSF of three considered experimental groups, except for a slight increase in PCSK9 levels of the AD group. Interestingly all the three patient's groups displayed significantly higher CSF PCSK9 levels as compared to those of a control group previously analysed by our research group, whose mean levels were 0.63 ± 0.47 ng/ml [287] (****p<0.0001 vs all).

In serum (**Figure 17B**), PCSK9 levels were found to be approximately 100-fold higher as compared to those present in CSF. Interestingly, while no significant changes in PCSK9 concentration were detected between MCI and AD subjects, MCI-AD displayed significantly higher PCSK9 levels as compared to AD patients (**p<0.01).

FIGURE 17

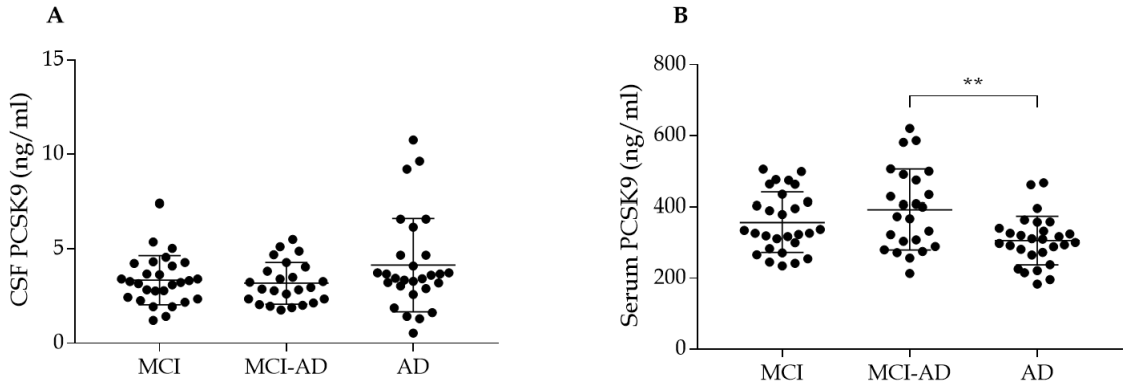

***Figure 17**. CSF (**A**) and Serum (**B**) PCSK9 levels in MCI, MCI-AD and AD patients.* Each point of the scatter plot represents the mean percentage of duplicate quantification of CSF and serum samples. The Kolmogorov-Smirnov test was used to determine the normality of the distribution. The one-way ANOVA test was used to compare the three groups with data normally distributed, while skewed variables were compared by the Kruskal-Wallis test. Dunnett's post-hoc test was performed multiple comparisons. **p<0.01.

3.1.1 PCSK9 levels and apoE genotype

Furtherly, as reported in **Figure 18**, PCSK9 levels were stratified between carriers and non-carriers of the apoE Ɛ4 isoform. Considering all the 83 subjects as a whole experimental group (**Figure 18A**), no differences were detected between CSF PCSK9 levels in apoE Ɛ4 non-carriers and carriers. By individually analysing the patients based on their clinical diagnosis, a similar situation was found in MCI and MCI-AD groups (**Figure 18B** and **18C**, respectively), both characterized by comparable PCSK9 levels in CSF of the subjects, with no differences based on their apoE Ɛ4 isoform. Interestingly, only within AD patients (**Figure 18D**), apoE Ɛ4 carriers showed significantly higher CSF PCSK9 concentration as compared to apoE Ɛ4 non-carriers (+ 38%; * p<0.05).

FIGURE 18

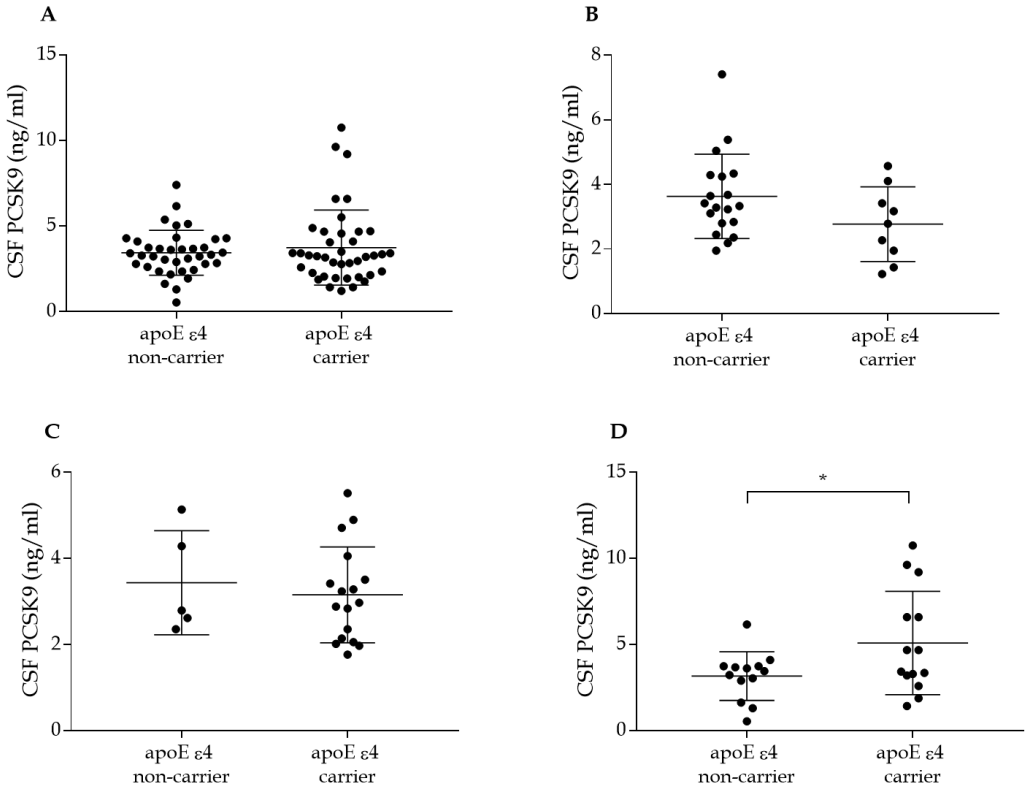

***Figure 18**. CSF PCSK9 levels stratified between apoE Ɛ4 non-carriers and apoE Ɛ4 carriers within all patients considered as a whole group (**A**), or in MCI (**B**), MCI-AD (**C**) and AD (**D**) subjects.* Each point of the scatter plot represents the mean percentage of duplicate quantification of CSF samples. The Kolmogorov-Smirnov test was used to determine the normality of the distribution. The unpaired t-test for data normally distributed or the Mann-Withney for data not-normally distributed test was used to compare the two groups. Dunnett's post-hoc test was performed for multiple comparisons. *p<0.05

The same stratification in serum PCSK9 levels didn't reveal significant differences when considering all the subjects as a whole group (data not shown). However, by evaluating the single group of subjects stratified based on their apoE Ɛ4 isoform, a significant reduction in serum PCSK9 levels of apoE Ɛ4 carriers compared to non-carriers was highlighted only in the MCI group (-22%: *p<0.05).

Finally, no significant differences were detected in PCSK9 CSF and serum concentration in males compared to female subjects (data not shown).

3.1.2 Correlation between PCSK9 levels in CSF and serum

Additionally, CSF PCSK9 levels were correlated to those in the serum of each patient (**Figure 19**). As seen in **Figure 19A**, considering all subjects as a whole group, no significant association was found (r=0.11; p=0.331). Interestingly, in analysing the same relationship and considering the three single experimental groups separately, a significant and linear correlation was observed only in the AD group (r=0.521; p=0.004), as reported in **Figure 19D**. On the other hand, no significant association between CSF and serum PCSK9 levels was detected neither in MCI (**Figure 19B**) nor in MCI-AD patients (**Figure 19C**).

FIGURE 19

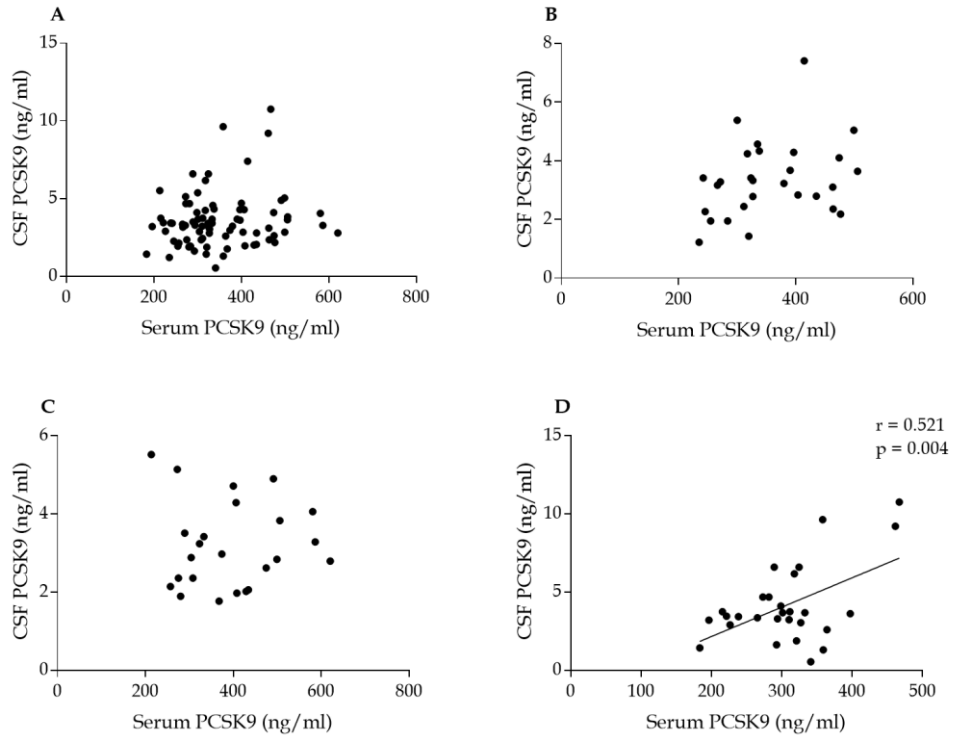

Figure 19*. Correlation between CSF and serum PCSK9 levels in all patients considered as a whole group (**A**), or in MCI (**B**), MCI-AD (**C**) and AD (**D**) subjects.* Relationships were established by non-parametric correlation analyses, and for the significant values, the Spearman r coefficient is reported.

3.2 CSF STEROLS QUANTIFICATION

Afterwards, cholesterol concentration in CSF was quantified and reported in **Table 3**. The obtained values are in line with CSF cholesterol values previously described [267]; in this context, no significant differences were detected among the three considered experimental groups.

TABLE 3

Experimental Group	n	CSF Cholesterol (μg/ml) Median	25th-75th percentile
MCI	28	1.08	0.857 - 1.34
MCI-AD	27	1.159	0.931 – 1.528
AD	28	1.013	0.773 – 1.505

***Table 3**. CSF Cholesterol levels in MCI, MCI-AD and AD patients.* Each CSF sample has been tested twice and the mean value has been considered. The table summarizes the experimental number in each patient's group, the median value of CSF cholesterol and the values included in the 25th and 75th percentile. The Kolmogorov-Smirnov test was used to determine the normality of the distribution. To compare the three groups, the one-way ANOVA was performed for data normally distributed, while skewed variables were compared by the Kruskal-Wallis test. The Dunnett's post-hoc test was performed for multiple comparisons.

In addition, similarly to the *ex-vivo* analyses previously described and performed in the murine models (**Figure 14**), the potential alteration of the levels of the three main hydroxysterols has been explored also in the recruited cohort of patients, as their alteration may help in lighten new AD-related pathogenic mechanisms as well as may serve as possible new disease biomarkers. To this aim, 24-, 25- and 27-OHC have been quantified in CSF through LC-MS/MS, as deeply described in the Material and Method section. As reported in **Figure 20A**, no differences were detected in 24-OHC levels between MCI, MCI-AD and AD subjects. A similar picture was also observed for 25-OHC (**Figure 20B**) and 27-OHC (**Figure 20C**) levels in MCI, MCI-AD and AD patients.

Within this context, no changes were found by stratifying subjects based on their apoE genotype or sex (data not shown).

FIGURE 20

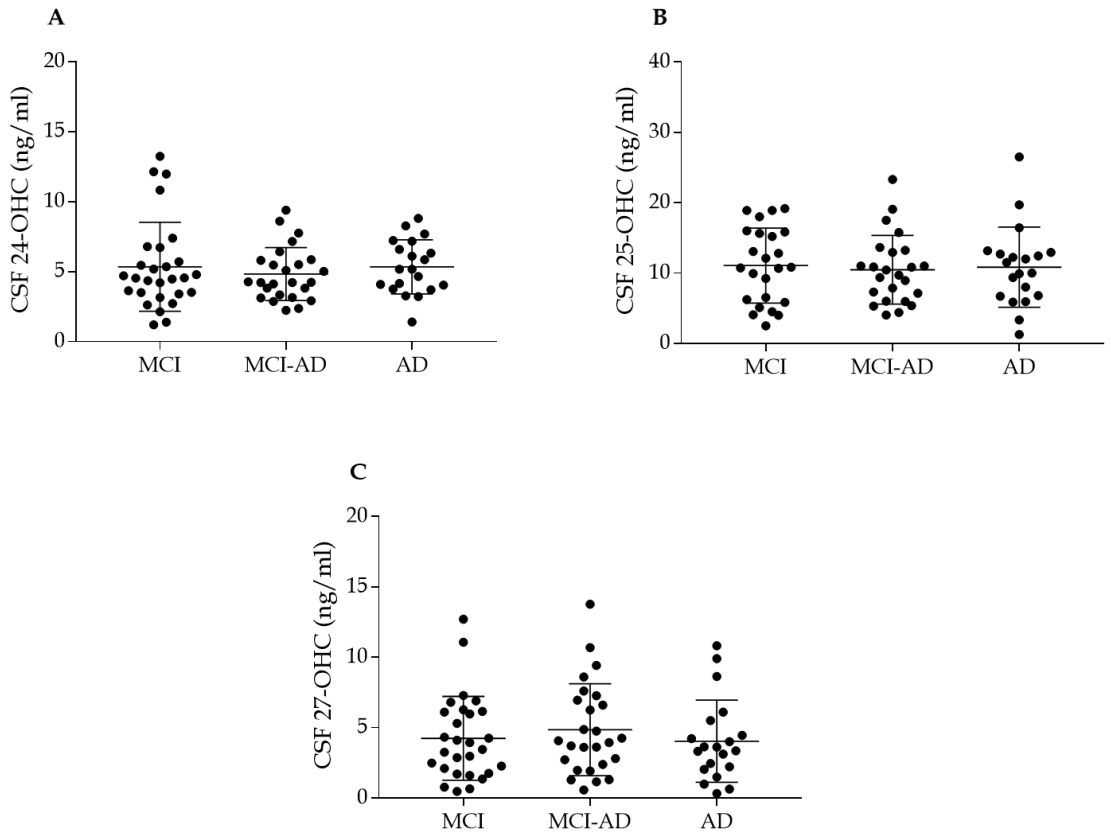

***Figure 20**. CSF levels of 24-OHC (**A**), 25-OHC (**B**) and 27-OHC (**C**) in MCI, MCI-AD and AD subjects.* Each point of the scatter plot represents the mean percentage of duplicate quantification of CSF. The horizontal, solid line represents the mean of each group. The Kolmogorov-Smirnov test was used to determine the normality of the distribution. To compare the three groups, the one-way ANOVA was performed for data normally distributed, while skewed variables were compared by the Kruskal-Wallis test. The Dunnett's post-hoc test was performed for multiple comparisons.

3.3 SERUM STEROLS QUANTIFICATION

In collaboration with Professor M. Bertolotti from the University of Modena and Reggio Emilia, the serum lipid profile of the above-mentioned patients has been evaluated. As reported in **Table 4**, Total cholesterol (TC) values were similar in MCI, MCI-AD and AD subjects and, similarly, no differences were observed in LDL-C and TG levels in the three considered populations. On the other side, AD patients were characterized by significantly increased HDL-C values as compared to MCI subjects (*p=0.037).

TABLE 4

	MCI (n=28)	**MCI-AD (n=27)**	**AD (n=28)**	**p-value**
TC (mg/dl)	206.6 ± 33.3	229.9 ± 49.43	231.7 ± 42.06	
HDL-C (mg/dl)	51.96 ± 12.29	58.22 ± 16.12	**62.14 ± 16.31**	0.037 (MCI vs AD)
LDL-C (mg/dl)	119.7 ± 25.53	133.4 ± 33.45	134 ± 28.5	
TG (mg/dl)	117 (79-149)	115 (89-149)	87.5 (72.25-130.8)	

***Table 4**. Lipid profile of MCI, MCI-AD and AD patients.* Each serum sample has been tested twice and the mean value has been considered. The Kolmogorov-Smirnov test was used to determine the normality of the distribution. Continuous variables were reported as mean ± standard deviation (SD) for normal distribution or median (interquartile range [IQR] defined as the 25th percentile – 75th percentile) for skewed distribution. To compare the three groups, the one-way ANOVA test was performed for data normally distributed, while skewed variables were compared by the Kruskal-Wallis test. Dunnett's post-hoc test was performed from multiple comparisons. Statistically significant values are reported in bold. TC: Total cholesterol; HDL-C: HDL cholesterol; LDL-C: LDL cholesterol; TG: triglycerides.

In addition, similarly to CSF analyses, hydroxysterols, namely 24-, 25- and 27-OHC, have been quantified in serum of the considered cohort of patients through LC/MC-MS. As shown in **Figure 21**, the serum concentration of all the three considered hydroxysterols was significantly higher as compared to the one retrieved in CSF (about a 15-20-fold increase as compared to CSF). No differences were detected in serum 24-OHC (**Figure 21A**) and 27-OHC (**Figure 21C**) among MCI, MCI-AD and AD subjects. Interestingly, as shown in **Figure 21B**, slightly higher levels of 25-OHC were found in MCI-AD as compared to AD subjects (*p<0.05).

FIGURE 21

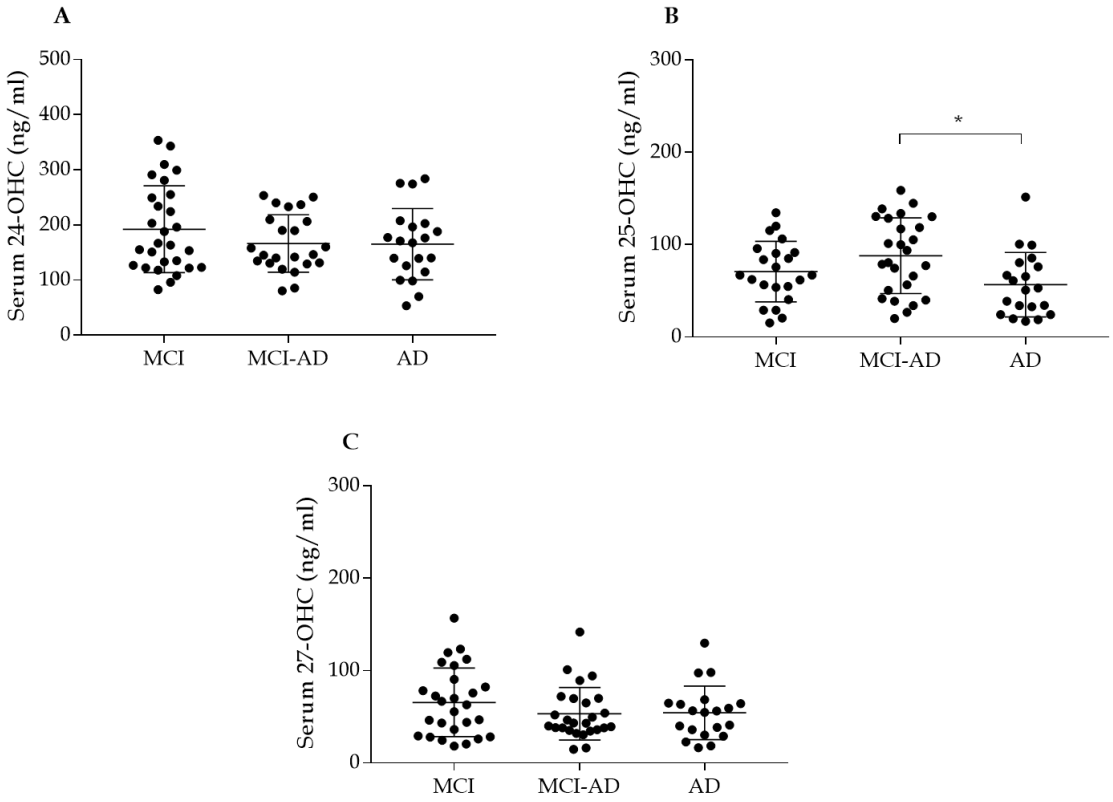

***Figure 21**. Serum levels of 24-OHC (**A**), 25-OHC (**B**) and 27-OHC (**C**) in MCI, MCI-AD and AD subjects.* Each point of the scatter plot represents the mean percentage of duplicate quantification of serum. The horizontal, solid line represents the mean of each group. The Kolmogorov-Smirnov test was used to determine the normality of the distribution. To compare the three groups, the one-way ANOVA was performed for data normally distributed, while skewed variables were compared by the Kruskal-Wallis test. The Dunnett's post-hoc test was performed for multiple comparisons.

Within this context, no changes were found by stratifying subjects based on their apoE genotype or sex (data not shown).

As previously discussed, AD pathogenesis is tightly linked to a dysregulation in cholesterol homeostasis; within this context, central and peripheral cholesterol pools are traditionally considered as separated districts due to the presence of BBB, even if the extent of this separation has been currently questioned and represents an interesting field of investigation. In this regard, the possible correlation between peripheral and central lipid values has been investigated. As reported in **Figure 22A**, a significant association was found between serum HDL-C values and CSF 24-OHC levels when considering all the subjects as a whole group (r=0.242; p=0.04). Interestingly, this linear correlation acquires even more strength when considering only apoE Ɛ4 carriers (r=0.526; p=0.001;

Figure 22B), while it disappears when only the non-apoE Ɛ4 carriers subjects are analysed (data not shown).

FIGURE 22

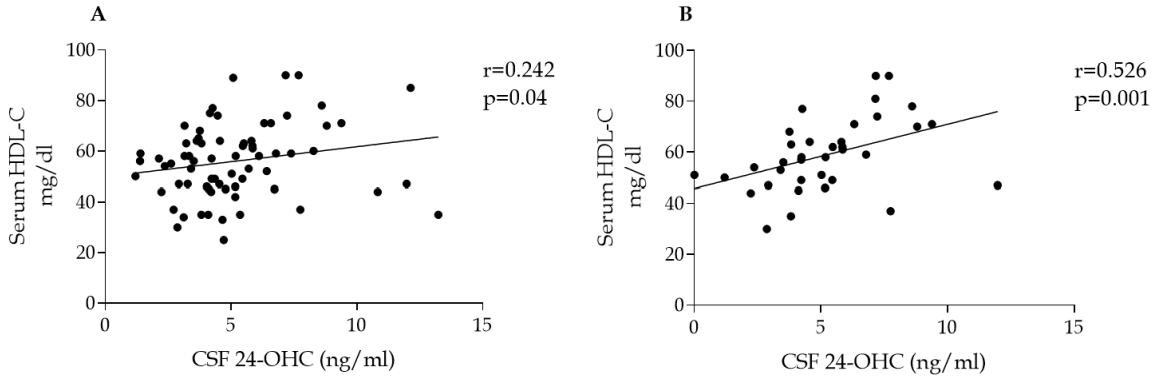

***Figure 22**. Correlation between Serum HDL-C and CSF 24-OHC levels in all patients considered as a whole group (**A**) and in apoE Ɛ4 carriers (**B**).* Relationships were established by non-parametric correlation analyses, and for the significant values, the Spearman r coefficient is reported.

3.4 CORRELATIONS BETWEEN PCSK9 AND HYDROXYSTEROLS

Considering the great impact of both PCSK9 and hydroxysterols in cerebral lipid metabolism, the possible correlation between these two parameters has been evaluated.

As reported in **Figure 23**, a significant, inverse association between 27-OHC and PCSK9 was found when considering all the subjects as a whole group. Specifically, CSF PCSK9 levels inversely associated with CSF 27-OHC levels (r=-0.238, p=0.047; **Figure 23A**) and with serum 27-OHC levels (r=-0.228; p=0.05; **Figure 23B**).

FIGURE 23

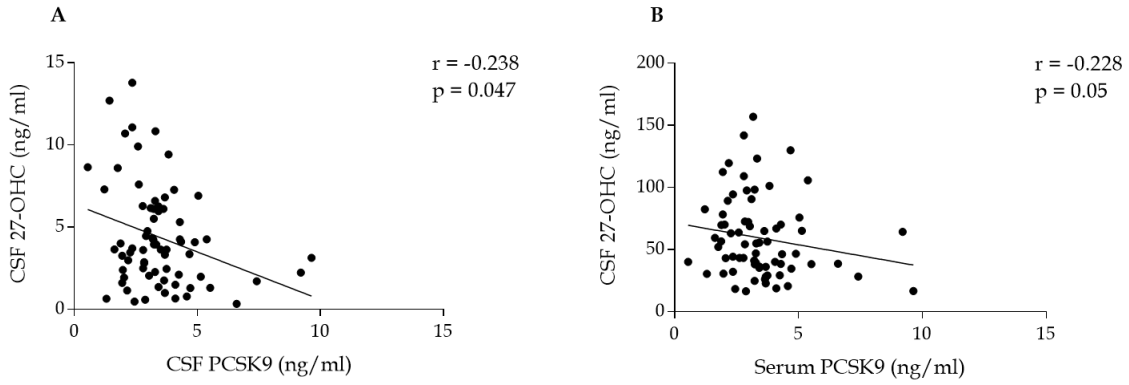

***Figure 23**. Correlation between CSF 27-OHC and CSF PCSK9 (**A**) and serum PCSK9 (**B**) levels in all patients considered as a whole group.* Relationships were established by non-parametric correlation analyses, and for the significant values, the Spearman r coefficient is reported.

Furthermore, considering CSF, no significant correlations were found between PCSK9 and 24-OHC levels when considering all the subjects as a whole group (Figure 24A). Interestingly, by separately analysing only the apoE Ɛ4 carriers (Figure 24B), a significant, inverse correlation emerged (r= -0.340; p= 0.036).

FIGURE 24

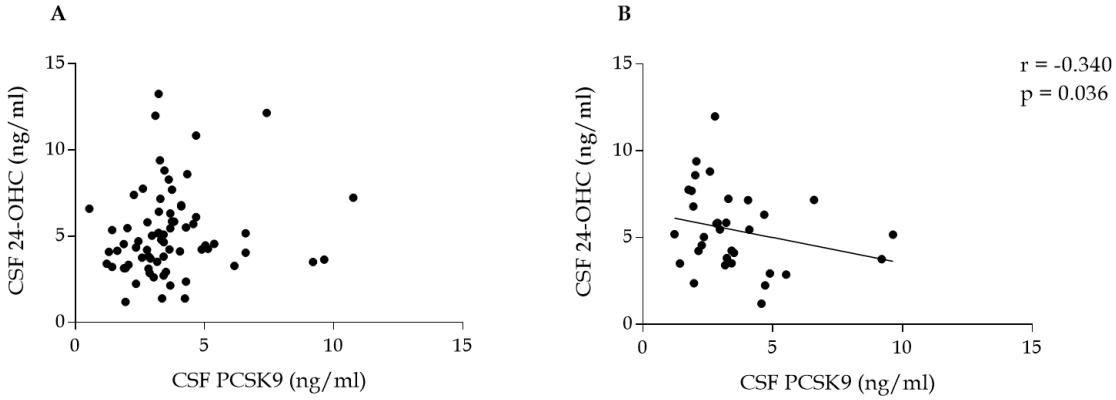

***Figure 24**. Correlation between CSF 24-OHC and CSF PCSK9 levels in all patients considered as a whole group (**A**), or in apoE Ɛ4 carriers only (**B**).* Relationships were established by non-parametric correlation analyses, and for the significant values, the Spearman r coefficient is reported

Finally, no significant correlations were found between either CSF or serum PCSK9 levels and the specific AD biomarkers, such as $A\beta_{1\text{-}42}$, total-tau, phospho-tau and the specific scores aimed at evaluating the patient's cognitive impairment, such as MMSE, ADL and iADL (data not shown).

DISCUSSION

In the present research work the potential involvement of PCSK9 in brain cholesterol dysregulation, which represents a central aspect of AD [374], has been investigated, providing new evidence that contributes to identifying PCSK9 as a possible disease-related biomarker and a pharmacological target. PCSK9, one of the major regulators of plasma LDL-C levels due to its degrading activity on LDLR [233], is also expressed in CNS [243], where it takes part in the modulation of several relevant processes [243,246–249]. Since lipoprotein receptors may be sensitive to the degrading activity of brain PCSK9, as in peripheral tissues, a direct involvement of PCSK9 in cholesterol metabolism has been postulated [250–252,344,345].

Aiming in investigating the possible relationship between PCSK9 and cerebral cholesterol homeostasis in AD, a translational study was set up, following three different experimental approaches including *in vitro* studies on cultured astrocytes and neuronal cell models, and *ex vivo* analyses upon samples isolated from both animal models of the disease and patients with different degrees of cognitive impairment.

In the first part of the research work, by conducting *in vitro* experiments upon human cell models of astrocytes and neurons, the impact of PCSK9 on the most relevant steps of brain cholesterol transport has been explored. Cholesterol is indeed extremely relevant for cerebral homeostasis [126,130] and brain cholesterol metabolism disturbances have been described in several neurodegenerative diseases, including AD [133,137,138,140]. Brain relies on *in situ* cholesterol biosynthesis, due to the presence of BBB, which impedes access to peripheral cholesterol [126,167]. Adult neurons strongly depend on cholesterol provided by astrocytes, as their endogenous cholesterol rate, high during the embryogenesis, progressively decreases [170]. Hence, brain cholesterol transport represents a crucial step for neuronal homeostasis and, specifically, newly-synthesized cholesterol and apoE from astrocytes are complexed in apoE-containing lipoparticles, finally internalized into neurons, thus contributing to their cholesterol supply [186,187]. In this study, U373 astrocytoma cells were used as an *in vitro* model of astrocytes, that represents the most abundant glial cells and play a relevant role in CNS both by providing neurons with several trophic factors, including cholesterol [185], and by presiding over brain immune surveillance [75]. Furthermore, cultured astrocytes were incubated with $A\beta_{1-42}$ fibrils in order to reproduce an AD-like experimental setting. Specifically, $A\beta_{1-42}$ fibrils' selection derives from a preliminary analysis of the impact of $A\beta_{1-42}$ at different concentrations and degrees of oligomerizations, namely $A\beta_{1-42}$ oligomers and fibrils, on cellular viability. Interestingly, in absence of any cytotoxic effect exerted by PCSK9, $A\beta_{1-42}$ oligomers were

able to significantly impact astrocytes' viability already at lower concentrations as compared to $A\beta_{1-42}$ fibrils. In this regard, the available evidence aiming at investigating whether oligomeric or fibrillar $A\beta_{1-42}$ species are most toxic is still controversial, and may possibly be related to several parameters that may affect the clarity of this outcome, including the assay used to monitor cell viability, the experimental protocol followed to reconstitute the above-mentioned $A\beta_{1-42}$ aggregates, as well as the use of primary or continuous cell lines [375]. However, there is consensus in acknowledging that $A\beta_{1-42}$ oligomers and fibrils promote a differential profile of pro-inflammatory cytokines and chemokines release, probably as a consequence of their differential size and structure, thus of their interaction with cellular receptors and channel [376], that may finally impact their differential effect on astrocytes' viability. Since $A\beta_{1-42}$ fibrils represent the most common neuropathological oligomerization form retrieved in AD brains [370], this aggregation form at [1μM] was selected to explore the impact of PCSK9 on cholesterol-related parameters in AD-like conditions, in absence of any cytotoxic effect derived from the incubation with $A\beta_{1-42}$ fibrils. Furthermore, $A\beta_{1-42}$ fibrils [1μM] is the most commonly used concentration reported in the literature. However, since AD patients are characterized by a deposition of $A\beta_{1-42}$ that is present and acts for many years, it would be extremely interesting to evaluate an incubation time longer than 48 hours.

Focusing on the impact of PCSK9 on brain cholesterol transport, in U373 astrocytoma cells PCSK9 induced a dose-dependent increase in endogenous cholesterol synthesis. Interestingly, this effect was independent of the presence of $A\beta_{1-42}$ fibrils. This observation was interpreted as a possible consequence of the activation of a feedback mechanism involving SREBP transcription factor in response to the degrading activity of PCSK9 on receptors in astrocytes responsible for cholesterol internalization, similarly to PCSK9's activity on hepatic receptors [233]. PCSK9 involvement in the regulation of brain lipoprotein receptors has been previously questioned, showing, however, contrasting evidence. During brain development as well as after a transient ischemic stroke, PCSK9 has been shown to downregulate LDLR expression in mice [252]. Similar evidence was reported for other receptors involved in neuronal cholesterol internalization belonging to the same family, such as apoER2, VLDLR and LRP1 [206,250,377]. Conversely, however, in a separate study performed upon adult mouse brains, PCSK9 didn't impact LDLR and other lipoprotein receptors expression [251]. In the present study, the incubation of astrocytes with human recombinant PCSK9 led to a marked reduction in LDLR and apoER2. This observation is furtherly confirmed by the significant reduction in the uptake of apoE-

containing reconstituted HDL in astrocytes incubated with PCSK9, whose internalization is specifically mediated by the interaction with lipoprotein receptors and apoE on rHDL surface [157]. Furthermore, PCSK9-mediated downregulation of LDLR and apoER2 expression in astrocytes occurred independently of the presence of $A\beta_{1-42}$ fibrils. Having observed a PCSK9-induced increase in endogenous cholesterol synthesis, possibly as a consequence of the reduced cholesterol internalization due to the degrading activity of the receptors involved in exogenous uptake, the net intracellular cholesterol content was subsequently analysed, highlighting that PCSK9 led to an overall reduction in total cholesterol content in astrocytes. Interestingly, the treatment with $A\beta_{1-42}$ fibrils also lowered astrocytic cholesterol content, with a more pronounced effect when co-incubated with PCSK9. These observations are peculiar and suggest that the significant increase in endogenous cholesterol biosynthesis induced by PCSK9 wasn't able to completely counterbalance the reduced cholesterol uptake derived from the degrading activity of the enzyme on the lipoprotein receptors. Furthermore, $A\beta_{1-42}$ fibrils, whose incubation has been performed to simulate the AD-like experimental conditions, were able to furtherly reduce the net intracellular cholesterol content by synergistically acting with PCSK9. The molecular mechanisms of the specific $A\beta_{1-42}$ fibrils-dependent intracellular cholesterol content reduction are not yet fully understood and deserve further investigations, but they're probably not related to lipoprotein receptors, since our results showed that $A\beta_{1-42}$ fibrils didn't impact either on LDLR or on apoER2 expression. Within this contest, membrane cholesterol content represents one of the main and most relevant cellular pools of free cholesterol, playing an extremely relevant role due to its involvement in cholesterol efflux and in mediating cellular functions in CNS [372]. Interestingly, the PCSK9-induced reduction of the overall intracellular cholesterol content, however, didn't affect the membrane cholesterol pool in astrocytes. On the other side, the presence of $A\beta_{1-42}$ fibrils led to a moderate but significant reduction in the amount of free cholesterol contained in the plasma membrane of astrocytes. In addition, since the intracellular cholesterol pool is constituted by a dynamic balance between the newly synthesized rate, the fraction internalized from the extracellular milieu as well as the fraction of cholesterol that flows outside the cells through the active efflux process, the impact of PCSK9 was evaluated in this latter mechanism. PCSK9, indeed, exerted a neutral impact on astrocytic cholesterol efflux mediated by the two main membrane transporters, namely ABCA1 [197] ad ABCG1 [196]. Interestingly, $A\beta_{1-42}$ fibrils were associated with a reduction in cholesterol efflux to apoE as extracellular acceptor, suggesting a peculiar interference of $A\beta_{1-42}$ fibrils with

ABCA1-mediated efflux, that has been furtherly confirmed by quantifying the transporter expression through Western Blot analysis. This observation is consistent with the previously described $A\beta_{1-42}$ fibrils-mediated reduction of membrane cholesterol content. Indeed, a reduction in cholesterol efflux from reactive cultured astrocytes, possibly related to the $A\beta_{1-42}$ fibrils-induced downregulation of ABCA1-expression was also previously observed [378]. The evidence that $A\beta_{1-42}$ fibrils may inhibit ABCA1 expression is consistent with previous findings in brain of AβPP/PS1 transgenic mice, characterized by increased Aβ processing and deposition [379]. Conversely, a recent study reported an increase in ABCA1 levels following $A\beta_{1-42}$ fibrils treatment in primary cultured astrocytes, in presence, however, of a decreased cholesterol efflux; the molecular mechanisms of this apparently contrasting evidence have not been fully elucidated but are probably related to an interference of apoE lipidation process [380].

Globally, within this experimental setting, the net effect resulting from PCSK9-induced increased synthesis and impaired endocytosis led to a reduction in astrocyte cholesterol content that was furtherly lowered by the co-incubation with $A\beta_{1-42}$ fibrils. The mechanism underlying this effect is now under investigation, but these observations clearly point to an impaired astrocyte cholesterol homeostasis, namely reduced intracellular cholesterol that, eventually, may translate in reduced supply to neurons.

Concerning the impact of PCSK9 on the last step of the cholesterol transport towards neurons, human neuroblastoma SH-SY5Y cells were retrovirally transduced to overexpress PCSK9. In addition, PCSK9-overexpressing and control neuroblastoma cells were induced to differentiate in neuronal-like cells following the incubation with all-trans-retinoic acid (ATRA), able to promote metabolic and morphological changes to mimic neuronal responses [355]. Interestingly, PCSK9 overexpression in differentiated neuroblastoma cells was associated with a significant reduction in cholesterol internalization from apoE-containing reconstituted HDL, which occurs independently of $A\beta_{1-42}$ fibrils, as also previously observed in astrocytes. The PCSK9-mediated reduction of exogenous cholesterol uptake is consistent with the strong reduction of both LDLR and apoER2 expression occurring in PCSK9-overexpressing neuroblastoma cells, which has been preliminarily demonstrated by our research group. Furthermore, this observation is in accordance with previous reports indicating that PCSK9 was able to downregulate cerebral LDLR expression during embryogenesis and transient ischemic stroke in mice [252].

The impact of PCSK9 on neuronal cholesterol biosynthesis was then evaluated and, differently from the observation previously described in astrocytes, PCSK9 acted by

furtherly downregulating the already low cholesterol biosynthesis in neurons. This observation also suggests that the regulatory mechanisms in neuronal cells may differ from those in astrocytes. Indeed, despite the enzymatic reactions leading to endogenous cholesterol biosynthesis being common in all tissues, two different, despite interlinked, processes have been proposed, namely the Kandutsch-Russell pathway for adult neurons and the Bloch pathway for astrocytes and developing neurons [170,174]. Within this context, it has previously been demonstrated that neurons prematurely abandon the energetic expensive cholesterol biosynthesis and depend on the less expensive uptake of cholesterol synthesized in astrocytes, that, on the other side, still maintain a high biosynthetic efficiency with a higher ability to up-regulate the synthetic pathway with respect to the cellular needs [170]. Hence, this observation, together with those related to the PCSK9-mediated impairment of cholesterol uptake, may suggest that the overall effect of the enzyme in neurons is linked to the reduction in intracellular cholesterol levels, which may have deleterious consequences on neuronal survival [24]. As a possible consequence, the increased apoptosis due to the dysregulation of a plethora of intracellular mechanisms leads to a dysfunction in neuronal metabolism eventually leading to cellular loss [381]. Consistently, also in the present experimental model, both cholesterol depletion, but also excess cholesterol were associated with a reduction in neuronal viability, which is furtherly worsened by the presence of PCSK9, thus confirming the possible pro-apoptotic role of PCSK9 previously hypothesized through *in vitro* studies [382].

Furthermore, PCSK9-mediated worsening of neurotoxicity was observed also in neurons exposed to $A\beta_{1-42}$ at different aggregation forms, namely $A\beta_{1-42}$ oligomers and fibrils. Interestingly, both $A\beta_{1-42}$ oligomers and fibrils induced a significant and dose-dependent worsening of neuronal viability, consistently with previous experimental observations [383]. The molecular mechanisms and the specific apoptotic pathways related to the deleterious impact of PCSK9 on neuronal viability are currently poorly understood. In this regard, it has been previously demonstrated that PCSK9 may promote neuronal apoptosis through its degrading activity on lipoprotein receptors such as apoER2 and VLDLR, critically involved in the anti-apoptotic reelin pathway [247].

Hence, data obtained through *in vitro* studies point to a possible disturbance of cerebral cholesterol metabolism induced by PCSK9, also acting in cooperation with $A\beta_{1-42}$ fibrils. In astrocytes, indeed, PCSK9 may act by reducing the overall intracellular cholesterol content and thus possibly compromising the first step of brain cholesterol transport, while

in neurons PCSK9 may promote cellular cholesterol depletion, possibly resulting in compromised neuronal viability.

The second part of the present research work focused on the impact of PCSK9 on lipid levels in transgenic mice model of AD with heterozygous or homozygous deletion of PCSK9, specifically generated for this project. In particular, serum and cerebral tissue were isolated from 10 months old mice and cholesterol, as well as the three main oxysterols, were quantified. As expected, a gene-dependent reduction in total cholesterol levels was highlighted in PCSK9^{he} and PCSK9^{ko} as compared to WT- PCSK9^{wt} mice. Furthermore, the presence of the 5 mutations leading to the development of an AD-like phenotype in 5XFAD^{he} mice was associated with an overall reduction of circulating cholesterol levels, maintaining, however, a further gene-dependent reduction related to PCSK9 gene expression. The reduction in serum total cholesterol levels in PCSK9^{ko} mice as compared to those carrying two working PCSK9 alleles has already been observed and well-characterized [384] and it's one of the most relevant *in vivo* pre-clinical evidence supporting the use of anti-PCSK9 agents (mAbs, RNAi) to treat hypercholesterolemia [239,242].

Furthermore, in absence of any differences in brain weight, a trend towards the reduction of cerebral cholesterol content was observed in WT mice with PCSK9^{he} and PCSK9^{ko} allelic background as compared to WT-PCSK9^{wt} mice. This observation is consistent with previous findings and suggests that PCSK9 may act also in the cerebral district by downregulating total brain cholesterol content, possibly through its degrading activity on lipoprotein receptors, similarly as in peripheral tissues [233].

In accordance, the administration of a PCSK9 inhibitor in rats fed with a high-fat diet was associated with lower hippocampal PCSK9 expression, accompanied with lower neuroinflammation, an amelioration in cognitive functions and, interestingly, with a reduction in cerebral cholesterol content [385]. Interestingly, 5XFAD^{he} mice overall displayed significantly lower brain cholesterol levels as compared to their WT littermates. In this regard, contrasting experimental evidence has been reported. Indeed, while Mast and colleagues reported that control and 5XFAD^{he} mice were characterized by similar brain cholesterol levels [386], other experimental evidence highlighted that both brain cholesterol content, as well as sterol dynamics, were altered in 5XFAD^{he} mice as compared to controls, with lower cerebral cholesterol and several fluctuations over the course of mice's life [387]. Such specific cholesterol alteration observed by ourselves suggests that in 5XFAD^{he} mice the presence of mutant human APP and PSEN1 is associated with a disturbance of

brain cholesterol homeostasis, that accompanies the cognitive functions and anatomopathological alterations that have been previously described in this specific animal model [367]. No differences in terms of brain cholesterol content were retrieved in 5XFAD^{he} mice based on the heterozygous or homozygous PCSK9 expression. One possible explanation may be related to the fact that in 5XFAD^{he} mice, characterized by already lower cerebral cholesterol content as compared to their WT littermates, the cholesterol-lowering effect of PCSK9 observed in WT mice may be covered. In addition, the increased BBB permeability previously reported in 5XFAD^{he} mice as compared to controls [386] may furtherly represent a disturbing element in brain cholesterol homeostasis, as peripheral and cerebral free cholesterol as well as PCSK9 pools, considered as separate districts, can come into contact [135,244]. Besides cholesterol, also its mono-oxygenated derivatives, hydroxysterols, are known to play a central role in brain metabolism, and their alteration in AD has been previously described [388]. Furthermore, several pieces of evidence suggest that also altered serum hydroxysterols levels may contribute to AD degeneration [334], despite the currently available experimental evidence being inconsistent, as hydroxysterols in serum and CSF of AD subjects were reported as increased, decreased or even unaltered [388,389]. Hence, the most relevant oxysterols, 24-, 25- and 27-OHC were quantified in both serum and cerebral tissue of the considered animal models, observing that nor the presence of heterozygous and homozygous mutations in PCSK9 encoding sequence, nor the 5XFAD^{he} allelic background were able to affect oxysterol balance. One possible limitation of this latter observation may be assumed to the relatively small sample size of PCSK9^{wt} mice, both in animals with the WT or 5XFAD^{he} genic background and representing the internal control groups, that necessitates further analyses, still ongoing.

In the third part of the present research work, a case-control study has been performed by recruiting 83 subjects with different degrees of cognitive impairment, namely subjects with stable MCI, patients with MCI that furtherly degenerated to AD at follow-up, and patients with clinically diagnosed AD. As expected, the main specific AD diagnostic parameters such as $A\beta_{1-42}$, Total-Tau and phospho-Tau were significantly increased in both AD and MCI-AD patients; in addition, AD patients displayed poorer cognitive performances. These observations are in line with previous evidence suggesting that the alterations in the main molecular biomarkers used to formulate an AD diagnosis may precede the cognitive decline [390]. Interestingly, apoE ε4 genotype was the most prevalent in MCI-AD and AD subjects. This observation is in line with previous evidence, pointing

apoE ε4 isoform as the major genetic risk factor that predisposes to AD development [59]. ApoE, in fact, is an apolipoprotein known to play a relevant role in cerebral homeostasis in both physiological and pathological conditions. ApoE is directly synthesized *in situ*, where it participates in several processes including brain cholesterol transport, the maintenance of synaptic plasticity as well as the modulation of the Aβ aggregation process [391]. Within this context, different lines of evidence showed that apoE ε4 isoform is dysfunctional for several reasons, as it has been shown to be hypolipidated as compared to the most common apo ε3 isoform, it accelerates the Aβ deposition as well as it reduces its clearance, and accelerates the disruption of BBB integrity [392]. Accordingly, the apoE ε4 isoform in heterozygosis is associated with a 2-4-fold risk to develop AD, while its presence in homozygosis furtherly increases this risk up to 8-12-fold. In this regard, a similar prevalence of subjects carrying two apoE ε4 alleles was found in AD and MCI-AD patients recruited in the present study, while, interestingly, no stable MCI patient was homozygous for the apoE ε4 allele. Furthermore, MCI-AD patients were slightly older as compared to AD and, even more, to MCI subjects. This observation is consistent with the high prevalence of apoE ε4 genotype among MCI-AD, since apoE ε4 represents the major risk factor for LOAD, affecting older subjects as compared to EOAD [59].

CSF PCSK9 levels were similar among stable MCI, MCI-AD and AD subjects, possibly suggesting that this parameter may not be reliable to discriminate the different phases of the disease, nor to predict the further degeneration to AD in patients with MCI. In this regard, a study previously conducted by our research group showed that CSF PCSK9 levels were increased in AD subjects as compared to controls [287], and, interestingly, the absolute CSF PCSK9 values of the 83 patients recruited in the present research work were overall higher as compared to those of control patients previously analysed. Altogether, these observations suggest that PCSK9 levels in CSF may be increased since the early phases of the disease. Furthermore, consistently with previous findings [287], a significant increase in CSF PCSK9 levels was observed specifically in AD patients carrying at least one apoE ε4 allele and reinforces the possible existence of a mechanistic connection between apoE ε4 and PCSK9 in AD, that may also involve PCSK9's degrading activity on neuronal lipoprotein receptors, able to recognize and bind apoE [187]. In this regard, apoE ε4 binding to receptors involved in lipoprotein uptake has been recently investigated, providing evidence of an alteration in the modulation of LDLR and LRP1 shedding as compared to the most common apoE ε3 isoform, resulting in a reduced Aβ elimination and, possibly, also in altered delivery of apoE-containing lipoproteins [393].

Serum PCSK9 levels, on the other side, were about 100-fold higher as compared to those retrieved in CSF, as expected [394]. Unexpectedly, AD patients displayed slightly low PCSK9 serum levels as compared to MCI-AD subjects; the reasons beyond this observation are not yet fully clarified and currently under investigation; one possible explanation may be related to a different lipid profile among the single patients [395]. PCSK9 levels, indeed, are known to correlate with several lipid parameters [395]; furthermore, their levels may be influenced by specific pharmacological treatments [396], possibly explaining the observed difference.

Interestingly, PCSK9 levels in CSF were found to positively correlate with those in serum, specifically in patients affected by AD. This observation may suggest that in this latter subgroup of patients, characterized by an increased permeability of BBB that has been previously reported [122], an exchange between peripheral and central PCSK9 levels may occur. Hence, the increased CSF PCSK9 levels previously described in AD patients as compared to controls, and furtherly confirmed in the present cohort of patients with different degrees of cognitive impairment, may be a consequence of both an enhanced PCSK9 crossing of BBB from the periphery to CNS, as well as an increased local PCSK9 expression. Supporting the latter hypothesis, it has been previously demonstrated that apoE -/- mice fed with a high-fat diet, presenting synaptic loss and impaired cognitive functions and therefore considered an AD-like experimental model, were characterized by increased hippocampal apoptosis, accompanied by higher BACE1 and PCSK9 expression [341]. Furthermore, apoE ε4 carriers displayed an accelerated breakdown of BBB integrity in the hippocampus and temporal lobe, possibly contributing to cognitive decline [397], thus supporting the evidence of increased CSF PCSK9 specifically retrieved in AD patients carrying apoE ε4 genotype. Consistently, the observed association between HDL-C and CSF 24-OHC which is specifically strengthened in apoE ε4 carriers is suggestive of an alteration of BBB integrity occurring in this specific patient's population [397]. Following this observation, it's conceivable to hypothesize that the increased BBB permeability allows circulating HDLs to flow into CNS, where excess cholesterol is furtherly converted by enzyme CYP46A1, specifically expressed in neurons [389], into the more hydrophilic 24-OHC, finally diffusing through CSF across BBB for its final elimination. In this regard, the ability of HDL to cross BBB has been recently investigated through *in vitro* assays, showing that in physiological conditions discoidal HDLs were able to flow from the periphery to CNS, suggesting that the lipidation state of HDL's apoA-I may be a key

factor for their BBB crossing [180]. Hence, in presence of an AD-related increase of BBB permeability, a strengthened passage of peripheric HDLs to CNS may be conceivable.
Within this contest, PCSK9 may possibly directly contribute to the worsening of BBB integrity. In this regard, in rats fed with a high-fat diet and characterized by cognitive decline, hippocampal apoptosis, BBB disruption and Aβ deposition, PCSK9 inhibition induced a significative amelioration of both the above-listed anatomopathological as well as behavioural parameters, with a significant increase in occludin expression, a key structural component of BBB [385].
Furthermore, CSF cholesterol, whose levels were in line with previously reported quantifications [267], as well the most relevant oxysterols, 24-, 25- and 27-OHC, were similar among the three considered patient groups. Similarly, no changes were observed in circulating total cholesterol, LDL-C and triglycerides. Interestingly, AD patients displayed the highest plasmatic HDL-C levels; however, in this regard, literature data are inconsistent, reporting either increased [301] or lower HDL-C in AD patients [195], in the absence, however, of a causal risk of AD, as reported by Mendelian randomization studies [195]. In addition, concerning the circulating levels of the three most relevant oxysterols, namely 24-, 25- and 27-OHC, no marked differences were observed in the three analysed patients group. This evidence, combined with the observations previously described in the animal models, don't support the reliability of oxysterols as specific AD biomarkers.
Interestingly, however, an inverse correlation was found between CSF PCSK9 levels and both CSF and serum 27-OHC levels when considering all the subjects as a whole population, while CSF PCSK9 levels negatively correlated with CSF 24-OHC levels specifically in apoE ε4 carriers. Altogether, these observations suggest a possible interaction between these two parameters that deserves additional investigations.
In conclusion, the results of this translational study, performed upon *in vitro* as well as *ex vivo* experimental approaches, indicate the involvement of PCSK9 in AD pathogenesis. Indeed, *in vitro* results revealed an interference with cerebral cholesterol metabolism, by specifically disrupting brain cholesterol transport, resulting in decreased cholesterol supply to neurons, with negative consequences on neuronal viability. Furthermore, *ex vivo* studies on animal models of AD confirmed an involvement of PCSK9 on brain cholesterol homeostasis in mice, as its genetic silencing was associated with an altered cerebral cholesterol profile. These observations are also strengthened by a parallel study conducted on the same experimental model, clearly showing that PCSK9 genetic silencing led to a significant improvement of cognitive performances, possibly as a consequence of

reduced Aβ deposition and neuroinflammation. Finally, the results of the case-control study suggest that PCSK9 levels in CSF may start to increase since the prodromal phases of the disease. In addition, AD subjects, in which an increased BBB permeability has been previously described, circulating PCSK9 may flow to CNS, thus contributing to the already increased PCSK9 levels.

Altogether, these data support the possibility to identify cerebral PCSK9 as a pharmacological target for the treatment of AD, for which available therapies are still lacking. In this regard, the currently available anti-PCSK9 drugs, namely the monoclonal antibodies evolocumab and alirocumab, are mainly aimed at a hepatic modulation of PCSK9 levels, and their ability to access CNS is estimated to be about 0.1% [398], while siRNA inclisiran was specifically designed to target the liver [399]. Hence, the development of small lipophilic molecules targeting PCSK9 and able to cross BBB may represent an interesting future pharmacological perspective, that may pave the way to an innovative therapeutic approach. Cerebral PCSK9 inhibition, indeed, could restore brain cholesterol homeostasis, especially in the early phases of the disease. With this perspective, this novel pharmacological approach may open new perspectives in AD treatment, leading to an enormous social and medical impact.

BIBLIOGRAPHY

1. 2021 Alzheimer's disease facts and figures - Alzheimer's Association Report. *Alzheimer's Dement.* **17**, 327–406 (2021).

2. Möller, H.-J. & Graeber, M. B. The case described by Alois Alzheimer in 1911. *Eur. Arch. Psychiatry Clin. Neurosci.* **248**, 111–122 (1998).

3. Atri, A. The Alzheimer's Disease Clinical Spectrum: Diagnosis and Management. *Med. Clin. North Am.* **103**, 263–293 (2019).

4. Scheltens, P. *et al.* Alzheimer's disease. *Lancet* **397**, 1577–1590 (2021).

5. Alzheimer Europe. Dementia in Europe Yearbook. Estimating the prevalence of dementia in Europe. *Alzheimer Eur.* 108 (2019).

6. Todd, S., Barr, S., Roberts, M. & Passmore, A. P. Survival in dementia and predictors of mortality: a review. *Int. J. Geriatr. Psychiatry* **28**, 1109–1124 (2013).

7. Vermunt, L. *et al.* Duration of preclinical, prodromal, and dementia stages of Alzheimer's disease in relation to age, sex, and APOE genotype. *Alzheimer's Dement.* **15**, 888–898 (2019).

8. Nasreddine, Z. S. *et al.* The Montreal Cognitive Assessment, MoCA: a brief screening tool for mild cognitive impairment. *J. Am. Geriatr. Soc.* **53**, 695–699 (2005).

9. Xu, W. *et al.* Meta-analysis of modifiable risk factors for Alzheimer's disease. *J. Neurol. Neurosurg. Psychiatry* **86**, 1299–1306 (2015).

10. Barber, I. S. *et al.* Mutation analysis of sporadic early-onset Alzheimer's disease using the NeuroX array. *Neurobiol. Aging* **49**, 215.e1-215.e8 (2017).

11. Jarmolowicz, A. I., Chen, H.-Y. & Panegyres, P. K. The patterns of inheritance in early-onset dementia: Alzheimer's disease and frontotemporal dementia. *Am. J. Alzheimers. Dis. Other Demen.* **30**, 299–306 (2015).

12. Glenner, G. G. & Wong, C. W. Alzheimer's disease: initial report of the purification and characterization of a novel cerebrovascular amyloid protein. *Biochem. Biophys. Res. Commun.* **120**, 885–890 (1984).

13. Paroni, G., Bisceglia, P. & Seripa, D. Understanding the Amyloid Hypothesis in Alzheimer's Disease. *J. Alzheimer's Dis.* **68**, 493–510 (2019).

14. Tanzi, R. E. & Bertram, L. Twenty years of the Alzheimer's disease amyloid hypothesis: a genetic perspective. *Cell* **120**, 545–555 (2005).

15. Bandyopadhyay, S., Goldstein, L. E., Lahiri, D. K. & Rogers, J. T. Role of the APP non-amyloidogenic signaling pathway and targeting alpha-secretase as an alternative drug target for treatment of Alzheimer's disease. *Curr. Med. Chem.* **14**, 2848–2864 (2007).

16. Tiwari, S., Venkata, A., Kaushik, A., Adriana, Y. & Nair, M. Alzheimer ' s Disease Diagnostics And Therapeutics Market. *Int J Nanomedicine .* **Jul 2019**, 5541–5554 (2019).

17. Young-Pearse, T. L. *et al.* A critical function for β-amyloid precursor protein in neuronal migration revealed by in utero RNA interference. *J. Neurosci.* **27**, 14459–14469 (2007).

18. Lee, S. J. C., Nam, E., Lee, H. J., Savelieff, M. G. & Lim, M. H. Towards an

understanding of amyloid-β oligomers: Characterization, toxicity mechanisms, and inhibitors. *Chem. Soc. Rev.* **46**, 310–323 (2017).

19. Barz, B., Liao, Q. & Strodel, B. Pathways of Amyloid-β Aggregation Depend on Oligomer Shape. *J. Am. Chem. Soc.* **140**, 319–327 (2018).

20. Benseny-Cases, N., Klementieva, O. & Cladera, J. In vitro oligomerization and fibrillogenesis of amyloid-beta peptides. *Subcell. Biochem.* **65**, 53–74 (2012).

21. Hellström-Lindahl, E., Ravid, R. & Nordberg, A. Age-dependent decline of neprilysin in Alzheimer's disease and normal brain: inverse correlation with A beta levels. *Neurobiol. Aging* **29**, 210–221 (2008).

22. Heneka, M. T. *et al.* Neuroinflammation in Alzheimer's disease. *Lancet. Neurol.* **14**, 388–405 (2015).

23. Moreira, P. I. Alzheimer's disease and diabetes: An integrative view of the role of mitochondria, oxidative stress, and insulin. *J. Alzheimer's Dis.* **30**, (2012).

24. Koudinov, A. R. & Koudinova, N. V. Cholesterol homeostasis failure as a unifying cause of synaptic degeneration. *J. Neurol. Sci.* **229–230**, 233–240 (2005).

25. Lanoiselée, H.-M. *et al.* APP, PSEN1, and PSEN2 mutations in early-onset Alzheimer disease: A genetic screening study of familial and sporadic cases. *PLoS Med.* **14**, e1002270 (2017).

26. Müller, M. K., Jacobi, E., Sakimura, K., Malinow, R. & von Engelhardt, J. NMDA receptors mediate synaptic depression, but not spine loss in the dentate gyrus of adult amyloid Beta (Aβ) overexpressing mice. *Acta Neuropathol. Commun.* **6**, 110 (2018).

27. Zhou, Z. *et al.* The C-terminal tails of endogenous GluA1 and GluA2 differentially contribute to hippocampal synaptic plasticity and learning. *Nat. Neurosci.* **21**, 50–62 (2018).

28. Talantova, M. *et al.* Aβ induces astrocytic glutamate release, extrasynaptic NMDA receptor activation, and synaptic loss. *Proc. Natl. Acad. Sci. U. S. A.* **110**, E2518-27 (2013).

29. Um, J. W. *et al.* Alzheimer amyloid-β oligomer bound to postsynaptic prion protein activates Fyn to impair neurons. *Nat. Neurosci.* **15**, 1227–1235 (2012).

30. Resende, R., Ferreiro, E., Pereira, C. & Resende de Oliveira, C. Neurotoxic effect of oligomeric and fibrillar species of amyloid-beta peptide 1-42: involvement of endoplasmic reticulum calcium release in oligomer-induced cell death. *Neuroscience* **155**, 725–737 (2008).

31. Luo, Y. *et al.* Mice deficient in BACE1, the Alzheimer's beta-secretase, have normal phenotype and abolished beta-amyloid generation. *Nat. Neurosci.* **4**, 231–232 (2001).

32. Moussa-Pacha, N. M., Abdin, S. M., Omar, H. A., Alniss, H. & Al-Tel, T. H. BACE1 inhibitors: Current status and future directions in treating Alzheimer's disease. *Med. Res. Rev.* **40**, 339–384 (2020).

33. Holmes, C. *et al.* Long-term effects of Abeta42 immunisation in Alzheimer's disease: follow-up of a randomised, placebo-controlled phase I trial. *Lancet (London, England)* **372**, 216–223 (2008).

34. Orgogozo, J.-M. *et al.* Subacute meningoencephalitis in a subset of patients with AD after Abeta42 immunization. *Neurology* **61**, 46–54 (2003).

35. Sevigny, J. *et al.* Addendum: The antibody aducanumab reduces Aβ plaques in Alzheimer's disease. *Nature* **546**, 564 (2017).

36. Tolar, M., Abushakra, S. & Sabbagh, M. The path forward in Alzheimer's disease therapeutics: Reevaluating the amyloid cascade hypothesis. *Alzheimer's Dement.* **16**, 1553–1560 (2020).

37. Desikan, R. S. *et al.* Amyloid-β--associated clinical decline occurs only in the presence of elevated P-tau. *Arch. Neurol.* **69**, 709–713 (2012).

38. Gao, Y., Tan, L., Yu, J.-T. & Tan, L. Tau in Alzheimer's Disease: Mechanisms and Therapeutic Strategies. *Curr. Alzheimer Res.* **15**, 283–300 (2018).

39. Dent, E. W. & Baas, P. W. Microtubules in neurons as information carriers. *J. Neurochem.* **129**, 235–239 (2014).

40. Buée, L., Bussière, T., Buée-Scherrer, V., Delacourte, A. & Hof, P. R. Tau protein isoforms, phosphorylation and role in neurodegenerative disorders. *Brain Res. Brain Res. Rev.* **33**, 95–130 (2000).

41. Iqbal, K., Liu, F., Gong, C.-X. & Grundke-Iqbal, I. Tau in Alzheimer disease and related tauopathies. *Curr. Alzheimer Res.* **7**, 656–664 (2010).

42. Martin, L. *et al.* Tau protein kinases: involvement in Alzheimer's disease. *Ageing Res. Rev.* **12**, 289–309 (2013).

43. Liu, F. *et al.* Role of glycosylation in hyperphosphorylation of tau in Alzheimer's disease. *FEBS Lett.* **512**, 101–106 (2002).

44. Liu, F., Iqbal, K., Grundke-Iqbal, I., Rossie, S. & Gong, C.-X. Dephosphorylation of tau by protein phosphatase 5: impairment in Alzheimer's disease. *J. Biol. Chem.* **280**, 1790–1796 (2005).

45. Köpke, E. *et al.* Microtubule-associated protein tau. Abnormal phosphorylation of a non-paired helical filament pool in Alzheimer disease. *J. Biol. Chem.* **268**, 24374–24384 (1993).

46. Min, S.-W. *et al.* Acetylation of tau inhibits its degradation and contributes to tauopathy. *Neuron* **67**, 953–966 (2010).

47. Lee, G., Neve, R. L. & Kosik, K. S. The microtubule binding domain of tau protein. *Neuron* **2**, 1615–1624 (1989).

48. Barghorn, S. & Mandelkow, E. Toward a unified scheme for the aggregation of tau into Alzheimer paired helical filaments. *Biochemistry* **41**, 14885–14896 (2002).

49. Fitzpatrick, A. W. P. *et al.* Cryo-EM structures of tau filaments from Alzheimer's disease. *Nature* **547**, 185–190 (2017).

50. Congdon, E. E. & Sigurdsson, E. M. Tau-targeting therapies for Alzheimer disease. *Nat. Rev. Neurol.* **14**, 399–415 (2018).

51. Rozenstein-Tsalkovich, L. *et al.* Repeated immunization of mice with phosphorylated-tau peptides causes neuroinflammation. *Exp. Neurol.* **248**, 451–456 (2013).

52. Novak, P. *et al.* AADvac1, an Active Immunotherapy for Alzheimer's Disease and Non Alzheimer Tauopathies: An Overview of Preclinical and Clinical Development. *J. Prev. Alzheimer's Dis.* **6**, 63–69 (2019).

53. Karch, C. M. & Goate, A. M. Alzheimer's disease risk genes and mechanisms of disease pathogenesis. *Biol. Psychiatry* **77**, 43–51 (2015).

54. Wisniewski, K. E., Wisniewski, H. M. & Wen, G. Y. Occurrence of neuropathological changes and dementia of Alzheimer's disease in Down's syndrome. *Ann. Neurol.* **17**, 278–282 (1985).

55. Rovelet-Lecrux, A. *et al.* APP locus duplication causes autosomal dominant early-onset Alzheimer disease with cerebral amyloid angiopathy. *Nat. Genet.* **38**, 24–26 (2006).

56. Jonsson, T. *et al.* A mutation in APP protects against Alzheimer's disease and age-related cognitive decline. *Nature* **488**, 96–99 (2012).

57. Wallon, D. *et al.* The French series of autosomal dominant early onset Alzheimer's disease cases: mutation spectrum and cerebrospinal fluid biomarkers. *J. Alzheimers. Dis.* **30**, 847–856 (2012).

58. Gatz, M. *et al.* Role of genes and environments for explaining Alzheimer disease. *Arch. Gen. Psychiatry* **63**, 168–174 (2006).

59. Strittmatter, W. J. *et al.* Apolipoprotein E: high-avidity binding to beta-amyloid and increased frequency of type 4 allele in late-onset familial Alzheimer disease. *Proc. Natl. Acad. Sci. U. S. A.* **90**, 1977–1981 (1993).

60. Husain, M. A., Laurent, B. & Plourde, M. APOE and Alzheimer's Disease: From Lipid Transport to Physiopathology and Therapeutics. *Front. Neurosci.* **15**, 630502 (2021).

61. Kunkle, B. W. *et al.* Genetic meta-analysis of diagnosed Alzheimer's disease identifies new risk loci and implicates Aβ, tau, immunity and lipid processing. *Nat. Genet.* **51**, 414–430 (2019).

62. Desikan, R. S. *et al.* Genetic assessment of age-associated Alzheimer disease risk: Development and validation of a polygenic hazard score. *PLoS Med.* **14**, e1002258 (2017).

63. Whitehouse, P. J., Price, D. L., Clark, A. W., Coyle, J. T. & DeLong, M. R. Alzheimer disease: evidence for selective loss of cholinergic neurons in the nucleus basalis. *Ann. Neurol.* **10**, 122–126 (1981).

64. Davies, P. & Maloney, A. J. Selective loss of central cholinergic neurons in Alzheimer's disease. *Lancet (London, England)* vol. 2 1403 (1976).

65. Sun, Y., Lai, M.-S., Lu, C.-J. & Chen, R.-C. How long can patients with mild or moderate Alzheimer's dementia maintain both the cognition and the therapy of cholinesterase inhibitors: a national population-based study. *Eur. J. Neurol.* **15**, 278–283 (2008).

66. Nordberg, A. & Winblad, B. Reduced number of [3H]nicotine and [3H]acetylcholine binding sites in the frontal cortex of Alzheimer brains. *Neurosci. Lett.* **72**, 115–119 (1986).

67. Vaucher, E., Borredon, J., Bonvento, G., Seylaz, J. & Lacombe, P. Autoradiographic evidence for flow-metabolism uncoupling during stimulation of the nucleus basalis of Meynert in the conscious rat. *J. Cereb. blood flow Metab. Off. J. Int. Soc. Cereb. Blood Flow Metab.* **17**, 686–694 (1997).

68. Geula, C. & Mesulam, M. Cholinesterases and the pathology of Alzheimer disease. *Alzheimer Dis. Assoc. Disord.* (1995).

69. Beach, T. G. *et al.* The cholinergic deficit coincides with Abeta deposition at the earliest histopathologic stages of Alzheimer disease. *J. Neuropathol. Exp. Neurol.* **59**, 308–313 (2000).

70. Ramos-Rodriguez, J. J. *et al.* Rapid β-amyloid deposition and cognitive impairment after cholinergic denervation in APP/PS1 mice. *J. Neuropathol. Exp. Neurol.* **72**, 272–285 (2013).

71. Kalkman, H. O. & Feuerbach, D. Modulatory effects of α7 nAChRs on the immune system and its relevance for CNS disorders. *Cell. Mol. Life Sci.* **73**, 2511–2530 (2016).

72. Bott, J.-B. *et al.* APOE-Sensitive Cholinergic Sprouting Compensates for Hippocampal Dysfunctions Due to Reduced Entorhinal Input. *J. Neurosci.* **36**, 10472 LP – 10486 (2016).

73. Hansen, R. A. *et al.* Efficacy and safety of donepezil, galantamine, and rivastigmine for the treatment of Alzheimer's disease: a systematic review and meta-analysis. *Clin. Interv. Aging* **3**, 211–225 (2008).

74. Nimmerjahn, A., Kirchhiff, F. & Helmchen, F. Resting Microglial Cells Are Highly Dynamic Surveillants of Brain Parenchyma in vivo. *Science (80-.).* **308**, 1314–1318 (2005).

75. Leng, F. & Edison, P. Neuroinflammation and microglial activation in Alzheimer disease: where do we go from here? *Nat. Rev. Neurol.* **17**, 157–172 (2021).

76. Lyman, M., Lloyd, D. G., Ji, X., Vizcaychipi, M. P. & Ma, D. Neuroinflammation: the role and consequences. *Neurosci. Res.* **79**, 1–12 (2014).

77. Halle, A. *et al.* The NALP3 inflammasome is involved in the innate immune response to amyloid-beta. *Nat. Immunol.* **9**, 857–865 (2008).

78. Mishra, A., Kim, H. J., Shin, A. H. & Thayer, S. A. Synapse loss induced by interleukin-1β requires pre- and post-synaptic mechanisms. *J. neuroimmune Pharmacol. Off. J. Soc. NeuroImmune Pharmacol.* **7**, 571–578 (2012).

79. Hong, S. *et al.* Complement and microglia mediate early synapse loss in Alzheimer mouse models. *Science* **352**, 712–716 (2016).

80. Landreth, G. E. & Reed-Geaghan, E. G. TLRs in Alzheimer's disease. *Curr. Top. Microbiol. Immunol.* **336**, 137–153 (2009).

81. Bolmont, T. *et al.* Dynamics of the microglial/amyloid interaction indicate a role in plaque maintenance. *J. Neurosci.* **28**, 4283–4292 (2008).

82. Sato, S. *et al.* Toll/IL-1 receptor domain-containing adaptor inducing IFN-beta (TRIF) associates with TNF receptor-associated factor 6 and TANK-binding kinase 1, and activates two distinct transcription factors, NF-kappa B and IFN-regulatory factor-3, in the Toll-like r. *J. Immunol.* **171**, 4304–4310 (2003).

83. Letiembre, M. *et al.* Screening of innate immune receptors in neurodegenerative diseases: a similar pattern. *Neurobiol. Aging* **30**, 759–768 (2009).

84. Walter, S. *et al.* Role of the toll-like receptor 4 in neuroinflammation in Alzheimer's disease. *Cell. Physiol. Biochem. Int. J. Exp. Cell. Physiol. Biochem. Pharmacol.* **20**, 947–956 (2007).

85. Minoretti, P. *et al.* Effect of the functional toll-like receptor 4 Asp299Gly polymorphism on susceptibility to late-onset Alzheimer's disease. *Neurosci. Lett.* **391**, 147–149 (2006).

86. Stewart, C. R. *et al.* CD36 ligands promote sterile inflammation through assembly of a Toll-like receptor 4 and 6 heterodimer. *Nat. Immunol.* **11**, 155–161 (2010).

87. Patel, N. S. *et al.* Inflammatory cytokine levels correlate with amyloid load in transgenic mouse models of Alzheimer's disease. *J. Neuroinflammation* **2**, 9 (2005).

88. Bate, C., Veerhuis, R., Eikelenboom, P. & Williams, A. Microglia kill amyloid-beta1-42 damaged neurons by a CD14-dependent process. *Neuroreport* **15**, 1427–1430 (2004).

89. Yang, Y. & Zhang, Z. Microglia and Wnt Pathways: Prospects for Inflammation in Alzheimer's Disease. *Front. Aging Neurosci.* **12**, 1–13 (2020).

90. Van Steenwinckel, J. *et al.* Decreased microglial Wnt/β-catenin signalling drives microglial pro-inflammatory activation in the developing brain. *Brain* **142**, 3806–3833 (2019).

91. Toledo, E. M. & Inestrosa, N. C. Activation of Wnt signaling by lithium and rosiglitazone reduced spatial memory impairment and neurodegeneration in brains of an APPswe/PSEN1ΔE9 mouse model of Alzheimer's disease. *Mol. Psychiatry* **15**, 272–285 (2010).

92. He, P. & Shen, Y. Interruption of beta-catenin signaling reduces neurogenesis in Alzheimer's disease. *J. Neurosci.* **29**, 6545–6557 (2009).

93. Liu, E. *et al.* Tau acetylates and stabilizes β-catenin thereby promoting cell survival. *EMBO Rep.* **21**, e48328 (2020).

94. Kuhn, J. & Sharman, T. Cerebral Amyloid Angiopathy. in (2021).

95. Attems, J. Sporadic cerebral amyloid angiopathy: pathology, clinical implications, and possible pathomechanisms. *Acta Neuropathol.* **110**, 345–359 (2005).

96. Soto-Rojas, L. O. *et al.* Insoluble Vascular Amyloid Deposits Trigger Disruption of the Neurovascular Unit in Alzheimer's Disease Brains. *Int. J. Mol. Sci.* **22**, (2021).

97. Mawuenyega, K. G. *et al.* Decreased clearance of CNS beta-amyloid in Alzheimer's disease. *Science* **330**, 1774 (2010).

98. Miyakawa, T. *et al.* Role of blood vessels in producing pathological changes in the brain with Alzheimer's disease. *Ann. N. Y. Acad. Sci.* **903**, 46–54 (2000).

99. Apátiga-Pérez, R. *et al.* Neurovascular dysfunction and vascular amyloid accumulation as early events in Alzheimer's disease. *Metab. Brain Dis.* (2021) doi:10.1007/s11011-021-00814-4.

100. Sengillo, J. D. *et al.* Deficiency in mural vascular cells coincides with blood-brain

barrier disruption in Alzheimer's disease. *Brain Pathol.* **23**, 303–310 (2013).

101. Halliday, M. R. *et al.* Accelerated pericyte degeneration and blood-brain barrier breakdown in apolipoprotein E4 carriers with Alzheimer's disease. *J. Cereb. blood flow Metab. Off. J. Int. Soc. Cereb. Blood Flow Metab.* **36**, 216–227 (2016).

102. Monzio Compagnoni, G. *et al.* The Role of Mitochondria in Neurodegenerative Diseases: the Lesson from Alzheimer's Disease and Parkinson's Disease. *Mol. Neurobiol.* **57**, 2959–2980 (2020).

103. Friedland, R. P. *et al.* Regional cerebral metabolic alterations in dementia of the Alzheimer type: positron emission tomography with [18F]fluorodeoxyglucose. *J. Comput. Assist. Tomogr.* **7**, 590–598 (1983).

104. Foster, N. L. *et al.* Alzheimer's disease: focal cortical changes shown by positron emission tomography. *Neurology* **33**, 961–965 (1983).

105. Kish, S. J. *et al.* Brain cytochrome oxidase in Alzheimer's disease. *J. Neurochem.* **59**, 776–779 (1992).

106. Szabados, T. *et al.* A chronic Alzheimer's model evoked by mitochondrial poison sodium azide for pharmacological investigations. *Behav. Brain Res.* **154**, 31–40 (2004).

107. Höglinger, G. U. *et al.* The mitochondrial complex I inhibitor rotenone triggers a cerebral tauopathy. *J. Neurochem.* **95**, 930–939 (2005).

108. Pereira, C., Santos, M. S. & Oliveira, C. Mitochondrial function impairment induced by amyloid beta-peptide on PC12 cells. *Neuroreport* **9**, 1749–1755 (1998).

109. Wang, X. *et al.* Amyloid-beta overproduction causes abnormal mitochondrial dynamics via differential modulation of mitochondrial fission/fusion proteins. *Proc. Natl. Acad. Sci. U. S. A.* **105**, 19318–19323 (2008).

110. Rhein, V. *et al.* Amyloid-beta and tau synergistically impair the oxidative phosphorylation system in triple transgenic Alzheimer's disease mice. *Proc. Natl. Acad. Sci. U. S. A.* **106**, 20057–20062 (2009).

111. Smirnov, D. S. *et al.* Trajectories of cognitive decline differ in hippocampal sclerosis and Alzheimer's disease. *Neurobiol. Aging* **75**, 169–177 (2019).

112. Chhatwal, J. P. *et al.* Preferential degradation of cognitive networks differentiates Alzheimer's disease from ageing. *Brain* **141**, 1486–1500 (2018).

113. Petersen, R. C. *et al.* Practice guideline update summary: Mild cognitive impairment report of theguideline development, dissemination, and implementation. *Neurology* **90**, 126–135 (2018).

114. Braak, H., Alafuzoff, I., Arzberger, T., Kretzschmar, H. & Tredici, K. Staging of Alzheimer disease-associated neurofibrillary pathology using paraffin sections and immunocytochemistry. *Acta Neuropathol.* **112**, 389–404 (2006).

115. Hyman, B. T. *et al.* National Institute on Aging-Alzheimer's Association guidelines for the neuropathologic assessment of Alzheimer's disease. *Alzheimer's Dement.* **8**, 1–13 (2012).

116. James, B. D. *et al.* TDP-43 stage, mixed pathologies, and clinical Alzheimer's-type

dementia. *Brain* **139**, 2983–2993 (2016).

117. Soria Lopez, J. A., González, H. M. & Léger, G. C. Alzheimer's disease. *Handb. Clin. Neurol.* **167**, 231–255 (2019).

118. Lloret, A. *et al.* When does Alzheimer's disease really start? The role of biomarkers. *Int. J. Mol. Sci.* **20**, 1–15 (2019).

119. Shaw, L. M. *et al.* Appropriate use criteria for lumbar puncture and cerebrospinal fluid testing in the diagnosis of Alzheimer's disease. *Alzheimer's Dement.* **14**, 1505–1521 (2018).

120. Anand, K. & Sabbagh, M. Amyloid Imaging: Poised for Integration into Medical Practice. *Neurotherapeutics* **14**, 54–61 (2017).

121. Bloudek, L. M., Spackman, D. E., Blankenburg, M. & Sullivan, S. D. Review and meta-analysis of biomarkers and diagnostic imaging in Alzheimer's disease. *J. Alzheimers. Dis.* **26**, 627–645 (2011).

122. Nation, D. A. *et al.* Blood-brain barrier brackdown is an early biomarker of human congitived dysfunction. *Nat. Med.* **25**, 270–276 (2019).

123. Sweeney, M. D. *et al.* Vascular dysfunction—The disregarded partner of Alzheimer's disease. *Alzheimer's Dement.* **15**, 158–167 (2019).

124. Schade, D. S., Shey, L. & Eaton, R. P. Cholesterol Review: A Metabolically Important Molecule. *Endocr. Pract.* **26**, 1514–1523 (2020).

125. Tabas, I. Cholesterol in health and disease. *J. Clin. Invest.* **110**, 583–590 (2002).

126. Dietschy, J. M. Central nervous system: cholesterol turnover, brain development and neurodegeneration. *Biol. Chem.* **390**, 287–293 (2009).

127. Lemus, H. N., Warrington, A. E. & Rodriguez, M. Multiple Sclerosis: Mechanisms of Disease and Strategies for Myelin and Axonal Repair. *Neurol. Clin.* **36**, 1–11 (2018).

128. Mauch, D. H. *et al.* CNS synaptogenesis promoted by glia-derived cholesterol. *Science* **294**, 1354–1357 (2001).

129. Suzuki, S. *et al.* Brain-derived neurotrophic factor regulates cholesterol metabolism for synapse development. *J. Neurosci.* **27**, 6417–6427 (2007).

130. Hussain, G. *et al.* Role of cholesterol and sphingolipids in brain development and neurological diseases. *Lipids Health Dis.* **18**, 26 (2019).

131. Grassi, S. *et al.* Lipid rafts and neurodegeneration: structural and functional roles in physiologic aging and neurodegenerative diseases. *J. Lipid Res.* **61**, 636–654 (2020).

132. Thiele, C., Hannah, M. J., Fahrenholz, F. & Huttner, W. B. Cholesterol binds to synaptophysin and is required for biogenesis of synaptic vesicles. *Nat. Cell Biol.* **2**, 42–49 (2000).

133. Goritz, C., Mauch, D. H. & Pfrieger, F. W. Multiple mechanisms mediate cholesterol-induced synaptogenesis in a CNS neuron. *Mol. Cell. Neurosci.* **29**, 190–201 (2005).

134. Linetti, A. *et al.* Cholesterol reduction impairs exocytosis of synaptic vesicles. *J. Cell*

Sci. **123**, 595–605 (2010).

135. Zhang, J. & Liu, Q. Cholesterol metabolism and homeostasis in the brain. *Protein Cell* **6**, 254–264 (2015).

136. Turri, M., Marchi, C., Adorni, M. P., Calabresi, L. & Zimetti, F. Emerging role of HDL in brain cholesterol metabolism and neurodegenerative disorders. *Biochim. Biophys. Acta - Mol. Cell Biol. Lipids* **1867**, 159123 (2022).

137. Song, Y., Liu, J., Zhao, K., Gao, L. & Zhao, J. Cholesterol-induced toxicity: An integrated view of the role of cholesterol in multiple diseases. *Cell Metab.* **33**, 1911–1925 (2021).

138. Wang, H. *et al.* Regulation of beta-amyloid production in neurons by astrocyte-derived cholesterol. *Proc. Natl. Acad. Sci. U. S. A.* **118**, (2021).

139. Wong, M. Y. *et al.* 25-Hydroxycholesterol amplifies microglial IL-1β production in an apoE isoform-dependent manner. *J. Neuroinflammation* **17**, 1–17 (2020).

140. Mouzat, K. *et al.* Regulation of brain cholesterol: What role do liver X receptors play in neurodegenerative diseases? *Int. J. Mol. Sci.* **20**, (2019).

141. Peet, D. J. *et al.* Cholesterol and bile acid metabolism are impaired in mice lacking the nuclear oxysterol receptor LXR alpha. *Cell* **93**, 693–704 (1998).

142. Yu, L. *et al.* Stimulation of cholesterol excretion by the liver X receptor agonist requires ATP-binding cassette transporters G5 and G8. *J. Biol. Chem.* **278**, 15565–15570 (2003).

143. Repa, J. J. *et al.* Regulation of absorption and ABC1-mediated efflux of cholesterol by RXR heterodimers. *Science* **289**, 1524–1529 (2000).

144. Kennedy, M. A. *et al.* Characterization of the human ABCG1 gene: liver X receptor activates an internal promoter that produces a novel transcript encoding an alternative form of the protein. *J. Biol. Chem.* **276**, 39438–39447 (2001).

145. Tontonoz, P. & Mangelsdorf, D. J. Liver X Receptor Signaling Pathways in Cardiovascular Disease. *Mol. Endocrinol.* **17**, 985–993 (2003).

146. Wang, B. & Tontonoz, P. Liver X receptors in lipid signalling and membrane homeostasis. *Nat. Rev. Endocrinol.* **14**, 452–463 (2018).

147. Murthy, S., Born, E., Mathur, S. N. & Field, F. J. LXR/RXR activation enhances basolateral efflux of cholesterol in CaCo-2 cells. *J. Lipid Res.* **43**, 1054–1064 (2002).

148. Muse, E. D. *et al.* Cell-specific discrimination of desmosterol and desmosterol mimetics confers selective regulation of LXR and SREBP in macrophages. *Proc. Natl. Acad. Sci.* **115**, E4680--E4689 (2018).

149. Janowski, B. A., Willy, P. J., Devi, T. R., Falck, J. R. & Mangelsdorf, D. J. An oxysterol signalling pathway mediated by the nuclear receptor LXR alpha. *Nature* **383**, 728–731 (1996).

150. Landis, M. S., Patel, H. V & Capone, J. P. Oxysterol activators of liver X receptor and 9-cis-retinoic acid promote sequential steps in the synthesis and secretion of tumor necrosis factor-alpha from human monocytes. *J. Biol. Chem.* **277**, 4713–4721 (2002).

151. Lee, J. H. *et al.* Differential SUMOylation of LXRalpha and LXRbeta mediates transrepression of STAT1 inflammatory signaling in IFN-gamma-stimulated brain astrocytes. *Mol. Cell* **35**, 806–817 (2009).

152. Thomas, D. G. *et al.* LXR Suppresses Inflammatory Gene Expression and Neutrophil Migration through cis-Repression and Cholesterol Efflux. *Cell Rep.* **25**, 3774-3785.e4 (2018).

153. Hong, C. *et al.* The E3 ubiquitin ligase IDOL induces the degradation of the low density lipoprotein receptor family members VLDLR and ApoER2. *J. Biol. Chem.* **285**, 19720–19726 (2010).

154. Eckert, G. P., Vardanian, L., Rebeck, G. W. & Burns, M. P. Regulation of central nervous system cholesterol homeostasis by the liver X receptor agonist TO-901317. *Neurosci. Lett.* **423**, 47–52 (2007).

155. Abildayeva, K. *et al.* 24(S)-hydroxycholesterol participates in a liver X receptor-controlled pathway in astrocytes that regulates apolipoprotein E-mediated cholesterol efflux. *J. Biol. Chem.* **281**, 12799–12808 (2006).

156. Wu, C.-H. *et al.* Treatment with TO901317, a synthetic liver X receptor agonist, reduces brain damage and attenuates neuroinflammation in experimental intracerebral hemorrhage. *J. Neuroinflammation* **13**, 62 (2016).

157. Spagnuolo, M. S. *et al.* Brain-derived neurotrophic factor modulates cholesterol homeostasis and Apolipoprotein E synthesis in human cell models of astrocytes and neurons. *J. Cell. Physiol.* **233**, 6925–6943 (2018).

158. Bengoechea-Alonso, M. T. & Ericsson, J. SREBP in signal transduction: cholesterol metabolism and beyond. *Curr. Opin. Cell Biol.* **19**, 215–222 (2007).

159. Horton, J. D., Goldstein, J. L. & Brown, M. S. SREBPs: activators of the complete program of cholesterol and fatty acid synthesis in the liver. *J. Clin. Invest.* **109**, 1125–1131 (2002).

160. Birolini, G. *et al.* SREBP2 gene therapy targeting striatal astrocytes ameliorates Huntington's disease phenotypes. *Brain* (2021) doi:10.1093/brain/awab186.

161. van Deijk, A.-L. F. *et al.* Astrocyte lipid metabolism is critical for synapse development and function in vivo. *Glia* **65**, 670–682 (2017).

162. Lee, S. *et al.* Deficiency of sterol regulatory element-binding protein-1c induces schizophrenia-like behavior in mice. *Genes. Brain. Behav.* **18**, e12540 (2019).

163. Ang, M. J. *et al.* Transcriptome Profiling Reveals Novel Candidate Genes Related to Hippocampal Dysfunction in SREBP-1c Knockout Mice. *Int. J. Mol. Sci.* **21**, (2020).

164. Ang, M. J. *et al.* SREBP-1c Deficiency Affects Hippocampal Micromorphometry and Hippocampus-Dependent Memory Ability in Mice. *Int. J. Mol. Sci.* **22**, (2021).

165. Spell, C. *et al.* SREBP-1a polymorphism influences the risk of Alzheimer's disease in carriers of the ApoE4 allele. *Dement. Geriatr. Cogn. Disord.* **18**, 245–249 (2004).

166. Tarr, P. T. & Edwards, P. A. ABCG1 and ABCG4 are coexpressed in neurons and astrocytes of the CNS and regulate cholesterol homeostasis through SREBP-2. *J. Lipid Res.* **49**, 169–182 (2008).

167. Dietschy, J. M. & Turley, S. D. Thematic review series: brain Lipids. Cholesterol metabolism in the central nervous system during early development and in the mature animal. *J. Lipid Res.* **45**, 1375–1397 (2004).

168. Suzuki, R., Ferris, H. A., Chee, M. J., Maratos-Flier, E. & Kahn, C. R. Reduction of the cholesterol sensor SCAP in the brains of mice causes impaired synaptic transmission and altered cognitive function. *PLoS Biol.* **11**, e1001532 (2013).

169. Quan, G., Xie, C., Dietschy, J. M. & Turley, S. D. Ontogenesis and regulation of cholesterol metabolism in the central nervous system of the mouse. *Brain Res. Dev. Brain Res.* **146**, 87–98 (2003).

170. Nieweg, K., Schaller, H. & Pfrieger, F. W. Marked differences in cholesterol synthesis between neurons and glial cells from postnatal rats. *J. Neurochem.* **109**, 125–134 (2009).

171. Wang, N. *et al.* ATP-binding cassette transporters G1 and G4 mediate cholesterol and desmosterol efflux to HDL and regulate sterol accumulation in the brain. *FASEB J. Off. Publ. Fed. Am. Soc. Exp. Biol.* **22**, 1073–1082 (2008).

172. Megha, Bakht, O. & London, E. Cholesterol precursors stabilize ordinary and ceramide-rich ordered lipid domains (lipid rafts) to different degrees. Implications for the Bloch hypothesis and sterol biosynthesis disorders. *J. Biol. Chem.* **281**, 21903–21913 (2006).

173. Benvenuti, S. *et al.* Neuronal differentiation of human mesenchymal stem cells: changes in the expression of the Alzheimer's disease-related gene seladin-1. *Exp. Cell Res.* **312**, 2592–2604 (2006).

174. Genaro-Mattos, T. C., Anderson, A., Allen, L. B., Korade, Z. & Mirnics, K. Cholesterol Biosynthesis and Uptake in Developing Neurons. *ACS Chem. Neurosci.* **10**, 3671–3681 (2019).

175. Linton, M. F. *et al.* Phenotypes of apolipoprotein B and apolipoprotein E after liver transplantation. *J. Clin. Invest.* **88**, 270–281 (1991).

176. Sweeney, M. D., Sagare, A. P. & Zlokovic, B. V. Blood-brain barrier breakdown in Alzheimer disease and other neurodegenerative disorders. *Nat. Rev. Neurol.* **14**, 133–150 (2018).

177. Solár, P., Zamani, A., Kubíčková, L., Dubový, P. & Joukal, M. Choroid plexus and the blood-cerebrospinal fluid barrier in disease. *Fluids Barriers CNS* **17**, 35 (2020).

178. Van Valkenburgh, J. *et al.* Understanding the Exchange of Systemic HDL Particles Into the Brain and Vascular Cells Has Diagnostic and Therapeutic Implications for Neurodegenerative Diseases. *Front. Physiol.* **12**, 700847 (2021).

179. Koch, S. *et al.* Characterization of four lipoprotein classes in human cerebrospinal fluid. *J. Lipid Res.* **42**, 1143–1151 (2001).

180. Dal Magro, R. *et al.* The Extent of Human Apolipoprotein A-I Lipidation Strongly Affects the β-Amyloid Efflux Across the Blood-Brain Barrier in vitro. *Front. Neurosci.* **13**, 419 (2019).

181. Demeester, N. *et al.* Characterization and functional studies of lipoproteins, lipid transfer proteins, and lecithin:cholesterol acyltransferase in CSF of normal individuals and patients with Alzheimer's disease. *J. Lipid Res.* **41**, 963–974 (2000).

182. Stukas, S. *et al.* Intravenously injected human apolipoprotein A-I rapidly enters the central nervous system via the choroid plexus. *J. Am. Heart Assoc.* **3**, e001156 (2014).

183. McCabe, S. M. & Zhao, N. The Potential Roles of Blood-Brain Barrier and Blood-Cerebrospinal Fluid Barrier in Maintaining Brain Manganese Homeostasis. *Nutrients* **13**, (2021).

184. Tumani, H., Huss, A. & Bachhuber, F. The cerebrospinal fluid and barriers - anatomic and physiologic considerations. *Handb. Clin. Neurol.* **146**, 21–32 (2017).

185. Vitali, C., Wellington, C. L. & Calabresi, L. HDL and cholesterol handling in the brain. *Cardiovasc. Res.* **103**, 405–413 (2014).

186. Chen, J., Zhang, X., Kusumo, H., Costa, L. G. & Guizzetti, M. Cholesterol efflux is differentially regulated in neurons and astrocytes: implications for brain cholesterol homeostasis. *Biochim. Biophys. Acta* **1831**, 263–275 (2013).

187. Bu, G. Apolipoprotein E and its receptors in Alzheimer's disease: pathways, pathogenesis and therapy. *Nat. Rev. Neurosci.* **10**, 333–344 (2009).

188. Fung, K. Y. *et al.* SR-BI mediated transcytosis of HDL in brain microvascular endothelial cells is independent of caveolin, clathrin, and PDZK1. *Front. Physiol.* **8**, 1–16 (2017).

189. Ladu, M. J. *et al.* Lipoproteins in the central nervous system. *Ann. N. Y. Acad. Sci.* **903**, 167–175 (2000).

190. Hirsch-Reinshagen, V. *et al.* LCAT synthesized by primary astrocytes esterifies cholesterol on glia-derived lipoproteins. *J. Lipid Res.* **50**, 885–893 (2009).

191. Albers, J. J., Tollefson, J. H., Wolfbauer, G. & Albright, R. E. J. Cholesteryl ester transfer protein in human brain. *Int. J. Clin. Lab. Res.* **21**, 264–266 (1992).

192. Wellington, C. L. & Frikke-Schmidt, R. Relation between plasma and brain lipids. *Curr. Opin. Lipidol.* **27**, 225–232 (2016).

193. van der Vorst, E. P. C. High-Density Lipoproteins and Apolipoprotein A1. *Subcell. Biochem.* **94**, 399–420 (2020).

194. Zhou, A. L. *et al.* Apolipoprotein A-I Crosses the Blood-Brain Barrier through Clathrin-Independent and Cholesterol-Mediated Endocytosis. *J. Pharmacol. Exp. Ther.* **369**, 481–488 (2019).

195. Marsillach, J. *et al.* HDL Proteome and Alzheimer's Disease: Evidence of a Link. *Antioxidants (Basel, Switzerland)* **9**, (2020).

196. Kim, W. S., Weickert, C. S. & Garner, B. Role of ATP-binding cassette transporters in brain lipid transport and neurological disease. *J. Neurochem.* **104**, 1145–1166 (2008).

197. Koldamova, R., Fitz, N. F. & Lefterov, I. ATP-binding cassette transporter A1: from metabolism to neurodegeneration. *Neurobiol. Dis.* **72 Pt A**, 13–21 (2014).

198. Fitz, N. F. *et al.* ABCA1 Deficiency Affects Basal Cognitive Deficits and Dendritic Density in Mice. *J. Alzheimers. Dis.* **56**, 1075–1085 (2017).

199. Fujiyoshi, M., Ohtsuki, S., Hori, S., Tachikawa, M. & Terasaki, T. 24S-hydroxycholesterol induces cholesterol release from choroid plexus epithelial cells

in an apical- and apoE isoform-dependent manner concomitantly with the induction of ABCA1 and ABCG1 expression. *J. Neurochem.* **100**, 968–978 (2007).

200. Kim, W. S. *et al.* Role of ABCG1 and ABCA1 in Regulation of Neuronal Cholesterol Efflux to Apolipoprotein E Discs and Suppression of Amyloid-β Peptide Generation*. *J. Biol. Chem.* **282**, 2851–2861 (2007).

201. Karten, B., Campenot, R. B., Vance, D. E. & Vance, J. E. Expression of ABCG1, but not ABCA1, correlates with cholesterol release by cerebellar astroglia. *J. Biol. Chem.* **281**, 4049–4057 (2006).

202. Yang, A. *et al.* Regulation of ABCG4 transporter expression by sterols and LXR ligands. *Biochim. Biophys. acta. Gen. Subj.* **1865**, 129769 (2021).

203. Bojanic, D. D. *et al.* Differential expression and function of ABCG1 and ABCG4 during development and aging. *J. Lipid Res.* **51**, 169–181 (2010).

204. Beffert, U., Stolt, P. C. & Herz, J. Functions of lipoprotein receptors in neurons. *J. Lipid Res.* **45**, 403–409 (2004).

205. Trommsdorff, M. *et al.* Reeler/Disabled-like disruption of neuronal migration in knockout mice lacking the VLDL receptor and ApoE receptor 2. *Cell* **97**, 689–701 (1999).

206. Lane-Donovan, C. & Herz, J. The ApoE receptors Vldlr and Apoer2 in central nervous system function and disease. *J. Lipid Res.* **58**, 1036–1043 (2017).

207. Kong, W.-J., Liu, J. & Jiang, J.-D. Human low-density lipoprotein receptor gene and its regulation. *J. Mol. Med. (Berl).* **84**, 29–36 (2006).

208. Fryer, J. D. *et al.* The low density lipoprotein receptor regulates the level of central nervous system human and murine apolipoprotein E but does not modify amyloid plaque pathology in PDAPP mice. *J. Biol. Chem.* **280**, 25754–25759 (2005).

209. Dlugosz, P. & Nimpf, J. The Reelin Receptors Apolipoprotein E receptor 2 (ApoER2) and VLDL Receptor. *Int. J. Mol. Sci.* **19**, (2018).

210. Gao, J. *et al.* The E3 ubiquitin ligase IDOL regulates synaptic ApoER2 levels and is important for plasticity and learning. *Elife* **6**, (2017).

211. Frykman, P. K., Brown, M. S., Yamamoto, T., Goldstein, J. L. & Herz, J. Normal plasma lipoproteins and fertility in gene-targeted mice homozygous for a disruption in the gene encoding very low density lipoprotein receptor. *Proc. Natl. Acad. Sci. U. S. A.* **92**, 8453–8457 (1995).

212. Shinohara, M., Tachibana, M., Kanekiyo, T. & Bu, G. Role of LRP1 in the pathogenesis of Alzheimer's disease: evidence from clinical and preclinical studies. *J. Lipid Res.* **58**, 1267–1281 (2017).

213. Zlokovic, B. V, Deane, R., Sagare, A. P., Bell, R. D. & Winkler, E. A. Low-density lipoprotein receptor-related protein-1: a serial clearance homeostatic mechanism controlling Alzheimer's amyloid β-peptide elimination from the brain. *J. Neurochem.* **115**, 1077–1089 (2010).

214. Liu, Q. *et al.* Amyloid precursor protein regulates brain apolipoprotein E and cholesterol metabolism through lipoprotein receptor LRP1. *Neuron* **56**, 66–78 (2007).

215. Griffiths, W. J. & Wang, Y. Oxysterol research: a brief review. *Biochem. Soc. Trans.* **47**, 517–526 (2019).

216. Björkhem, I. *et al.* Cholesterol homeostasis in human brain: turnover of 24S-hydroxycholesterol and evidence for a cerebral origin of most of this oxysterol in the circulation. *J. Lipid Res.* **39**, 1594–1600 (1998).

217. Gamba, P. *et al.* Oxidized cholesterol as the driving force behind the development of Alzheimer's disease. *Front. Aging Neurosci.* **7**, 119 (2015).

218. Han, M. *et al.* Therapeutic implications of altered cholesterol homeostasis mediated by loss of CYP46A1 in human glioblastoma. *EMBO Mol. Med.* **12**, e10924 (2020).

219. Wang, Y., Muneton, S., Sjövall, J., Jovanovic, J. N. & Griffiths, W. J. The effect of 24S-hydroxycholesterol on cholesterol homeostasis in neurons: quantitative changes to the cortical neuron proteome. *J. Proteome Res.* **7**, 1606–1614 (2008).

220. Radhakrishnan, A., Ikeda, Y., Kwon, H. J., Brown, M. S. & Goldstein, J. L. Sterol-regulated transport of SREBPs from endoplasmic reticulum to Golgi: Oxysterols block transport by binding to Insig. *Proc. Natl. Acad. Sci.* **104**, 6511–6518 (2007).

221. Ali, Z. *et al.* On the regulatory role of side-chain hydroxylated oxysterols in the brain. Lessons from CYP27A1 transgenic and Cyp27a1 -/- mice 1. *J. Lipid Res.* **54**, 1033–1043 (2013).

222. Makoukji, J. *et al.* Interplay between LXR and Wnt/β-catenin signaling in the negative regulation of peripheral myelin genes by oxysterols. *J. Neurosci.* **31**, 9620–9629 (2011).

223. Seidah, N. G., Awan, Z., Chrétien, M. & Mbikay, M. PCSK9: a key modulator of cardiovascular health. *Circ. Res.* **114**, 1022–1036 (2014).

224. Zhang, D.-W. *et al.* Binding of proprotein convertase subtilisin/kexin type 9 to epidermal growth factor-like repeat A of low density lipoprotein receptor decreases receptor recycling and increases degradation. *J. Biol. Chem.* **282**, 18602–18612 (2007).

225. Demers, A. *et al.* PCSK9 Induces CD36 Degradation and Affects Long-Chain Fatty Acid Uptake and Triglyceride Metabolism in Adipocytes and in Mouse Liver. *Arterioscler. Thromb. Vasc. Biol.* **35**, 2517–2525 (2015).

226. Huang, S., Henry, L., Ho, Y. K., Pownall, H. J. & Rudenko, G. Mechanism of LDL binding and release probed by structure-based mutagenesis of the LDL receptor. *J. Lipid Res.* **51**, 297–308 (2010).

227. Poirier, S. *et al.* Dissection of the endogenous cellular pathways of PCSK9-induced low density lipoprotein receptor degradation: evidence for an intracellular route. *J. Biol. Chem.* **284**, 28856–28864 (2009).

228. Saavedra, Y. G. L., Day, R. & Seidah, N. G. The M2 module of the Cys-His-rich domain (CHRD) of PCSK9 protein is needed for the extracellular low-density lipoprotein receptor (LDLR) degradation pathway. *J. Biol. Chem.* **287**, 43492–43501 (2012).

229. Maxwell, K. N., Soccio, R. E., Duncan, E. M., Sehayek, E. & Breslow, J. L. Novel putative SREBP and LXR target genes identified by microarray analysis in liver of cholesterol-fed mice. *J. Lipid Res.* **44**, 2109–2119 (2003).

230. Dubuc, G. *et al.* Statins upregulate PCSK9, the gene encoding the proprotein convertase neural apoptosis-regulated convertase-1 implicated in familial hypercholesterolemia. *Arterioscler. Thromb. Vasc. Biol.* **24**, 1454–1459 (2004).

231. Kourimate, S. *et al.* Dual mechanisms for the fibrate-mediated repression of proprotein convertase subtilisin/kexin type 9. *J. Biol. Chem.* **283**, 9666–9673 (2008).

232. Citrin, K. M., Fernández-Hernando, C. & Suárez, Y. MicroRNA regulation of cholesterol metabolism. *Ann. N. Y. Acad. Sci.* **1495**, 55–77 (2021).

233. Barale, C., Melchionda, E., Morotti, A. & Russo, I. PCSK9 Biology and Its Role in Atherothrombosis. *Int. J. Mol. Sci.* **22**, (2021).

234. Cohen, J. C., Boerwinkle, E., Mosley, T. H. J. & Hobbs, H. H. Sequence variations in PCSK9, low LDL, and protection against coronary heart disease. *N. Engl. J. Med.* **354**, 1264–1272 (2006).

235. Timms, K. M. *et al.* A mutation in PCSK9 causing autosomal-dominant hypercholesterolemia in a Utah pedigree. *Hum. Genet.* **114**, 349–353 (2004).

236. Tibolla, G., Norata, G. D., Artali, R., Meneghetti, F. & Catapano, A. L. Proprotein convertase subtilisin/kexin type 9 (PCSK9): from structure-function relation to therapeutic inhibition. *Nutr. Metab. Cardiovasc. Dis.* **21**, 835–843 (2011).

237. Ricci, C. *et al.* PCSK9 induces a pro-inflammatory response in macrophages. *Sci. Rep.* **8**, 2267 (2018).

238. Bjørklund, M. M. *et al.* Induction of atherosclerosis in mice and hamsters without germline genetic engineering. *Circ. Res.* **114**, 1684–1689 (2014).

239. Sabatine, M. S. *et al.* Evolocumab and Clinical Outcomes in Patients with Cardiovascular Disease. *N. Engl. J. Med.* **376**, 1713–1722 (2017).

240. Schwartz, G. G. *et al.* Alirocumab and Cardiovascular Outcomes after Acute Coronary Syndrome. *N. Engl. J. Med.* **379**, 2097–2107 (2018).

241. Nishikido, T. & Ray, K. K. Inclisiran for the treatment of dyslipidemia. *Expert Opin. Investig. Drugs* **27**, 287–294 (2018).

242. Raal, F. J. *et al.* Inclisiran for the Treatment of Heterozygous Familial Hypercholesterolemia. *N. Engl. J. Med.* **382**, 1520–1530 (2020).

243. Seidah, N. G. *et al.* The secretory proprotein convertase neural apoptosis-regulated convertase 1 (NARC-1): Liver regeneration and neuronal differentiation. *Proc. Natl. Acad. Sci. U. S. A.* **100**, 928–933 (2003).

244. Chen, Y. Q., Troutt, J. S. & Konrad, R. J. PCSK9 is present in human cerebrospinal fluid and is maintained at remarkably constant concentrations throughout the course of the day. *Lipids* **49**, 445–455 (2014).

245. Adorni, M. P., Ruscica, M., Ferri, N., Bernini, F. & Zimetti, F. Proprotein Convertase Subtilisin/Kexin Type 9, Brain Cholesterol Homeostasis and Potential Implication for Alzheimer's Disease. *Front. Aging Neurosci.* **11**, 120 (2019).

246. Poirier, S. *et al.* Implication of the proprotein convertase NARC-1/PCSK9 in the development of the nervous system. *J. Neurochem.* **98**, 838–850 (2006).

247. Kysenius, K., Muggalla, P., Mätlik, K., Arumäe, U. & Huttunen, H. J. PCSK9

regulates neuronal apoptosis by adjusting ApoER2 levels and signaling. *Cell. Mol. Life Sci.* **69**, 1903–1916 (2012).

248. Piao, M.-X., Bai, J.-W., Zhang, P.-F. & Zhang, Y.-Z. PCSK9 regulates apoptosis in human neuroglioma u251 cells via mitochondrial signaling pathways. *Int. J. Clin. Exp. Pathol.* **8**, 2787–2794 (2015).

249. Apaijai, N. *et al.* Pretreatment With PCSK9 Inhibitor Protects the Brain Against Cardiac Ischemia/Reperfusion Injury Through a Reduction of Neuronal Inflammation and Amyloid Beta Aggregation. *J. Am. Heart Assoc.* **8**, e010838 (2019).

250. Poirier, S. *et al.* The proprotein convertase PCSK9 induces the degradation of low density lipoprotein receptor (LDLR) and its closest family members VLDLR and ApoER2. *J. Biol. Chem.* **283**, 2363–2372 (2008).

251. Liu, M. *et al.* PCSK9 is not involved in the degradation of LDL receptors and BACE1 in the adult mouse brain. *J. Lipid Res.* **51**, 2611–2618 (2010).

252. Rousselet, E. *et al.* PCSK9 reduces the protein levels of the LDL receptor in mouse brain during development and after ischemic stroke. *J. Lipid Res.* **52**, 1383–1391 (2011).

253. Koldamova, R. P. *et al.* The liver X receptor ligand T0901317 decreases amyloid beta production in vitro and in a mouse model of Alzheimer's disease. *J. Biol. Chem.* **280**, 4079–4088 (2005).

254. Zelcer, N. *et al.* Attenuation of neuroinflammation and Alzheimer's disease pathology by liver x receptors. *Proc. Natl. Acad. Sci. U. S. A.* **104**, 10601–10606 (2007).

255. Cui, W. *et al.* Liver X receptor activation attenuates inflammatory response and protects cholinergic neurons in APP/PS1 transgenic mice. *Neuroscience* **210**, 200–210 (2012).

256. Adighibe, O., Arepalli, S., Duckworth, J., Hardy, J. & Wavrant-De Vrièze, F. Genetic variability at the LXR gene (NR1H2) may contribute to the risk of Alzheimer's disease. *Neurobiol. Aging* **27**, 1431–1434 (2006).

257. Natunen, T. *et al.* Effects of NR1H3 genetic variation on the expression of liver X receptor α and the progression of Alzheimer's disease. *PLoS One* **8**, e80700 (2013).

258. Mohamed, A., Saavedra, L., Di Pardo, A., Sipione, S. & Posse de Chaves, E. β-amyloid inhibits protein prenylation and induces cholesterol sequestration by impairing SREBP-2 cleavage. *J. Neurosci.* **32**, 6490–6500 (2012).

259. Mohamed, A., Viveiros, A., Williams, K. & Posse de Chaves, E. Aβ inhibits SREBP-2 activation through Akt inhibition. *J. Lipid Res.* **59**, 1–13 (2018).

260. Pierrot, N. *et al.* Amyloid precursor protein controls cholesterol turnover needed for neuronal activity. *EMBO Mol. Med.* **5**, 608–625 (2013).

261. Mandas, A. *et al.* Changes in cholesterol metabolism-related gene expression in peripheral blood mononuclear cells from Alzheimer patients. *Lipids Health Dis.* **11**, 39 (2012).

262. Barbero-Camps, E., Fernández, A., Martínez, L., Fernández-Checa, J. C. & Colell, A. APP/PS1 mice overexpressing SREBP-2 exhibit combined Aβ accumulation and

tau pathology underlying Alzheimer's disease. *Hum. Mol. Genet.* **22**, 3460–3476 (2013).

263. Picard, C. *et al.* Alterations in cholesterol metabolism–related genes in sporadic Alzheimer's disease. *Neurobiol. Aging* **66**, 180.e1-180.e9 (2018).

264. Wang, C. *et al.* The sterol regulatory element-binding protein 2 is dysregulated by tau alterations in Alzheimer disease. *Brain Pathol.* **29**, 530–543 (2019).

265. Greeve, I. *et al.* The human DIMINUTO/DWARF1 homolog seladin-1 confers resistance to Alzheimer's disease-associated neurodegeneration and oxidative stress. *J. Neurosci.* **20**, 7345–7352 (2000).

266. Fünfschilling, U., Saher, G., Xiao, L., Möbius, W. & Nave, K.-A. Survival of adult neurons lacking cholesterol synthesis in vivo. *BMC Neurosci.* **8**, 1 (2007).

267. Yassine, H. N. *et al.* ABCA1-Mediated Cholesterol Efflux Capacity to Cerebrospinal Fluid Is Reduced in Patients With Mild Cognitive Impairment and Alzheimer's Disease. *J. Am. Heart Assoc.* **5**, 1–10 (2016).

268. Marchi, C. *et al.* ABCA1- And ABCG1-mediated cholesterol efflux capacity of cerebrospinal fluid is impaired in Alzheimer's disease. *J. Lipid Res.* **60**, 1449–1456 (2019).

269. Sanders, A. E. *et al.* Association of a functional polymorphism in the cholesteryl ester transfer protein (CETP) gene with memory decline and incidence of dementia. *JAMA* **303**, 150–158 (2010).

270. Johnson, W. *et al.* No association of CETP genotype with cognitive function or age-related cognitive change. *Neurosci. Lett.* **420**, 189–192 (2007).

271. Chirackal Manavalan, A. P. *et al.* Phospholipid transfer protein is expressed in cerebrovascular endothelial cells and involved in high density lipoprotein biogenesis and remodeling at the blood-brain barrier. *J. Biol. Chem.* **289**, 4683–4698 (2014).

272. Zhou, T. *et al.* Phospholipid transfer protein (PLTP) deficiency impaired blood-brain barrier integrity by increasing cerebrovascular oxidative stress. *Biochem. Biophys. Res. Commun.* **445**, 352–356 (2014).

273. Vuletic, S. *et al.* Widespread distribution of PLTP in human CNS: evidence for PLTP synthesis by glia and neurons, and increased levels in Alzheimer's disease. *J. Lipid Res.* **44**, 1113–1123 (2003).

274. Lewis, T. L. *et al.* Overexpression of human apolipoprotein A-I preserves cognitive function and attenuates neuroinflammation and cerebral amyloid angiopathy in a mouse model of Alzheimer disease. *J. Biol. Chem.* **285**, 36958–36968 (2010).

275. Lefterov, I. *et al.* Apolipoprotein A-I deficiency increases cerebral amyloid angiopathy and cognitive deficits in APP/PS1DeltaE9 mice. *J. Biol. Chem.* **285**, 36945–36957 (2010).

276. Ciccone, L., Shi, C., di Lorenzo, D., Van Baelen, A.-C. & Tonali, N. The Positive Side of the Alzheimer's Disease Amyloid Cross-Interactions: The Case of the Aβ 1-42 Peptide with Tau, TTR, CysC, and ApoA1. *Molecules* **25**, (2020).

277. Merched, A., Xia, Y., Visvikis, S., Serot, J. M. & Siest, G. Decreased high-density

lipoprotein cholesterol and serum apolipoprotein AI concentrations are highly correlated with the severity of Alzheimer's disease. *Neurobiol. Aging* **21**, 27–30 (2000).

278. Johansson, P. *et al.* Reduced Cerebrospinal Fluid Concentration of Apolipoprotein A-I in Patients with Alzheimer's Disease. *J. Alzheimer's Dis.* **59**, 1017–1026 (2017).

279. Button, E. B. *et al.* ApoA-I deficiency increases cortical amyloid deposition, cerebral amyloid angiopathy, cortical and hippocampal astrogliosis, and amyloid-associated astrocyte reactivity in APP/PS1 mice. *Alzheimers. Res. Ther.* **11**, 44 (2019).

280. Kloske, C. M. & Wilcock, D. M. The Important Interface Between Apolipoprotein E and Neuroinflammation in Alzheimer's Disease. *Front. Immunol.* **11**, 754 (2020).

281. Tachibana, M. *et al.* APOE4-mediated amyloid-β pathology depends on its neuronal receptor LRP1. *J. Clin. Invest.* **129**, 1272–1277 (2019).

282. Shi, Y. *et al.* APOE4 markedly exacerbates tau-mediated neurodegeneration in a mouse model of tauopathy. *Nature* **549**, 523–527 (2017).

283. Farfel, J. M., Yu, L., De Jager, P. L., Schneider, J. A. & Bennett, D. A. Association of APOE with Tau-Tangle Pathology with and without β-amyloid. *Neurobiol Aging.* **176**, 19–25 (2016).

284. Konings, S. C., Torres-Garcia, L., Martinsson, I. & Gouras, G. K. Astrocytic and Neuronal Apolipoprotein E Isoforms Differentially Affect Neuronal Excitability. *Front. Neurosci.* **15**, 734001 (2021).

285. Heinsinger, N. M., Gachechiladze, M. A. & Rebeck, G. W. Apolipoprotein e genotype affects size of ApoE complexes in cerebrospinal fluid. *J. Neuropathol. Exp. Neurol.* **75**, 918–924 (2016).

286. Rawat, V. *et al.* ApoE4 Alters ABCA1 Membrane Trafficking in Astrocytes. *J. Neurosci.* **39**, 9611–9622 (2019).

287. Zimetti, F. *et al.* Increased PCSK9 cerebrospinal fluid concentrations in Alzheimer's disease. *J. Alzheimer's Dis.* **55**, 315–320 (2017).

288. Noe, C. R., Noe-Letschnig, M., Handschuh, P., Noe, C. A. & Lanzenberger, R. Dysfunction of the Blood-Brain Barrier-A Key Step in Neurodegeneration and Dementia. *Front. Aging Neurosci.* **12**, 185 (2020).

289. Montagne, A. *et al.* APOE4 leads to blood–brain barrier dysfunction predicting cognitive decline. *Nature* **581**, 71–76 (2020).

290. Lynch, J. R. *et al.* APOE genotype and an ApoE-mimetic peptide modify the systemic and central nervous system inflammatory response. *J. Biol. Chem.* **278**, 48529–48533 (2003).

291. Cioffi, F., Adam, R. H. I., Bansal, R. & Broersen, K. A Review of Oxidative Stress Products and Related Genes in Early Alzheimer's Disease. *J. Alzheimers. Dis.* **83**, 977–1001 (2021).

292. Xiong, M. *et al.* APOE immunotherapy reduces cerebral amyloid angiopathy and amyloid plaques while improving cerebrovascular function. *Sci. Transl. Med.* **13**, (2021).

293. Nordestgaard, L. T., Tybjaerg-Hansen, A., Rasmussen, K. L., Nordestgaard, B. G. & Frikke-Schmidt, R. Genetic variation in clusterin and risk of dementia and ischemic vascular disease in the general population - cohort studies and meta-analyses of 362,338 individuals. *Atherosclerosis* **275**, e29–e30 (2018).

294. Narayan, P. *et al.* The extracellular chaperone clusterin sequesters oligomeric forms of the amyloid-β(1-40) peptide. *Nat. Struct. Mol. Biol.* **19**, 79–83 (2011).

295. Cascella, R. *et al.* Extracellular chaperones prevent Aβ42-induced toxicity in rat brains. *Biochim. Biophys. Acta - Mol. Basis Dis.* **1832**, 1217–1226 (2013).

296. Shepherd, C. E., Affleck, A. J., Bahar, A. Y., Carew-Jones, F. & Halliday, G. M. Intracellular and secreted forms of clusterin are elevated early in Alzheimer's disease and associate with both Aβ and tau pathology. *Neurobiol. Aging* **89**, 129–131 (2020).

297. Hirsch-Reinshagen, V. *et al.* The absence of ABCA1 decreases soluble ApoE levels but does not diminish amyloid deposition in two murine models of Alzheimer disease. *J. Biol. Chem.* **280**, 43243–43256 (2005).

298. Fitz, N. F. *et al.* Abca1 deficiency affects Alzheimer's disease-like phenotype in human ApoE4 but not in ApoE3-targeted replacement mice. *J. Neurosci.* **32**, 13125–13136 (2012).

299. Morizawa, Y. M. *et al.* Reactive astrocytes function as phagocytes after brain ischemia via ABCA1-mediated pathway. *Nat. Commun.* **8**, 28 (2017).

300. Cascorbi, I. *et al.* Association of ATP-binding cassette transporter variants with the risk of Alzheimer's disease. *Pharmacogenomics* **14**, 485–494 (2013).

301. Nordestgaard, L. T., Tybjærg-Hansen, A., Nordestgaard, B. G. & Frikke-Schmidt, R. Loss-of-function mutation in ABCA1 and risk of Alzheimer's disease and cerebrovascular disease. *Alzheimer's Dement.* **11**, 1430–1438 (2015).

302. Tansley, G. H. *et al.* The cholesterol transporter ABCG1 modulates the subcellular distribution and proteolytic processing of beta-amyloid precursor protein. *J. Lipid Res.* **48**, 1022–1034 (2007).

303. Burgess, B. L. *et al.* ABCG1 influences the brain cholesterol biosynthetic pathway but does not affect amyloid precursor protein or apolipoprotein E metabolism in vivo. *J. Lipid Res.* **49**, 1254–1267 (2008).

304. Wollmer, M. A. *et al.* Association study of cholesterol-related genes in Alzheimer's disease. *Neurogenetics* **8**, 179–188 (2007).

305. Uehara, Y. *et al.* ATP-binding cassette transporter G4 is highly expressed in microglia in Alzheimer's brain. *Brain Res.* **1217**, 239–246 (2008).

306. Dodacki, A. *et al.* Expression and function of Abcg4 in the mouse blood-brain barrier: role in restricting the brain entry of amyloid-β peptide. *Sci. Rep.* **7**, 13393 (2017).

307. Cao, D., Fukuchi, K., Wan, H., Kim, H. & Li, L. Lack of LDL receptor aggravates learning deficits and amyloid deposits in Alzheimer transgenic mice. *Neurobiol. Aging* **27**, 1632–1643 (2006).

308. Kim, J. *et al.* Overexpression of low-density lipoprotein receptor in the brain

markedly inhibits amyloid deposition and increases extracellular A beta clearance. *Neuron* **64**, 632–644 (2009).

309. Basak, J. M., Verghese, P. B., Yoon, H., Kim, J. & Holtzman, D. M. Low-density lipoprotein receptor represents an apolipoprotein E-independent pathway of Aβ uptake and degradation by astrocytes. *J. Biol. Chem.* **287**, 13959–13971 (2012).

310. Castellano, J. M. *et al.* Low-density lipoprotein receptor overexpression enhances the rate of brain-to-blood Aβ clearance in a mouse model of β-amyloidosis. *Proc. Natl. Acad. Sci. U. S. A.* **109**, 15502–15507 (2012).

311. Lämsä, R. *et al.* Genetic study evaluating LDLR polymorphisms and Alzheimer's disease. *Neurobiol. Aging* **29**, 848–855 (2008).

312. Motoi, Y. *et al.* Apolipoprotein E receptor 2 is involved in neuritic plaque formation in APP sw mice. *Neurosci. Lett.* **368**, 144–147 (2004).

313. Hoe, H.-S. *et al.* Interaction of reelin with amyloid precursor protein promotes neurite outgrowth. *J. Neurosci.* **29**, 7459–7473 (2009).

314. Fuentealba, R. A. *et al.* ApoER2 expression increases Abeta production while decreasing Amyloid Precursor Protein (APP) endocytosis: Possible role in the partitioning of APP into lipid rafts and in the regulation of gamma-secretase activity. *Mol. Neurodegener.* **2**, 14 (2007).

315. Hoe, H.-S. & Rebeck, G. W. Regulation of ApoE receptor proteolysis by ligand binding. *Brain Res. Mol. Brain Res.* **137**, 31–39 (2005).

316. Hoe, H.-S., Tran, T. S., Matsuoka, Y., Howell, B. W. & Rebeck, G. W. DAB1 and Reelin effects on amyloid precursor protein and ApoE receptor 2 trafficking and processing. *J. Biol. Chem.* **281**, 35176–35185 (2006).

317. Deane, R. *et al.* apoE isoform-specific disruption of amyloid beta peptide clearance from mouse brain. *J. Clin. Invest.* **118**, 4002–4013 (2008).

318. Rebeck, G. W. *et al.* Association of membrane-bound amyloid precursor protein APP with the apolipoprotein E receptor LRP. *Brain Res. Mol. Brain Res.* **87**, 238–245 (2001).

319. Lleó, A. *et al.* Low density lipoprotein receptor-related protein (LRP) interacts with presenilin 1 and is a competitive substrate of the amyloid precursor protein (APP) for gamma-secretase. *J. Biol. Chem.* **280**, 27303–27309 (2005).

320. Liu, C.-C. *et al.* Astrocytic LRP1 Mediates Brain Aβ Clearance and Impacts Amyloid Deposition. *J. Neurosci.* **37**, 4023–4031 (2017).

321. Storck, S. E. *et al.* Endothelial LRP1 transports amyloid-β(1-42) across the blood-brain barrier. *J. Clin. Invest.* **126**, 123–136 (2016).

322. Wilhelmus, M. M. M. *et al.* Lipoprotein receptor-related protein-1 mediates amyloid-beta-mediated cell death of cerebrovascular cells. *Am. J. Pathol.* **171**, 1989–1999 (2007).

323. Pritchard, A. *et al.* Association study and meta-analysis of low-density lipoprotein receptor related protein in Alzheimer's disease. *Neurosci. Lett.* **382**, 221–226 (2005).

324. Rebeck, G. W., Harr, S. D., Strickland, D. K. & Hyman, B. T. Multiple, diverse senile

plaque-associated proteins are ligands of an apolipoprotein E receptor, the alpha 2-macroglobulin receptor/low-density-lipoprotein receptor-related protein. *Ann. Neurol.* **37**, 211–217 (1995).

325. Yamanaka, Y. *et al.* Antisense RNA controls LRP1 Sense transcript expression through interaction with a chromatin-associated protein, HMGB2. *Cell Rep.* **11**, 967–976 (2015).

326. Sultana, R., Banks, W. A. & Butterfield, D. A. Decreased levels of PSD95 and two associated proteins and increased levels of BCl2 and caspase 3 in hippocampus from subjects with amnestic mild cognitive impairment: Insights into their potential roles for loss of synapses and memory, accumulation of Ab. *J. Neurosci. Res.* **88**, 469–477 (2010).

327. Testa, G. *et al.* Changes in brain oxysterols at different stages of Alzheimer's disease: Their involvement in neuroinflammation. *Redox Biol.* **10**, 24–33 (2016).

328. Wang, H.-L. *et al.* Cholesterol, 24-Hydroxycholesterol, and 27-Hydroxycholesterol as Surrogate Biomarkers in Cerebrospinal Fluid in Mild Cognitive Impairment and Alzheimer's Disease: A Meta-Analysis. *J. Alzheimers. Dis.* **51**, 45–55 (2016).

329. Kölsch, H. *et al.* CYP46A1 variants influence Alzheimer's disease risk and brain cholesterol metabolism. *Eur. Psychiatry* **24**, 183–190 (2009).

330. Kotti, T., Head, D. D., McKenna, C. E. & Russell, D. W. Biphasic requirement for geranylgeraniol in hippocampal long-term potentiation. *Proc. Natl. Acad. Sci. U. S. A.* **105**, 11394–11399 (2008).

331. Djelti, F. *et al.* CYP46A1 inhibition, brain cholesterol accumulation and neurodegeneration pave the way for Alzheimer's disease. *Brain* **138**, 2383–2398 (2015).

332. Famer, D. *et al.* Regulation of alpha- and beta-secretase activity by oxysterols: cerebrosterol stimulates processing of APP via the alpha-secretase pathway. *Biochem. Biophys. Res. Commun.* **359**, 46–50 (2007).

333. Hudry, E. *et al.* Adeno-associated virus gene therapy with cholesterol 24-hydroxylase reduces the amyloid pathology before or after the onset of amyloid plaques in mouse models of Alzheimer's disease. *Mol. Ther.* **18**, 44–53 (2010).

334. Loera-Valencia, R., Goikolea, J., Parrado-Fernandez, C., Merino-Serrais, P. & Maioli, S. Alterations in cholesterol metabolism as a risk factor for developing Alzheimer's disease: Potential novel targets for treatment. *J. Steroid Biochem. Mol. Biol.* **190**, 104–114 (2019).

335. Heverin, M. *et al.* 27-hydroxycholesterol mediates negative effects of dietary cholesterol on cognition in mice. *Behav. Brain Res.* **278**, 356–359 (2015).

336. Merino-Serrais, P. *et al.* 27-Hydroxycholesterol Induces Aberrant Morphology and Synaptic Dysfunction in Hippocampal Neurons. *Cereb. Cortex* **29**, 429–446 (2019).

337. Shafaati, M. *et al.* Marked accumulation of 27-hydroxycholesterol in the brains of Alzheimer's patients with the Swedish APP 670/671 mutation. *J. Lipid Res.* **52**, 1004–1010 (2011).

338. Prasanthi, J. R. *et al.* Differential effects of 24-hydroxycholesterol and 27-hydroxycholesterol on beta-amyloid precursor protein levels and processing in

human neuroblastoma SH-SY5Y cells. *Mol. Neurodegener.* **4**, 1 (2009).

339. Marwarha, G., Dasari, B. & Ghribi, O. Endoplasmic reticulum stress-induced CHOP activation mediates the down-regulation of leptin in human neuroblastoma SH-SY5Y cells treated with the oxysterol 27-hydroxycholesterol. *Cell. Signal.* **24**, 484–492 (2012).

340. Ismail, M.-A.-M. *et al.* 27-Hydroxycholesterol impairs neuronal glucose uptake through an IRAP/GLUT4 system dysregulation. *J. Exp. Med.* **214**, 699–717 (2017).

341. Zhao, X.-S. *et al.* Hyperlipidemia-induced apoptosis of hippocampal neurons in apoE(-/-) mice may be associated with increased PCSK9 expression. *Mol. Med. Rep.* **15**, 712–718 (2017).

342. Wang, L. *et al.* Inhibition of proprotein convertase subtilisin/kexin type 9 attenuates neuronal apoptosis following focal cerebral ischemia via apolipoprotein E receptor 2 downregulation in hyperlipidemic mice. *Int. J. Mol. Med.* **42**, 2098–2106 (2018).

343. Jonas, M. C., Costantini, C. & Puglielli, L. PCSK9 is required for the disposal of non-acetylated intermediates of the nascent membrane protein BACE1. *EMBO Rep.* **9**, 916–922 (2008).

344. Mulder, M. *et al.* LDL receptor deficiency results in decreased cell proliferation and presynaptic bouton density in the murine hippocampus. *Neurosci. Res.* **59**, 251–256 (2007).

345. Ding, Z. *et al.* PCSK9 regulates expression of scavenger receptors and ox-LDL uptake in macrophages. *Cardiovasc. Res.* **114**, 1145–1153 (2018).

346. Wollmer, M. A. Cholesterol-related genes in Alzheimer's disease. *Biochim. Biophys. Acta* **1801**, 762–773 (2010).

347. Shibata, N. *et al.* No genetic association between PCSK9 polymorphisms and Alzheimer's disease and plasma cholesterol level in Japanese patients. *Psychiatr. Genet.* **15**, 239 (2005).

348. Reynolds, C. A. *et al.* Analysis of lipid pathway genes indicates association of sequence variation near SREBF1/TOM1L2/ATPAF2 with dementia risk. *Hum. Mol. Genet.* **19**, 2068–2078 (2010).

349. Mefford, M. T. *et al.* PCSK9 Variants, Low-Density Lipoprotein Cholesterol, and Neurocognitive Impairment: Reasons for Geographic and Racial Differences in Stroke Study (REGARDS). *Circulation* **137**, 1260–1269 (2018).

350. Benn, M., Nordestgaard, B. G., Frikke-Schmidt, R. & Tybjærg-Hansen, A. Low LDL cholesterol, PCSK9 and HMGCR genetic variation, and risk of Alzheimer{\textquoteright}s disease and Parkinson{\textquoteright}s disease: Mendelian randomisation study. *BMJ* **357**, (2017).

351. Picard, C. *et al.* Proprotein convertase subtilisin/kexin type 9 (PCSK9) in Alzheimer's disease: A genetic and proteomic multi-cohort study. *PLoS One* **14**, 1–18 (2019).

352. Giugliano, R. P. *et al.* Cognitive Function in a Randomized Trial of Evolocumab. *N. Engl. J. Med.* **377**, 633–643 (2017).

353. Janik, M. J. *et al.* Alirocumab treatment and neurocognitive function according to the CANTAB scale in patients at increased cardiovascular risk: A prospective, randomized, placebo-controlled study. *Atherosclerosis* **331**, 20–27 (2021).

354. Seyedzadeh, M. H. *et al.* Study of curcumin immunomodulatory effects on reactive astrocyte cell function. *Int. Immunopharmacol.* **22**, 230–235 (2014).

355. Cheung, Y.-T. *et al.* Effects of all-trans-retinoic acid on human SH-SY5Y neuroblastoma as in vitro model in neurotoxicity research. *Neurotoxicology* **30**, 127–135 (2009).

356. Garton, K. J., Ferri, N. & Raines, E. W. Efficient expression of exogenous genes in primary vascular cells using IRES-based retroviral vectors. *Biotechniques* **32**, 830, 832, 834 passim (2002).

357. Cazzaniga, E. *et al.* Abeta peptide toxicity is reduced after treatments decreasing phosphatidylethanolamine content in differentiated neuroblastoma cells. *Neurochem. Res.* **36**, 863–869 (2011).

358. Gobbi, M. *et al.* Lipid-based nanoparticles with high binding affinity for amyloid-beta1-42 peptide. *Biomaterials* **31**, 6519–6529 (2010).

359. Balducci, C. *et al.* Synthetic amyloid-beta oligomers impair long-term memory independently of cellular prion protein. *Proc. Natl. Acad. Sci. U. S. A.* **107**, 2295–2300 (2010).

360. Spagnuolo, M. S. *et al.* Haptoglobin increases with age in rat hippocampus and modulates Apolipoprotein E mediated cholesterol trafficking in neuroblastoma cell lines. *Front. Cell. Neurosci.* **8**, 212 (2014).

361. Favari, E. *et al.* Small discoidal pre-β1 HDL particles are efficient acceptors of cell cholesterol via ABCA1 and ABCG1. *Biochemistry* **48**, 11067–11074 (2009).

362. Lupo, M. G. *et al.* Cholesterol-Lowering Action of a Novel Nutraceutical Combination in Uremic Rats: Insights into the Molecular Mechanism in a Hepatoma Cell Line. *Nutrients* **12**, (2020).

363. Schneider, C. A., Rasband, W. S. & Eliceiri, K. W. NIH Image to ImageJ: 25 years of image analysis. *Nat. Methods* **9**, 671–675 (2012).

364. Favari, E. *et al.* Probucol inhibits ABCA1-mediated cellular lipid efflux. *Arterioscler. Thromb. Vasc. Biol.* **24**, 2345–2350 (2004).

365. Adorni, M. P. *et al.* Inhibitory effect of PCSK9 on Abca1 protein expression and cholesterol efflux in macrophages. *Atherosclerosis* **256**, 1–6 (2017).

366. Krimbou, L. *et al.* Molecular interactions between apoE and ABCA1: impact on apoE lipidation. *J. Lipid Res.* **45**, 839–848 (2004).

367. Oakley, H. *et al.* Intraneuronal beta-amyloid aggregates, neurodegeneration, and neuron loss in transgenic mice with five familial Alzheimer's disease mutations: potential factors in amyloid plaque formation. *J. Neurosci.* **26**, 10129–10140 (2006).

368. Del Puppo, M., Kienle, M. G., Petroni, M. L., Crosignani, A. & Podda, M. Serum 27-hydroxycholesterol in patients with primary biliary cirrhosis suggests alteration of cholesterol catabolism to bile acids via the acidic pathway. *J. Lipid Res.* **39**, 2477–2482 (1998).

369. Borah, K. *et al.* A quantitative LC-MS/MS method for analysis of mitochondrial - specific oxysterol metabolism. *Redox Biol.* **36**, 101595 (2020).

370. Kollmer, M. *et al.* Cryo-EM structure and polymorphism of Aβ amyloid fibrils purified from Alzheimer's brain tissue. *Nat. Commun.* **10**, 4760 (2019).

371. Lopez, L. M. Rosuvastatin: a high-potency HMG-CoA reductase inhibitor. *J. Am. Pharm. Assoc. (2003).* **45**, 503–513 (2005).

372. Ehehalt, R., Keller, P., Haass, C., Thiele, C. & Simons, K. Amyloidogenic processing of the Alzheimer beta-amyloid precursor protein depends on lipid rafts. *J. Cell Biol.* **160**, 113–123 (2003).

373. Schwendeman, A. *et al.* The effect of phospholipid composition of reconstituted HDL on its cholesterol efflux and anti-inflammatory properties. *J. Lipid Res.* **56**, 1727–1737 (2015).

374. Feringa, F. M. & van der Kant, R. Cholesterol and Alzheimer's Disease; From Risk Genes to Pathological Effects. *Front. Aging Neurosci.* **13**, 690372 (2021).

375. Sondag, C. M., Dhawan, G. & Combs, C. K. Beta amyloid oligomers and fibrils stimulate differential activation of primary microglia. *J. Neuroinflammation* **6**, 1 (2009).

376. Hou, L. *et al.* The effects of amyloid-β42 oligomer on the proliferation and activation of astrocytes in vitro. *Vitr. Cell. Dev. Biol. - Anim.* **47**, 573 (2011).

377. Spuch, C., Ortolano, S. & Navarro, C. LRP-1 and LRP-2 receptors function in the membrane neuron. Trafficking mechanisms and proteolytic processing in Alzheimer's disease. *Front. Physiol.* **3**, 269 (2012).

378. Sierri, G. *et al.* Reduced Levels of ABCA1 Transporter Are Responsible for the Cholesterol Efflux Impairment in β-Amyloid-Induced Reactive Astrocytes: Potential Rescue from Biomimetic HDLs. *Int. J. Mol. Sci.* **23**, (2021).

379. Canepa, E. *et al.* Cholesterol and amyloid-β: evidence for a cross-talk between astrocytes and neuronal cells. *J. Alzheimers. Dis.* **25**, 645–653 (2011).

380. Azizidoost, S., Babaahmadi-Rezaei, H., Nazeri, Z., Cheraghzadeh, M. & Kheirollah, A. Amyloid beta increases ABCA1 and HMGCR protein expression, and cholesterol synthesis and accumulation in mice neurons and astrocytes. *Biochim. Biophys. acta. Mol. cell Biol. lipids* **1867**, 159069 (2022).

381. Fukui, K., Ferris, H. A. & Kahn, C. R. Effect of cholesterol reduction on receptor signaling in neurons. *J. Biol. Chem.* **290**, 26383–26392 (2015).

382. Liu, L.-S. *et al.* PCSK9 Promotes oxLDL-Induced PC12 Cell Apoptosis Through the Bcl-2/Bax-Caspase 9/3 Signaling Pathway. *J. Alzheimers. Dis.* **57**, 723–734 (2017).

383. Dahlgren, K. N. *et al.* Oligomeric and fibrillar species of amyloid-beta peptides differentially affect neuronal viability. *J. Biol. Chem.* **277**, 32046–32053 (2002).

384. Mbikay, M. *et al.* Variable effects of gender and Western diet on lipid and glucose homeostasis in aged PCSK9-deficient C57BL/6 mice CSK9PC57BL/6. *J. Diabetes* **7**, 74–84 (2015).

385. Arunsak, B. *et al.* Proprotein convertase subtilisin/kexin type 9 (PCSK9) inhibitor

exerts greater efficacy than atorvastatin on improvement of brain function and cognition in obese rats. *Arch. Biochem. Biophys.* **689**, 108470 (2020).

386. Mast, N., El-Darzi, N., Petrov, A. M., Li, Y. & Pikuleva, I. A. CYP46A1-dependent and independent effects of efavirenz treatment. *Brain Commun.* **2**, fcaa180 (2020).

387. Mast, N. *et al.* Cholesterol-metabolizing enzyme cytochrome P450 46A1 as a pharmacologic target for Alzheimer's disease. *Neuropharmacology* **123**, 465–476 (2017).

388. Leoni, V. & Caccia, C. Potential diagnostic applications of side chain oxysterols analysis in plasma and cerebrospinal fluid. *Biochem. Pharmacol.* **86**, 26–36 (2013).

389. Gamba, P. *et al.* The Controversial Role of 24-S-Hydroxycholesterol in Alzheimer's Disease. *Antioxidants (Basel, Switzerland)* **10**, (2021).

390. Counts, S. E., Ikonomovic, M. D., Mercado, N., Vega, I. E. & Mufson, E. J. Biomarkers for the Early Detection and Progression of Alzheimer's Disease. *Neurotherapeutics* **14**, 35–53 (2017).

391. Zhao, N., Liu, C.-C., Qiao, W. & Bu, G. Apolipoprotein E, Receptors, and Modulation of Alzheimer's Disease. *Biol. Psychiatry* **83**, 347–357 (2018).

392. Safieh, M., Korczyn, A. D. & Michaelson, D. M. ApoE4: an emerging therapeutic target for Alzheimer's disease. *BMC Med.* **17**, 64 (2019).

393. Bachmeier, C. *et al.* Apolipoprotein E isoform-specific effects on lipoprotein receptor processing. *Neuromolecular Med.* **16**, 686–696 (2014).

394. Mohammadi, A. *et al.* Circulating PCSK9 affects serum LDL and cholesterol levels more than SREBP-2 expression. *Adv. Clin. Exp. Med. Off. organ Wroclaw Med. Univ.* **26**, 655–659 (2017).

395. Dounousi, E. *et al.* Association between PCSK9 Levels and Markers of Inflammation, Oxidative Stress, and Endothelial Dysfunction in a Population of Nondialysis Chronic Kidney Disease Patients. *Oxid. Med. Cell. Longev.* **2021**, 6677012 (2021).

396. Nozue, T. Lipid Lowering Therapy and Circulating PCSK9 Concentration. *J. Atheroscler. Thromb.* **24**, 895–907 (2017).

397. Montagne, A. *et al.* APOE4 leads to blood-brain barrier dysfunction predicting cognitive decline. *Nature* **581**, 71–76 (2020).

398. di Mauro, G. *et al.* PCSK9 Inhibitors and Neurocognitive Adverse Drug Reactions: Analysis of Individual Case Safety Reports from the Eudravigilance Database. *Drug Saf.* **44**, 337–349 (2021).

399. Tomlinson, B., Chow, E., Chan, P. & Lam, C. W. K. An evaluation of the pharmacokinetics of inclisiran in the treatment of atherosclerotic cardiovascular disease. *Expert Opin. Drug Metab. Toxicol.* 1–9 (2022) doi:10.1080/17425255.2021.2029402.